AD-784 901

TURBINE INLET GAS TEMPERATURE MEASUREMENT AND CONTROL SYSTEM

William L. Webb

Pratt and Whitney Aircraft

Prepared for:

Air Force Aeropropulsion Laboratory
National Aeronautics and Space Administration

December 1973

NOTICE

When Government drawings, specifications, or other data are used for any purpose other than in connection with a definitely related Government procurement operation, the United States Government thereby incurs no responsibility nor any obligation whatsoever; and the fact that the Government may have formulated, furnished, or in any way supplied the said drawings, specifications, or other data, is not to be regarded by implication or otherwise as in any manner licensing the holder or any other person or corporation, or conveying any rights or permission to manufacture, use, or sell any patented invention that may in any way be related thereto.

Unclassified
Security Classification

AD-784 901

DOCUMENT CONTROL DATA - R & D

(Security classification of title, body of abstract and indexing annotation must be entered when the overall report is classified)

1. ORIGINATING ACTIVITY (Corporate author) Pratt & Whitney Aircraft	2a. REPORT SECURITY CLASSIFICATION Unclassified
	2b. GROUP

3. REPORT TITLE

TURBINE INLET GAS TEMPERATURE MEASUREMENT AND CONTROL SYSTEM

4. DESCRIPTIVE NOTES (Type of report and inclusive dates)
Final Report (1 April 1972 through 30 September 1973)

5. AUTHOR(S) (First name, middle initial, last name)

William L. Webb

6. REPORT DATE December 1973	7a. TOTAL NO. OF PAGES 114	7b. NO. OF REFS 3

8a. CONTRACT OR GRANT NO. USAF MIPR FY14557200404	9a. ORIGINATOR'S REPORT NUMBER(S) AFAPL-TR-73-116
b. PROJECT NO. 3066	
c. 306603	9b. OTHER REPORT NO(S) (Any other numbers that may be assigned this report)
d.	NASA ID No. 4 PR 72-148

10. DISTRIBUTION STATEMENT

Approved for Public Release: Distribution Unlimited

11. SUPPLEMENTARY NOTES	12. SPONSORING MILITARY ACTIVITY

13. ABSTRACT

A fluidic Turbine Inlet Gas Temperature (TIGT) Measurement and Control System was developed for use on a Pratt & Whitney Aircraft J58 engine. Based on engine operating requirements, criteria for high temperature materials selection, system design, and system performance were established. To minimize development and operational risk, the TIGT control system was designed to interface with an existing Exhaust Gas Temperature (EGT) Trim System and thereby modulate steady-state fuel flow to maintain a desired TIGT level. Extensive component and system testing was conducted including heated (2300°F) vibration tests for the fluidic sensor and gas sampling probe, temperature and vibration tests on the system electronics, burner rig testing of the TIGT measurement system, and in excess of 100 hours of system testing on a J58 engine. Due to the time variant level of turbine inlet gas temperature at a single measurement point, the TIGT control system, when operated in conjunction with the existing J58 trim system, caused the engine operating point to wander considerably. For improved performance, a second generation system would most probably utilize a multiple fluidic TIGT sampling point system similar to the existing EGT thermocouple harness. During the extensive bench and engine test program, the TIGT Measurement and Control System demonstrated the necessary durability and reliability for flight tests under the conditions existing on the YF-12 aircraft. Consequently, two complete flight qualified systems were delivered to NASA Flight Research Center for subsequent YF-12 flight testing during 1974.

DD FORM 1 NOV 65 1473

Unclassified
Security Classification

14. KEY WORDS	LINK A		LINK B		LINK C	
	ROLE	WT	ROLE	WT	ROLE	WT
Turbine Inlet Gas Temperature						
Fluidic Temperature Sensor						
Thorium Dispersed Nickel Chrome Aluminum						
Columbium						
Silicide Coating						

AFAPL-TR-73-116

TURBINE INLET GAS TEMPERATURE MEASUREMENT AND CONTROL SYSTEM

W. L. Webb

DECEMBER 1973

Approved for Public Release; Distribution Unlimited

i (c)

FOREWORD

This final report describes the technical work accomplished during the "Turbine Inlet Gas Temperature Measurement and Control System" program conducted under USAF MIPR No. FY14557200404, Air Force Aero Propulsion Laboratory (AFAPL), Project No. 3066, Task No. 306603. The work described was performed during the period 1 April 1972 through 30 September 1973. This contract with the Pratt & Whitney Aircraft Division of United Aircraft Corporation, Florida Research and Development Center, West Palm Beach, Florida, was sponsored by the National Aeronautics and Space Administration, Flight Research Center, Edwards Air Force Base, California, NASA Identification No. 4PR-72-148. Mr. Paul J. Reukauf was the Project Engineer.

Mr. W. L. Webb was the Program Manager with Messrs. L. D. Emerson and L. O. Churchill providing Senior Technical and Managerial direction. Mr. Ralph H. Pamperin was Program Manager for the Government and Aeronautical Projects Division of Honeywell, Inc. that was a major subcontractor in this effort. Acknowledgement is given to Mr. L. L. Small of AFAPL for his support and advice throughout the program. Pratt & Whitney Aircraft participation in past research and development programs funded by the Controls Group at AFAPL under the direction of Mr. C. E. Bentz formed the background on which this program was based.

This report was submitted by Pratt & Whitney Aircraft in October 1973 and carried the internal designation of FR-6094.

Publication of this report does not constitute Air Force approval of the report's findings or conclusions. It is published only for the exchange and stimulation of ideas.

Ernest C. Simpson
Director, Turbine Engine Division
Air Force Aero Propulsion Laboratory

ABSTRACT

A fluidic Turbine Inlet Gas Temperature (TIGT) Measurement and Control System was developed for use on a Pratt & Whitney Aircraft J58 engine. Based on engine operating requirements, criteria for high temperature materials selection, system design, and system performance were established. To minimize development and operational risk, the TIGT control system was designed to interface with an existing Exhaust Gas Temperature (EGT) Trim System and thereby modulate steady-state fuel flow to maintain a desired TIGT level. Extensive component and system testing was conducted including heated (2300°F) vibration tests for the fluidic sensor and gas sampling probe, temperature and vibration tests on the system electronics, burner rig testing of the TIGT measurement system, and in excess of 100 hours of system testing on a J58 engine. Due to the time variant level of turbine inlet gas temperature at a single measurement point, the TIGT control system, when operated in conjunction with the existing J58 trim system, caused the engine operating point to wander considerably. For improved performance, a second generation system would most probably utilize a multiple fluidic TIGT sampling point system similar to the existing EGT thermocouple harness. During the extensive bench and engine test program, the TIGT Measurement and Control System demonstrated the necessary durability and reliability for flight tests under the conditions existing on the YF-12 aircraft. Consequently, two complete flight qualified systems were delivered to NASA Flight Research Center for subsequent YF-12 flight testing during 1974.

CONTENTS

ILLUSTRATIONS

ILLUSTRATIONS (Continued)

TABLES

SECTION I

INTRODUCTION

The size and weight of a gas turbine are strongly affected by the maximum allowable turbine inlet gas temperature (TIGT). The maximum temperature is limited by the metallurgical properties of the turbine. Once an engine has been qualified and enters service, the effect of increased temperature is decreased engine life and the effect of lower temperature is to increase thrust specific fuel consumption. Parametrically, the effect of turbine metal temperature on engine life is as shown in figure 1 for IN100 material. Thrust specific fuel consumption increases are on the order of 3%/100°F decrease in turbine inlet gas temperature for modern engines. These relationships generate a requirement for a direct measurement of TIGT.

Turbine engines presently in service with turbine inlet gas temperature above 2000°F are developed and controlled to operate with turbine temperature sensed (by state-of-the-art thermocouples) at some station downstream of the turbine inlet where the response time - temperature level relationship is an acceptable compromise. Future turbine engines will incorporate variable turbine inlet geometry to improve performance. Turbine inlet temperature will increase to minimize engine size and weight thereby requiring an increase of turbine cooling airflow to maintain turbine hardware within metallurgical limits. However, at power conditions less than maximum, where most turbine engines operate for approximately 95% of the service life, turbine cooling airflow will need to be regulated to minimize the performance degradation associated with excessive cooling flow. These added turbine engine controlled variables will create a requirement for turbine inlet gas temperature measurement that does not exist in present fixed geometry turbine engines with unregulated cooling airflow.

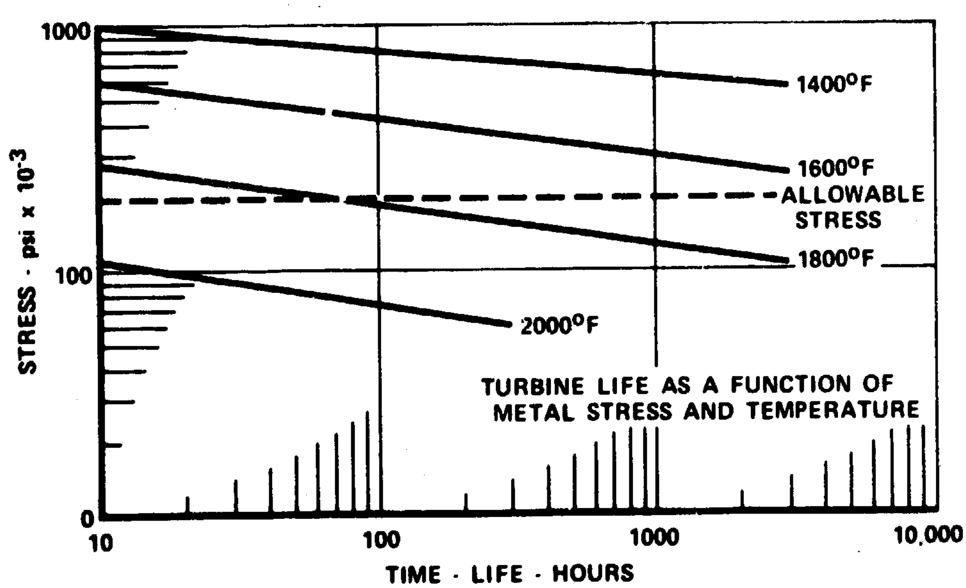

Figure 1. Turbine Life As A Function of Metal Stress and Temperature FD 74950

Turbine inlet gas temperature in the 2000 to 2500°F range can be measured with noble metal thermocouples. However, because of low mechanical strength, thermocouple sensing junctions must be relatively large to achieve the life required in turbine engines, some models of which have overhaul cycles in excess of 10,000 hours. Since a thermocouple is a thermoelectric device, its response to temperature change is directly related to the size of the sensing junction. This relation is illustrated in figure 2 (Reference 1). Therefore, noble metal thermocouples with reasonable life have relatively poor response characteristics. On the other hand fluidic temperature sensors can be used to measure TIGT and have demonstrated the ability to operate at a 4000°F sensed temperature for short periods while providing rapid transient response.

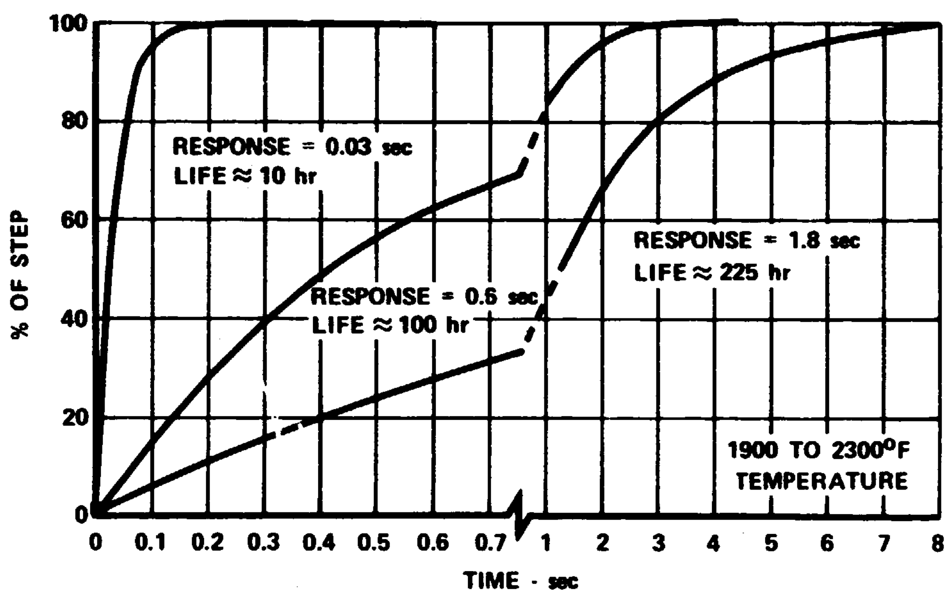

Figure 2. Ideal Response of Thermocouples FD 74951

Pratt & Whitney Aircraft, with Honeywell, Inc. as the subcontractor, has built a fluidic TIGT measurement and control system which is intended to be flight tested on a YF-12 airplane at the NASA Flight Research Center, Edwards, California. References 2 and 3 provide development and capability information for fluidic temperature sensors upon which this program is based. The general objectives of this program were to: (1) complete development of a Turbine Inlet Gas Temperature (TIGT) measurement system, initiated in the Hybrid Control Program (Contract No. F33615-68-C-1207), to a point suitable for flight test, (2) deliver two TIGT measurement systems for laboratory tests, (3) deliver two TIGT measurement systems for flight test in a YF-12, and (4) deliver one gas sampling probe for a TF30 engine. The flight test TIGT measurement system consists of a hot gas sampling probe, a fluidic temperature sensor, a piezoelectric frequency sensor, a pressure sensor, and a signal conditioning interface/selector. The TIGT measurement system operated through the J58 engine exhaust gas temperature (EGT) vernier control, to provide a TIGT control system.

The program was completed in 16 months scheduled in four phases as illustrated in figure 3.

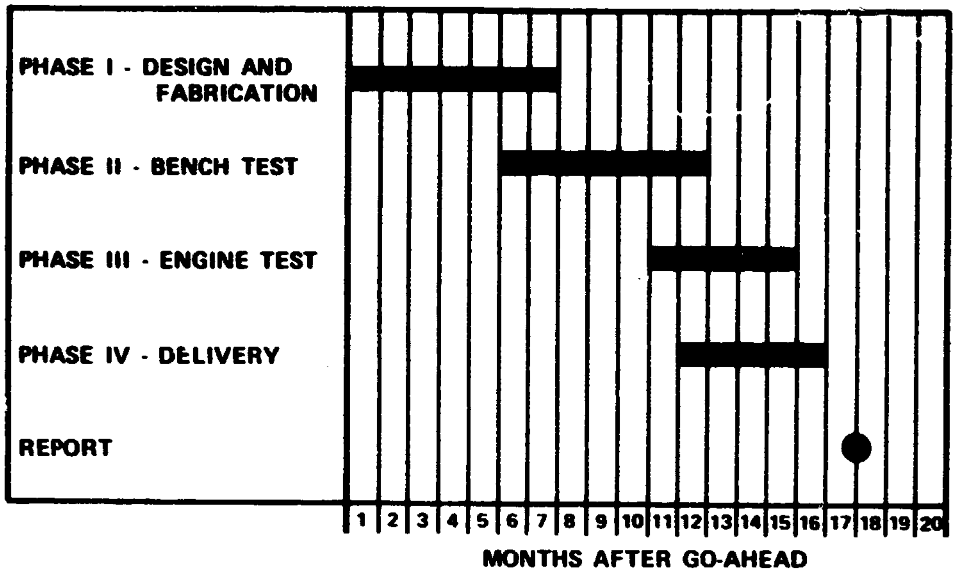

Figure 3. TIGT Measurement System Program Schedule FD 76207

SECTION II

PHASE I: DESIGN AND FABRICATION

A. REQUIREMENTS

Design and Fabrication of the Turbine Inlet Gas Temperature (TIGT) Measurement and Control System was accomplished using procedures and criteria for J58 engine control system components combined with those established during the Advanced Hybrid Propulsion Control System Program for the fluidic and electronic components.

The system configured to provide the functions required of a high response Turbine Inlet Gas Temperature Measurement and Control System is shown schematically in figure 4.

The design criteria and performance requirements were as follows:

1. Flight Suitability: Complete the equivalent of a Preliminary Flight Rating Test on a J58 engine.

2. Environmental Temperature

   a. Hot gas sampling probe - up to 2300°F
   b. Fluidic sensor - up to 2200°F
   c. Pressure sensor - -65 to 500°F
   d. Interface selector - -65 to 165°F
   e. Electronic control - -65 to 165°F

The performance goals for the TIGT system were as follows:

1. Steady State

   a. Accuracy ±40°F
   b. Repeatability ±20°F

2. Transient (step change of 200°F or less)

   a. Indicate 95% of a step change after 0.1 second
   b. Indicate 99% of a step change after 3 seconds
   c. Indicate within steady-state tolerance after 15 seconds

3. Transient (step change of greater than 200°F)

   a. Same as for step less than 200°F except indicate 99% after 7 seconds.

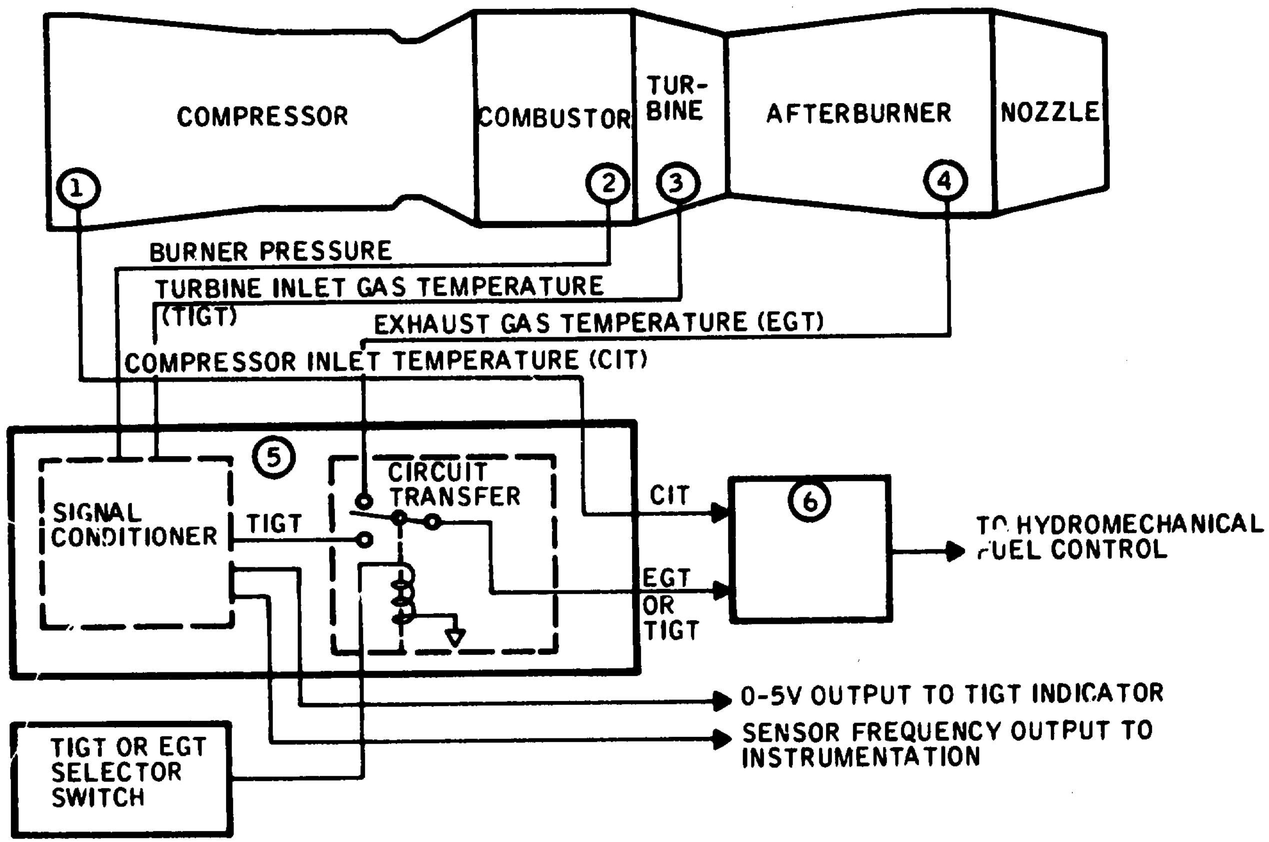

1. THERMOCOUPLES
2. STATHAM PRESSURE GAGE
3. HONEYWELL TG1009 TEMPERATURE SENSOR
4. THERMOCOUPLES
5. HONEYWELL DG1023 INTERFACE SELECTOR
6. HONEYWELL CG319 EGT VERNIER TRIM CONTROL

Figure 4. TIGT Measurement and Control System Block Diagram

The control part of the system utilizes the existing J58 engine Exhaust Gas Temperature (EGT) Vernier Control. The J58 EGT Vernier Control operates as a steady-state trim device in response to chromel alumel thermocouple signals for compressor inlet temperatures (CIT) and Exhaust Gas Temperature (EGT) each with a time constant of about one second. In order for the TIGT indicated signal to be compatible with a steady-state trim control and meet the very demanding response requirements, two outputs were selected. The two outputs were configured such that the slow response control signal had a range of 22 to 38 millivolts and fast response indicating signal had a range of 0 to 5 volts. A third output of TIGT sensor frequency was also included as part of the electronic interface selector. A combustor pressure bias was required to eliminate detrimental heat transfer effects on the sensor and and probe. To be compatible with the existing YF-12 system, means to select either EGT or TIGT control is required. The selector function is included in the electronic circuitry and is positioned by an external switch closure.

B. HOT GAS SAMPLING PROBES

The function of the hot gas sampling probe is to extract a sample of the combustion gas and deliver it to the fluidic sensor with no more than 10°F temperature change. Design of the hot gas sampling probe was initiated with a materials survey and selection. The criteria for selection of the probe material was that it operate for 60 hr in a 2300°F oxidizing environment at 0.3 to 0.45 Mach number and 225 psia with 9 g vibrational load. B-66 columbium with a silicide coating met all the requirements and was available through commercial channels. Several materials met many of the requirements but had some deficiency or shortcomings as listed below:

Columbium Alloy WC3015	- medium oxidation resistance and no available coating process
Silicon Carbide	- poor oxidation resistance between 1800°-2100°F
Beryllide of Tantalum	- poor low temperature ductility
Tantalum Alloy T-222 with coating	- poor oxidation resistance if coating fails
Beryllium Oxide	- low tensile strength, toxic and hydrates between 1800°-2100°F
Aluminum Oxide	- brittle and poor thermal shock resistance
Molybdenum Silicide	- poor thermal shock resistance
Silicon Nitride	- hydrates at ambient temperature
Boron Carbide	- low thermal shock resistance and incomplete development
TD Cobalt Alloy	- incomplete development and nonavailable.

Welding of B-66 is an uncertain process and past experience in the Hybrid Control Program indicated that some scrappage would occur. However, this deficiency was offset by the favorable experience gained at P&WA in experimental programs using this material and therefore it was selected as the hot gas sampling probe material.

A requirement of the program was to develop a J58 hot gas sampling probe for flight test and to design a TF30 sampling probe that could be incorporated in that engine during future testing. The fluidic sensor interface of each probe was identical so that the sensor developed for the J58 could also be used in the TF30 during future testing.

The TF30 probe design criteria differed only in configuration from the J58 probe. The J58 being cantilever mounted from the engine outer case and TF30 probe recessed mounted on the fan duct inner liner. The design of the J58 probe and its installation are presented in figure 5. The TF30 probe and sensor installation is shown in figure 6. Six J58 and two TF30 probes were fabricated for use in the experimental portion of the program. A photograph of the J58 probe after machining and before silicide coating is presented in figure 7.

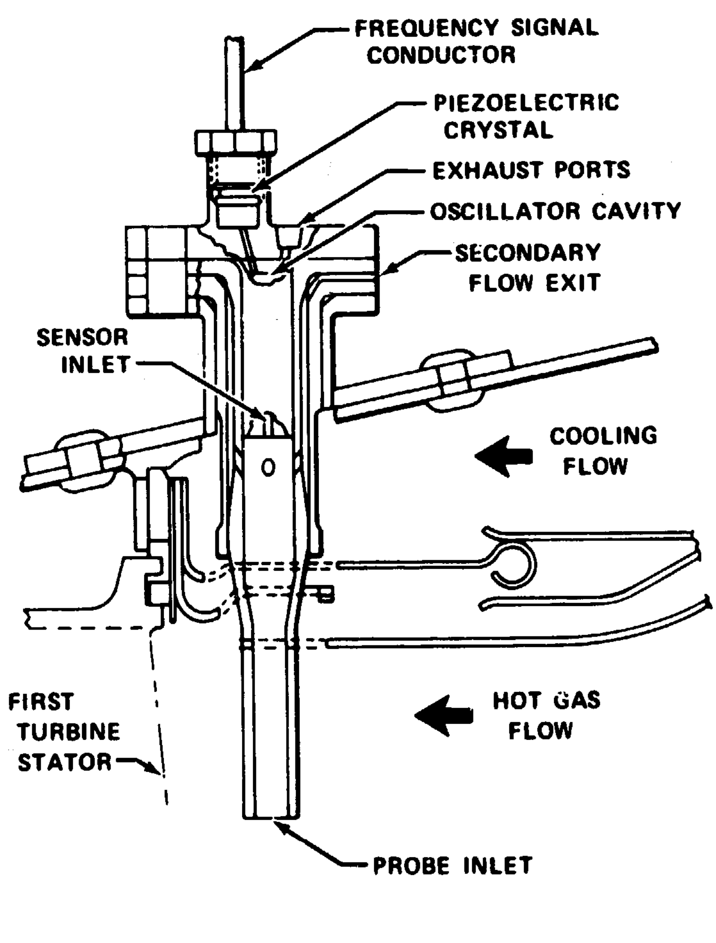

Figure 5. J58 TIGT Probe and Sensor Installation FD 74956

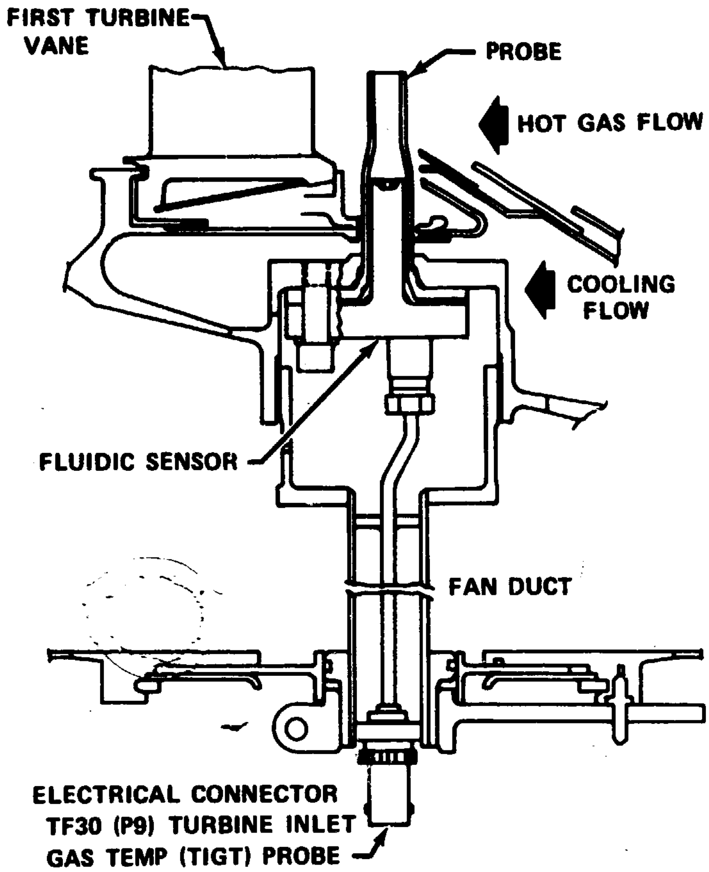

Figure 6. TF30 TIGT Probe and Sensor Installation FD 74969A

C. FLUIDIC TEMPERATURE SENSOR

1. Description

The TIGT sensor (Honeywell P/N TG1009) is an acoustic oscillator having an output frequency proportional to the square root of the average gas temperature. It is a flow-through device requiring a pressure differential, inlet to exhaust, to drive the gas through it and force oscillation. Figure 8 is a cutaway view showing major parts of the sensor. Gas enters the sensor through a slot nozzle, impinges on a splitter that excites acoustic oscillation, passes through resonant length cavities that amplify oscillation and exhausts through orifices.

The acoustic pressure signal is transmitted through a small passage to an acoustic cavity that is capped by a thin metal diaphragm. The diaphragm responds to the acoustic pressure wave and in turn excites a piezoelectric crystal. The piezoelectric crystal generates an electrical voltage when mechanically excited by the oscillatory pressure. This voltage is transmitted to the electronic converter by the electrode and lead wire that completes the fluidic sensor assembly.

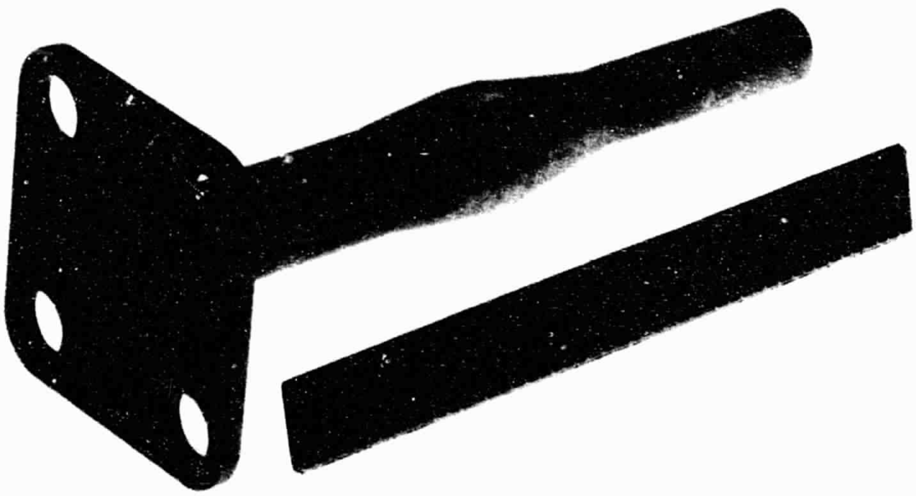

Figure 7. J58 Probe Before Silicide Coating FE 123560

Operation of the fluidic oscillator is described by the equations

$$f = K(\gamma RT)^{1/2} \tag{1}$$

for steady-state and by the transfer function for dynamic response

$$\frac{\text{Output}}{\text{Input}} \frac{[O(S)]}{[I(S)]} = \frac{K_1}{1 + \tau_1 S} + \frac{K_2}{1 + \tau_2 S} \tag{2}$$

In these equations,

f = output frequency

K = constant

γ = ratio of specific heats

R = gas constant

T = absolute gas temperature

K_1, K_2 = gain factors, $K_1 + K_2 = 1$

τ_1, τ_2 = time constants

S = Laplace transform operator

Values of various parameters are given in the section on Sensor Characteristics.

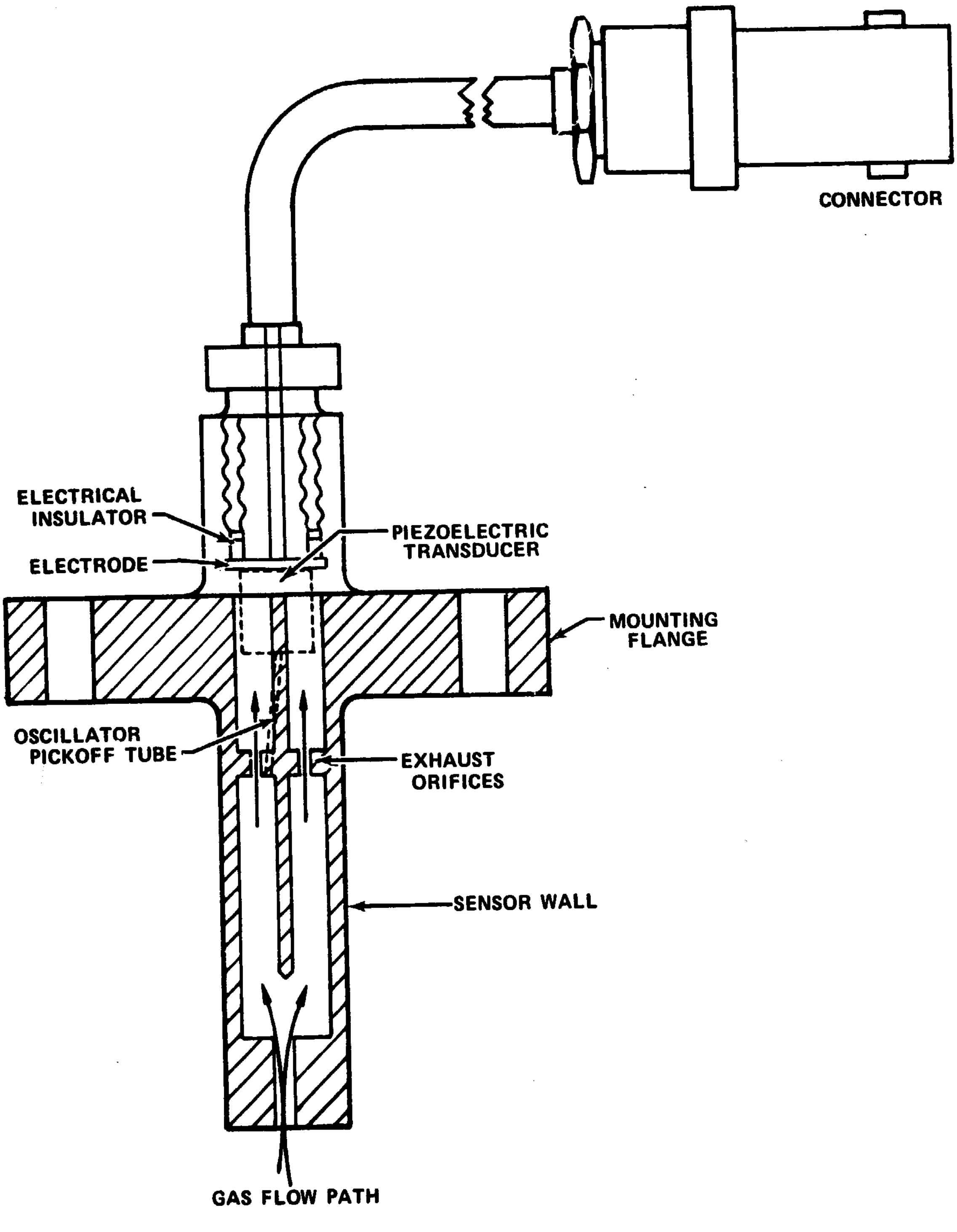

Figure 8. Cutaway View of Temperature Sensor FD 81180

2. Installation Requirements

The TIGT sensor design features are as follows:

1. Sensor mounting flange with four bolt holes in a rectangular pattern

2. Sensor body outside diameter compatible with the 0.355/0.350-inch probe inside diameter with nominal 0.010-inch clearance

3. Sensor body to mounting flange transition radius compatible with the 0.110/0.100-inch probe transition radius; provide maximum strength possible within this constraint

4. Sensor leadwire and sensor exhaust passage compatible with engine-installed envelope and environment

5. Sensor body and mounting flange materials compatible with probe material thermal coefficient of expansion.

3. Performance Requirements

Fluidic temperature sensor performance including accuracy and response are determined by the following:

1. Inherent design characteristics

   a. Size and mass of sensor
   b. Sensor material
   c. Size of flow passages, inlet and exhaust orifices

2. Installation effects

   a. Sensor mounting configuration
   b. Nature of flow around sensor
   c. Temperature and geometry of sensor mounting flange surroundings
   d. Thermal conductivity of surrounding material.

The inherent design characteristics are dependent on other performance requirements such as temperature capability, strength and life, and ruggedness and reliability. (Installation effects are largely fixed by design constraints of the application.)

The design requirements for sensor durability were as follows:

1. Sensor inlet temperature: 1500 to 2200°F

2. Ambient temperature: 1250°F

3. Sensor inlet pressure: 20 to 125 psia

4. Ambient pressure: 0.5 to 25 psia

5. Sensor life: 50 hours at 2200° F, 125 psia sensor inlet conditions

6. Vibration: Sensor operation with vibration as in MIL-STD-810B, figure 514-2, curve H with 13-1/2 g's substituted for 10 g's.

Accuracy and response performance were specified for the system and not for the sensor as a component. The sensor design, however, was directed at maximum accuracy and response possible within design constraints of above specifications.

4. Sensor Characteristics

In the steady-state, fluidic temperature sensor accuracy is affected by known characteristic errors. The most significant of these errors is caused by heat loss from the sample gas to the sensor walls as it flows through the device. This loss is dependent on the mounting configuration and installation of the sensor. An additional error is an inherent sensitivity to changes in pressure differential across the device and to changes in pressure level. For the sensor installed in a hot gas sampling probe (figure 5) steady-state accuracy of the sensor is influenced by heat losses to the probe and surroundings that vary with pressure differential and pressure level, i.e., sample gas flowrate and density. An illustration of the effect of sensor inlet pressure on sensor output frequency, when installed in a hot gas sampling probe is presented in figure 9.

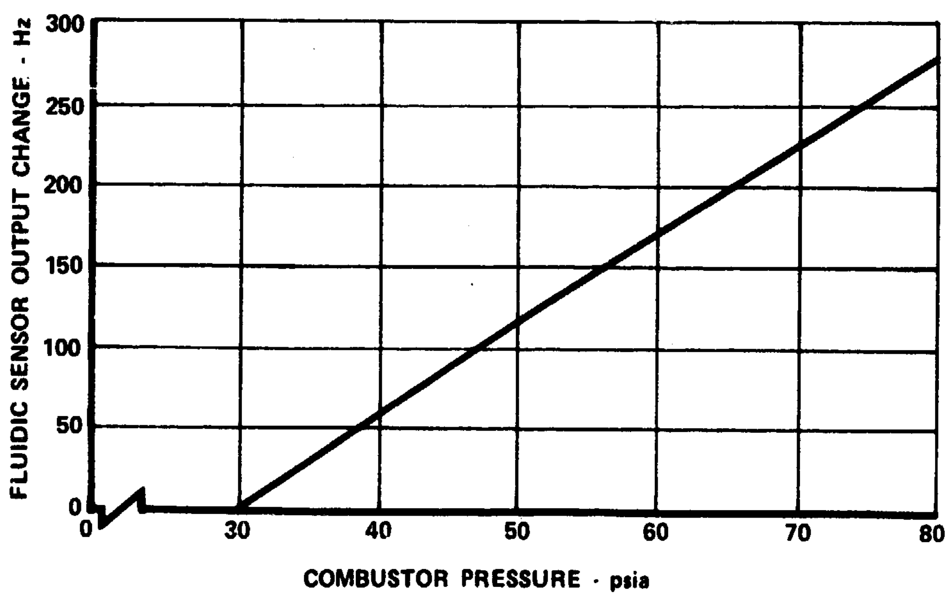

Figure 9. Pressure Bias of TIGT Sensor Output FD 81181

Transient response characteristics of a fluidic temperature sensor subjected to a step temperature change are determined by the amount of time required to flush the sensor cavity and to warm the sensor walls to an equilibrium temperature. The transfer function

$$\frac{O(S)}{I(S)} = \frac{K_1}{1 + \tau_1 S} + \frac{K_2}{1 + \tau_2 S} \tag{3}$$

expresses performance (figure 10). Assuming a sensor mounted with the oscillator body immersed in the hot gas, typical values of the parameters are:

$K_1 = 0.6$ to 0.7, $K_1 + K_2 = 1$

$\tau_1 = 0.02$ to 0.03 sec

$\tau_2 = 3$ to 6 sec

with the variations due to pressure effects. This performance is illustrated qualitatively in figure 11 by the curves labeled sensor only. For the sensor installed in the probe, the response is influenced by additional flushing time and thermal inertia of the probe and surroundings. The performance for this installation is illustrated qualitatively in figure 11 by the curves labeled sensor/probe. The additional probe effects tend to reduce the value of K_1 and increase the value and range of the constant τ_2. Interface electronics have been designed to compensate for these response errors as a function of pressure such that system requirements are met.

In the initial design phase, sensor/probe performance parameters and a range of possible values were estimated to permit design of interface electronic compensation circuits.

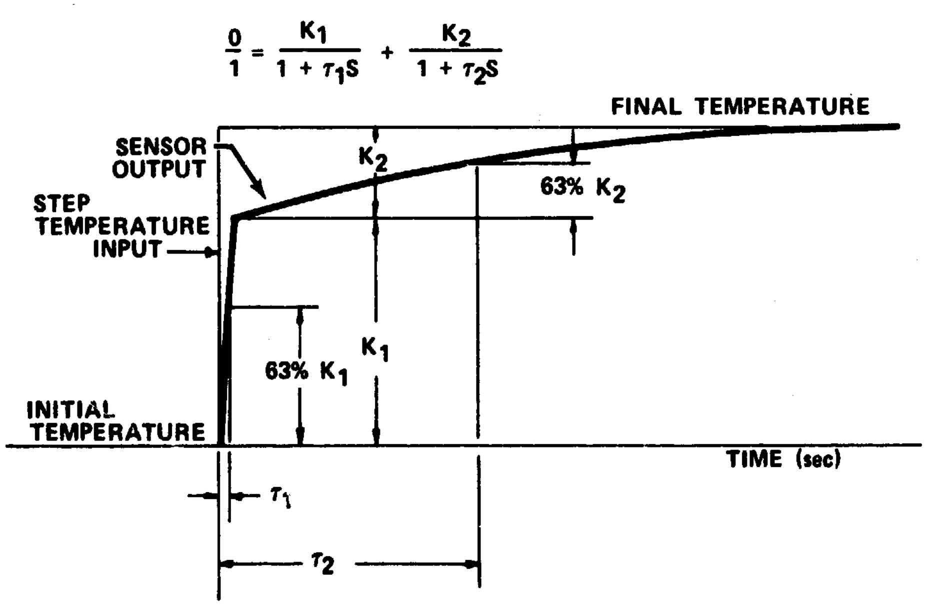

Figure 10. Transfer Function Definition - TIGT Sensor FD 81182

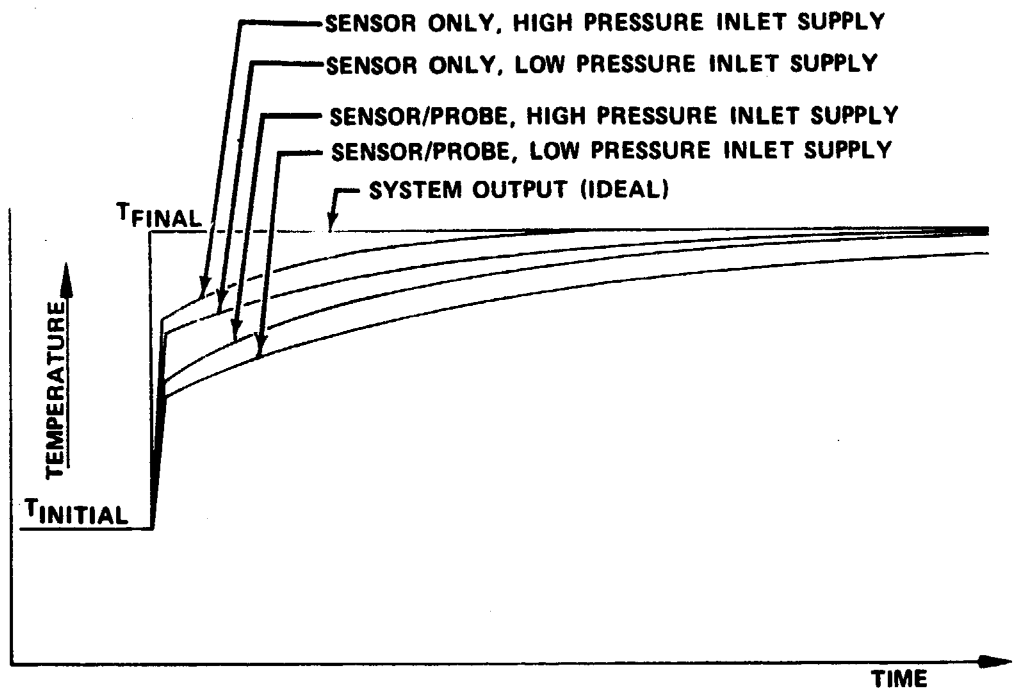

Figure 11. Transient Response Characteristics - TIGT Sensor FD 81183

5. Materials Selection

A requirement of the program was to survey candidate materials and select a suitable material for the sensor. Based on test experience of other programs as well as special tests conducted as part of the proposal effort for this program, thorium dispersion strengthened nickel chromium alloy with aluminum (TDNiCrAl) was selected as the material for sensor fabrication. Selection criteria included sensor performance specifications together with requirements of availability, machining, and fabrication.

The criteria for the fluidic sensor material selection was as follows:

1. Vibration as specified in MIL-STD-810B, figure 514-2, Curve H with 13-1/2 g's substituted for 10 g's

2. Sensed temperature level to 2200°F with ambient temperature 1250°F

3. Oxidation resistance to give 50 hour life capability at max temperature operating condition

4. Material compatibility with the probe material (B66)

5. Geometric configuration compatible with a 0.350 inch inside diameter.

A survey was made of past in-house Honeywell materials development and fluidic sensor development programs, NASA and Air Force development programs and Pratt & Whitney Aircraft materials development programs and a list of candidate materials compiled.

The materials considered and applicable comments are listed below:

1. KT Silicon Carbide - Poor thermal shock resistance excessive brittleness and special design for assembly required

2. Diborides - Requires metal support for strength and special features for mounting transducer

3. Chrome 90 - Excessive brittleness

4. Hastelloy Alloy X and Alloy S - High oxidation rate causing low life at 2200°F

5. TDNiCr - Excessive oxidation around bond joints at 2200°F

6. TDNiCrAl - Selected on the basis of (1) acceptable oxidation resistance, (2) tensile strength, (3) sensor/probe assembly requirements, (4) machineability, (5) fabricability, and (6) rough stock availability.

Figure 12 shows a sample of TDNiCrAl material following burner rig testing of 8 hr at 2000°F and 4 hr at 2200°F (TIGT sensor design point) with chamber pressure at 115 psia. The material loss during this test was 0.0002 grams.

6. Sensor Design

Design of the fluidic sensor was divided into three interrelated parts: (1) acoustic oscillator, (2) piezoelectric transducer, and (3) mounting flange. The acoustic oscillator used on the Advanced Hybrid Propulsion Control program (Reference 3) was used for the current program with a change in exhaust orifices. The piezoelectric transducer, a design developed at Honeywell for commercial gas temperature sensor programs, offered increased temperature capability over that of the Kistler Instruments Corporation devices used in earlier Honeywell development programs. The new design was sized to fit in approximately the same area as the Kistler units; however, it was designed as an integral part of the sensor allowing a lower device profile above the mounting flange. With these two parts of the sensor design established, the design integration into a unit was done concurrent with the mounting flange design and the prototype sensor design layout was completed. Areas receiving design emphasis were those that were identified as marginal or inadequate during the Hybrid Control Program. As shown in figure 8, these are as follows:

1. Transition section from the oscillator body to mounting flange

2. Sensor body wall thickness

3. Oscillator to transducer pickoff tube/sensor exhaust nozzle layout.

The first two resulted in a design with increased strength and ruggedness in critical areas. The latter resulted in a design permitting simplification of machining and assembly with complementary cost benefits. This prototype design evolved through the program test phases with only minor modifications to the final design as shown in figure 13.

7. Fabrication

The acoustic oscillator cavities and flow passages were fabricated using Electrostatic Discharge Machining (EDM) techniques, while remaining sensor piece parts were fabricated using conventional metal and ceramic machining techniques. The same procedures were followed in fabrication of: (1) one prototype unit for design and performance evaluation testing during Phase I design and fabrication, (2) four units for Phase II FRDC bench tests and Phase III: FRDC engine Preliminary Flight Rating Tests (PFRT), and (3) two units for Phase IV fabrication of flightworthy systems.

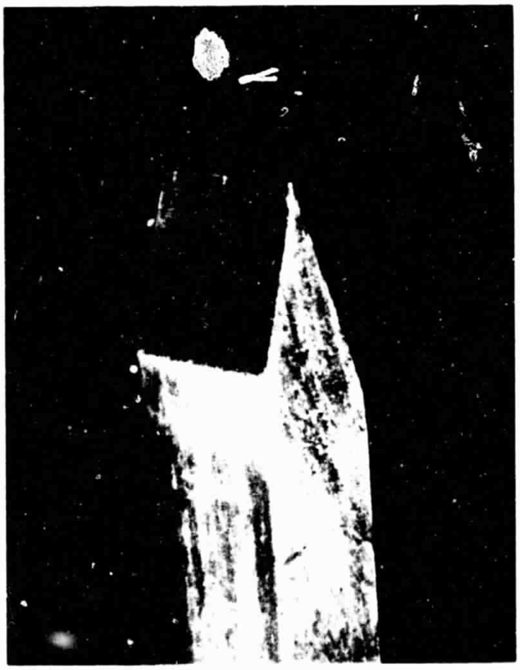

TDNi-CrAl AFTER TEST
4.5 TIMES ACTUAL SIZE

Figure 12. Fluidic Sensor Material Test Sample FD 74953

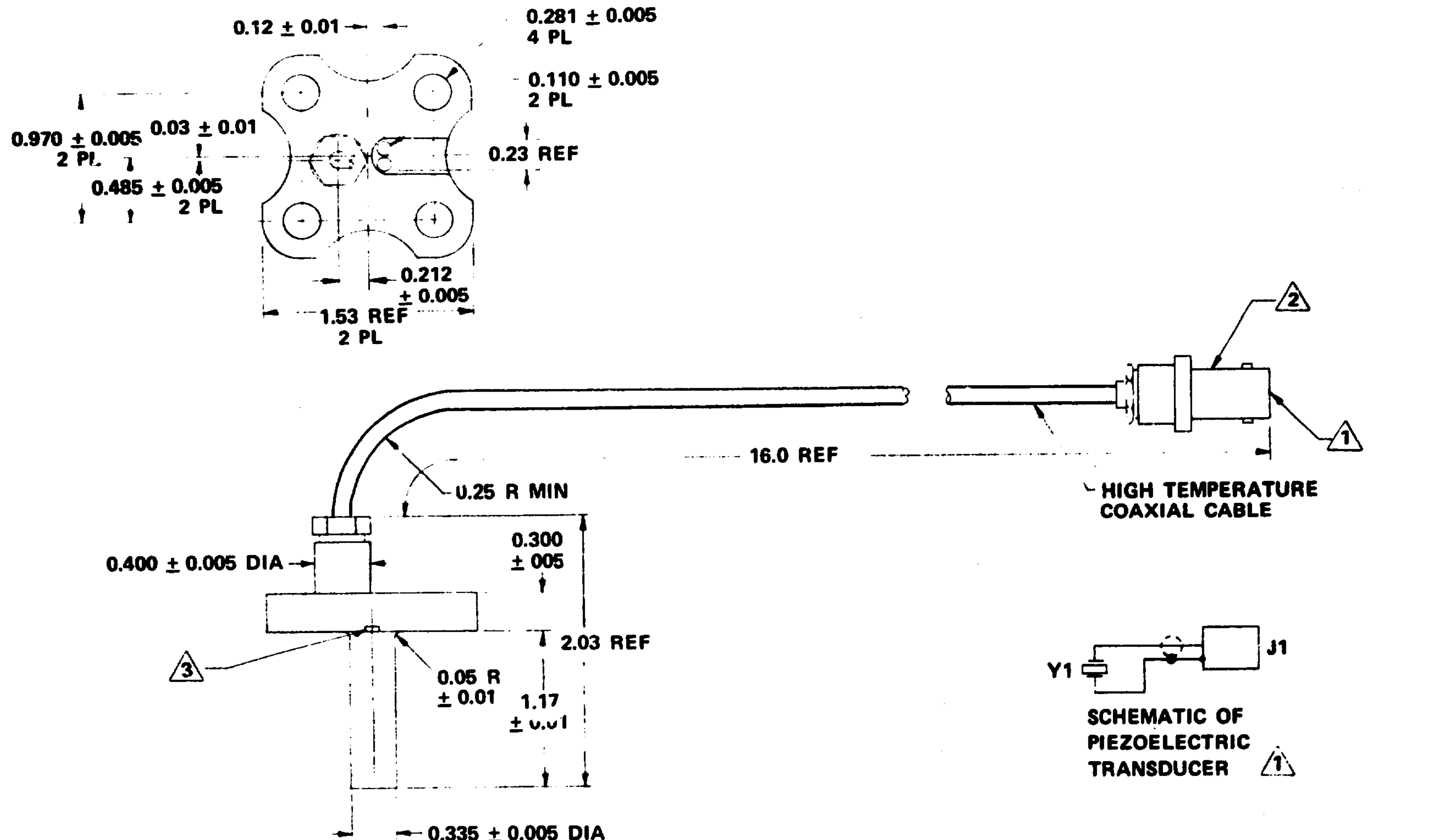

3 - 0.10 REF X 0.03 REF
SECONDARY AIR FLOW SLOT 3 PLACES

2 - TG1009 SERIES 2 CONNECTOR MATES WITH
KAMAN SCIENCES 850570-001 CONNECTOR
OR EQUIVALENT

1 - CONNECTS WITH UG88/U BNC CONNECTOR
OR EQUIVALENT

Figure 13. TIGT Sensor Installation Drawing

FD 81184

D. INTERFACE SELECTOR ELECTRONICS

1. Description

The Interface Selector (Honeywell P/N DG1023AA01) was developed on this program using the following general procedure. A breadboard model was constructed on which the electrical characteristics were studied and improved until they met program requirements. A prototype unit was then fabricated and packaged to the design criteria described in paragraph 3. This unit was tested for performance and durability and met program requirements with only minor component changes. Four units were manufactured and shipped during the program, two for Phase I and two for Phase IV. Based on results obtained during system bench testing and preliminary flight rating testing, the Phase IV hardware was calibrated to slightly modified requirements.

As shown previously in figure 4, the interface selector electronics provide signal conditioning circuitry for the temperature sensor and input selection means for choosing either the TIGT input or the EGT input for the trimmer (Honeywell P/N CG319A6). The outputs are TIGT/EGT, CIT, sensor frequency, and a 0- to 5-vdc signal of TIGT for possible indicator use. Means for selecting either the Exhaust Gas Temperature (EGT) thermocouples or the TIGT fluidic sensor (millivolt signal) for an input to the EGT trimmer is provided by a circuit transfer relay. The Compressor Input Temperature (CIT) thermocouples are routed through the box for interconnect convenience only.

The interface selector also has an input from a combustor pressure sensor. This input is used to compensate variations in both the steady-state and transient response temperature sensor performance parameters that vary as a function of the combustor pressure level.

2. Installation Requirements

a. Mechanical

The interface selector housing is approximately 7-1/2 in. long by 4 in. wide and 4 in. high. The unit is designed to be fastened down by four feet which have a hole pattern 4.75 x 4.75 in. between centers. The front panel contains five electrical connectors from the Bendix PT pigmy series. Four trim pots, R_1, R_2, R_3, and R_4 are also mounted on the front panel. These trim pots are used to match the box to a given temperature sensor and to change the TIGT output bias, pressure transducer zero and pressure transducer gain. Installation details are shown on the interface selector installation drawing, figure 14.

b. Electrical

The interface selector electronics contain five connectors used as follows: J1 contains power input, sensor frequency output, indicator output, and system grounds; J2 is the temperature sensor input; J3 is the pressure sensor input; J4 is the input for the EGT and CIT thermocouples; and J5 is for the output of EGT/TIGT signal and the CIT thermocouple. These signals are inputs to the EGT trimmer.

A TIGT measurement system interconnection diagram is shown in figure 15.

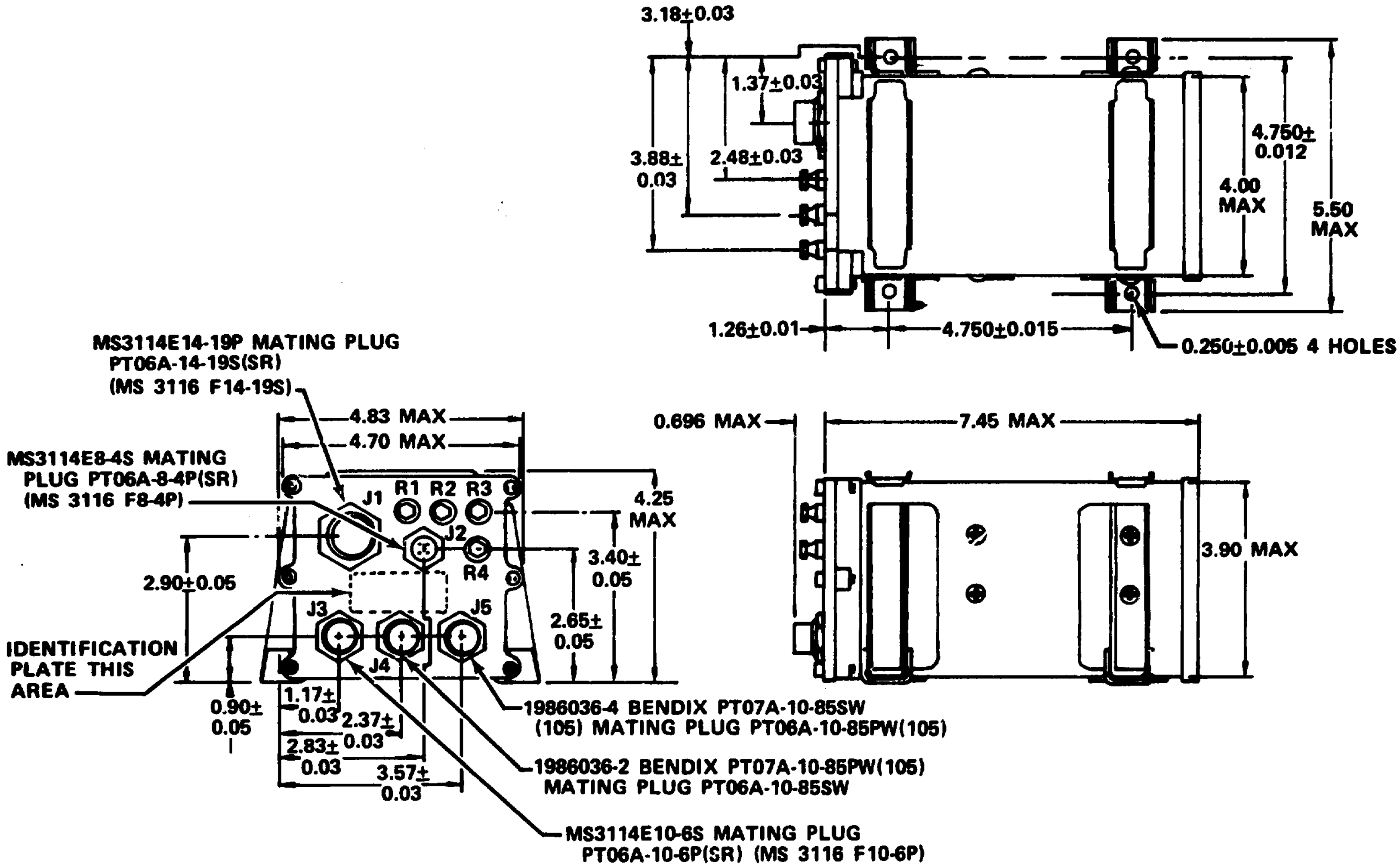

Figure 14. TIGT Interface Selector Installation Drawing FD 81186

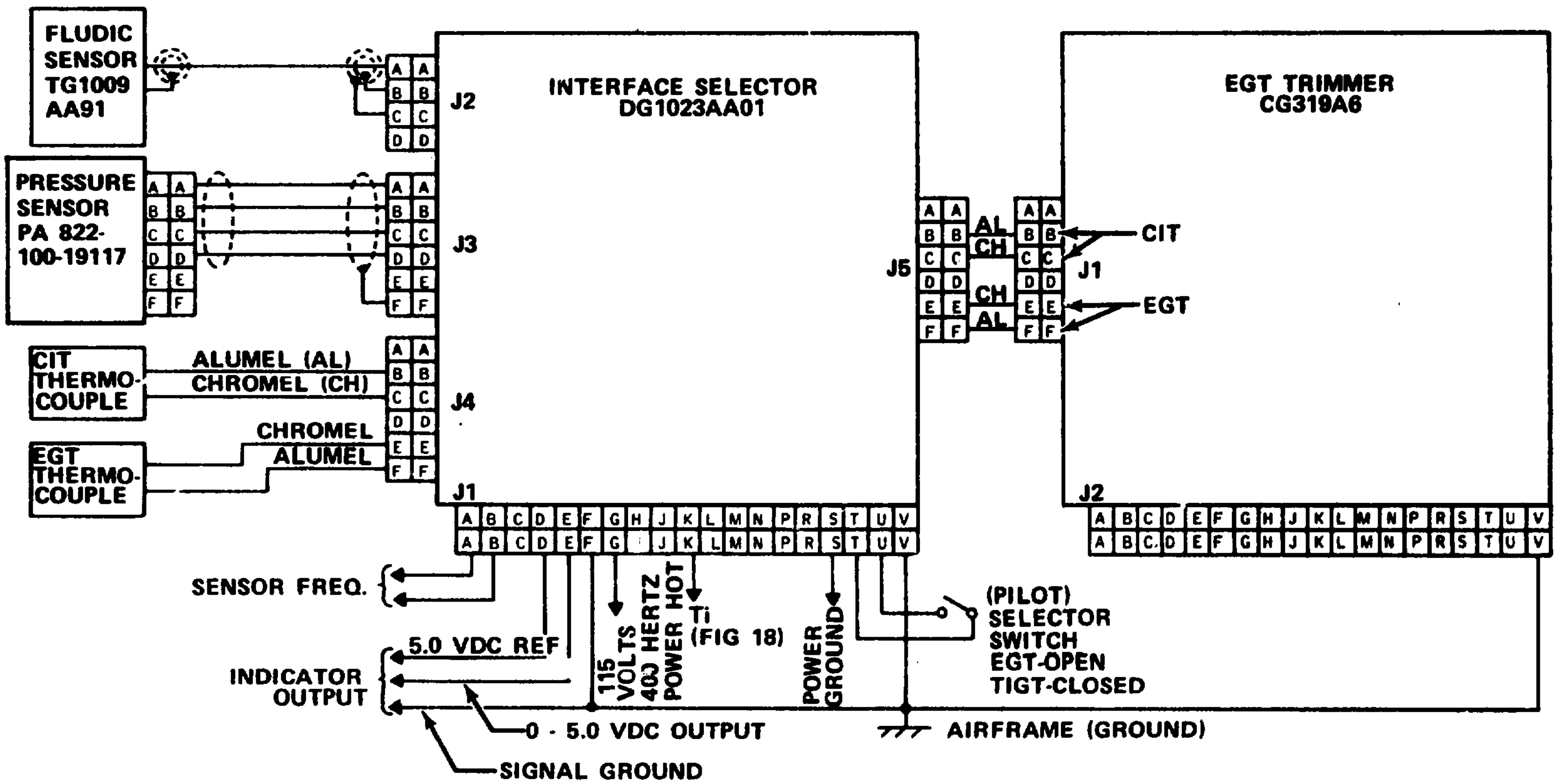

Figure 15. TIGT System Interconnect Diagram

FD 81187

3. Specifications

The interface selector performance specifications are as follows:

1. Range of operation inputs are:

   TIGT sensor = 1500° to 2200°F
   Pressure = 20 to 100 psia

2. Range of operation outputs are:

   Indicator = 0 to 5 volts
   TIGT = 21.95 to 38.14 mv

3. Ambient Temperature:

   -65°F to 160°F

4. Vibration:

   10g - 8 to 250 cycles

5. Accuracy: (Voltage versus frequency)

   ±20°F

6. EMI:

   MIL-I-6181
   MIL-E-5007

7. Power Input:

   115 volts, 400 Hz, 1 phase

8. Indicator Reference Voltage:

   5.00 ± 0.07 volts

9. Pressure Transducer Excitation Voltage:

   10.00 ± 0.10 volt dc

a. Steady-State Pressure Compensation

The fluidic sensor hot-gas sampling probe assembly is subject to heat transfer effects since the entire assembly cannot be submersed within the hot-gas stream. In addition to the heat transfer losses, the fluidic sensor operating frequency is a function of supply and cavity pressure since the speed of the wave propagating in the sensor cavity is a function of the gas density. This second effect of pressure is small when compared to the first and is estimated by some sources to be as low as 1% over the temperature range.

The electronic interface selector was designed to compensate for these pressure effects on the steady-state indicated temperature level. The system was designed so no steady-state compensation was made at 100 psia because this is the maximum pressure to which the system responds. The two development interface selectors Serial Numbers X1 and X2 steady-state compensation, based upon analytical studies initiated in the Hybrid Control Program, were 100°F at 2200°F and 77°F at 1500°F indicated temperature and sensed pressure of 20 psia. The form of compensation was linear with temperature and inverse with pressure. Bench tests, reported in Section III, of these two systems revealed that a more linear and larger compensation was required for the flight test systems.

The flight test systems, Serial Numbers W3 and W4, were calibrated to provide no compensation at 100 psia and 6 Hz/psia at 20 psia and no bias as a function of temperature level. This results in an addition of 480 Hz added to the sensor output at 20 psia sensed pressure.

b. Transient Compensation

The heat transfer effects described above also bias the system performance during temperature transients. This bias, described in paragraph C.4 and illustrated in figure 16 can be compensated as a function of the sensor input pressure. The two development interface selectors were calibrated for a τ_2; heat transfer time constant; of 6.6 sec at 100 psia and 11.0 sec at 20 psia. As shown in figure 10, the amplitude compensation K_2 selected was 0.33 or 50% amplitude added to the initial sensed change at all pressures. This selection was based upon transient tests conducted at Honeywell using a prototype sensor. Bench tests on the development systems at FRDC indicated the need for additional transient compensation. Experimental data are included in Appendix B.

The flight test systems were calibrated to provide a τ_2 of 7 sec at 100 psia and 35 sec at 20 psia. Amplitude compensation K_2 was increased to 0.5 or 100% amplitude added to the initial sensed change at all pressures. Bench test results of this configuration are presented in Section V.

1. Functional Description

Figure 17 is a photo of the interface selector chassis assembly, which shows the mechanical mounting of the four printed circuit card assemblies. One card is mounted below the chassis backbone and three above. Nine standoffs are used between cards to provide a rugged mechanical assembly. In addition, a "u" bracket between the top circuit board and second board down is bolted into the case to ensure that the top cards will be held from excessive swaying during shock and vibration.

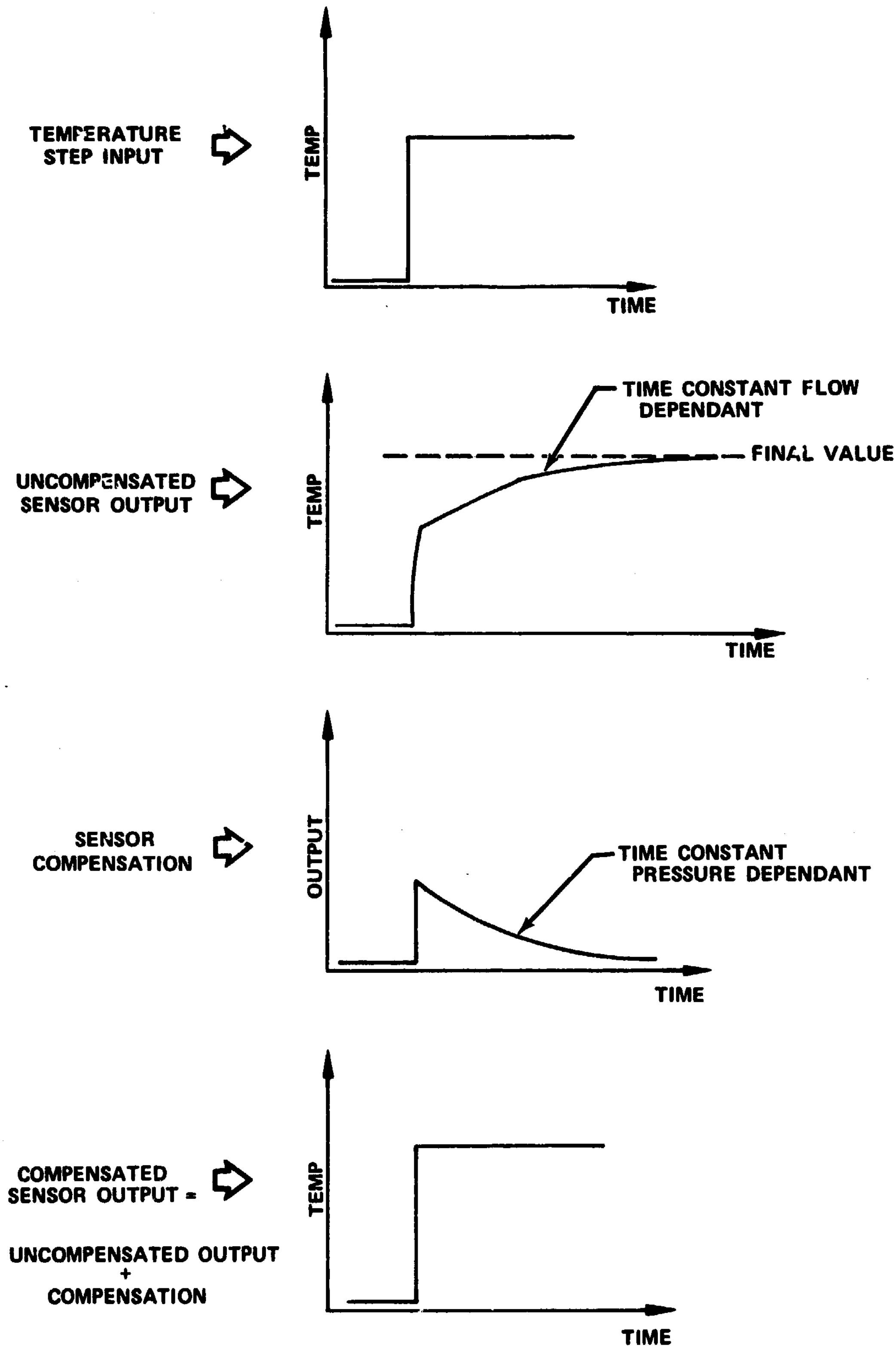

Figure 16. Illustration of Pressure Dependent Transient Compensation

FD 81183

Figure 17. Interface Selector Chassis Assembly

Figure 18 is a detailed block diagram of the interface selector. An input of 115v, 400 Hz, single phase power is used to develop the internal dc power supplies necessary to power the circuitry. The temperature sensor input is fed into a frequency-to-analog converter that converts the frequency to a dc voltage that varies between ±10 vdc to represent indicated temperature (Ti). The pressure sensor is excited by +10 vdc from the interface box. Output of the pressure sensor is a bridge type differential signal with approximately a 0- to 25-mv output that is fed into the pressure signal amplifier. The output of the amplifier is voltage analog (P_A) of pressure that varies from 0 to 10 vdc for 0 to 100 psia. The variable compensation computer accepts inputs of Ti and P_A and computes the compensation to bias the temperature sensor output. Scaling circuits are used to convert the temperature signal from between ±10 vdc to 0 to 5 vdc output for an indicator and 21.95 to 38.14 mv for a simulated thermocouple signal. The relay switching circuit provides the capability of selecting the EGT thermocouple or the TIGT simulated thermocouple signal. An open circuit connects the EGT trimmer with EGT and a closed circuit connects it with TIGT. Four adjustments provided for field calibration are shown on the block diagram (figure 18).

a. Frequency to Analog Converter

A block diagram of the frequency-to-analog converter is shown in figure 19. Input from the fluidic sensor is a frequency which varies approximately as the square root of the sensed temperature. This signal is amplified by a charge amplifier specially designed to detect the output of a crystal. It is designed as a bandpass amplifier with a range of 5,000 to 13,000 Hertz. The output of the charge amplifier is transformer coupled into a frequency-to-dc converter to provide ground isolation for the fluidic sensor. A phase lock loop (integrated circuit) is used to convert the input frequency to a dc output voltage. The output of the phase lock loop is amplified and fed into the two-slope linearization circuit. Internal adjustments are provided to set the zero voltage, low-temperature adjustment and high-temperature adjustment. The voltage analog output Ti is then fed into the variable compensation computer.

b. Variable Compensation Computer

The technique used to compensate for characteristics of the fluidic sensor is to simulate these characteristics in the feedback path of an operational amplifier. The voltage analog of temperature at the amplifier output then becomes a very good indication of the input temperature to the fluidic sensor. If characteristics of the fluidic sensor are accurately defined and simulated, the output will be accurate.

Figure 20 is a block diagram of the variable compensation computer. The basic ground rule followed in designing the fluidic sensor simulation was as follows: Ti = To at 100 psia pressure level; hence, the unit is calibrated to 100 psia curve and needs no correction to steady-state curve. The dynamic correction decays to zero after a sufficient length of time and contributes nothing to steady-state errors.

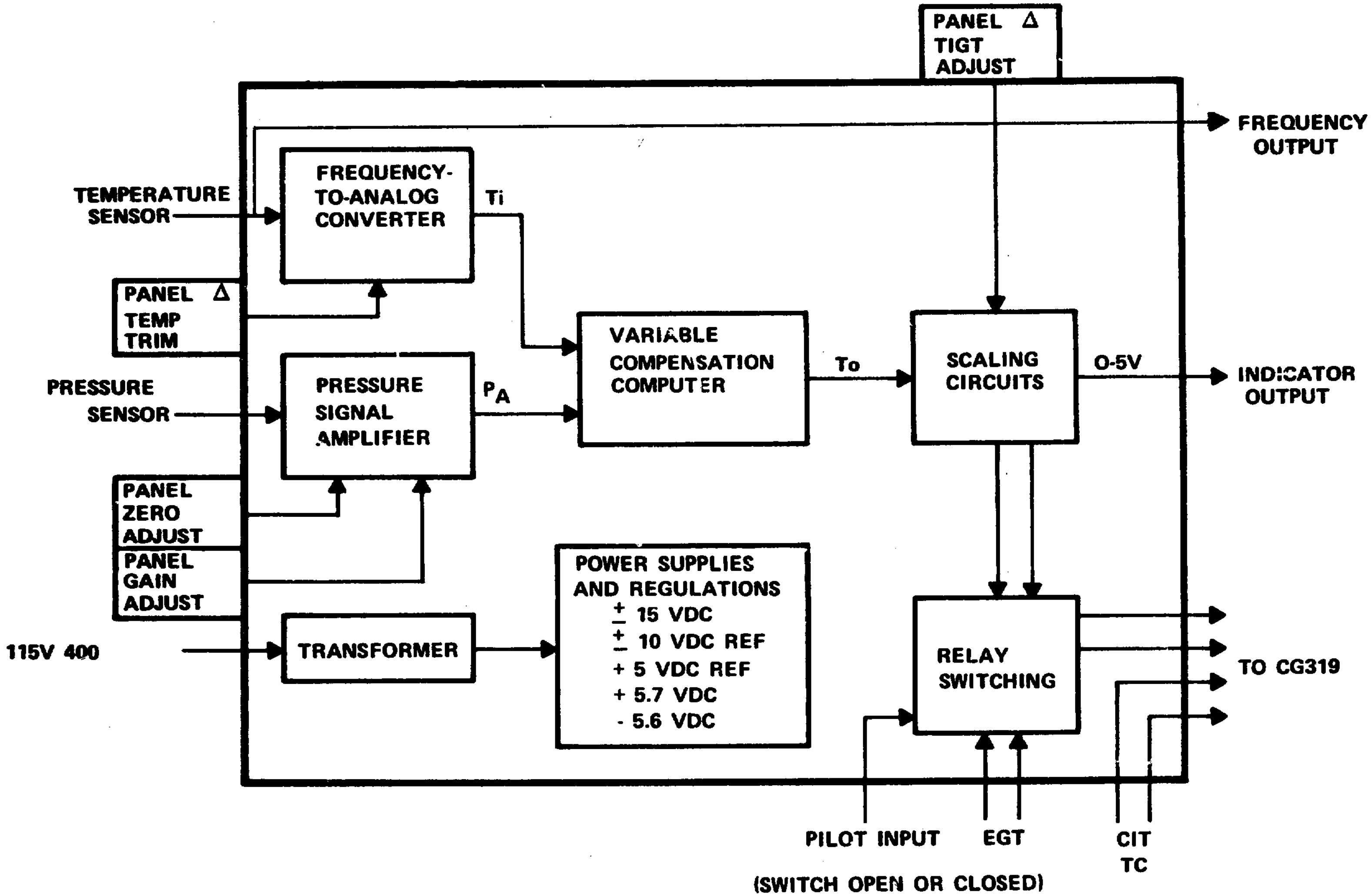

Figure 18. Interface Selector Block Diagram

FD 81188

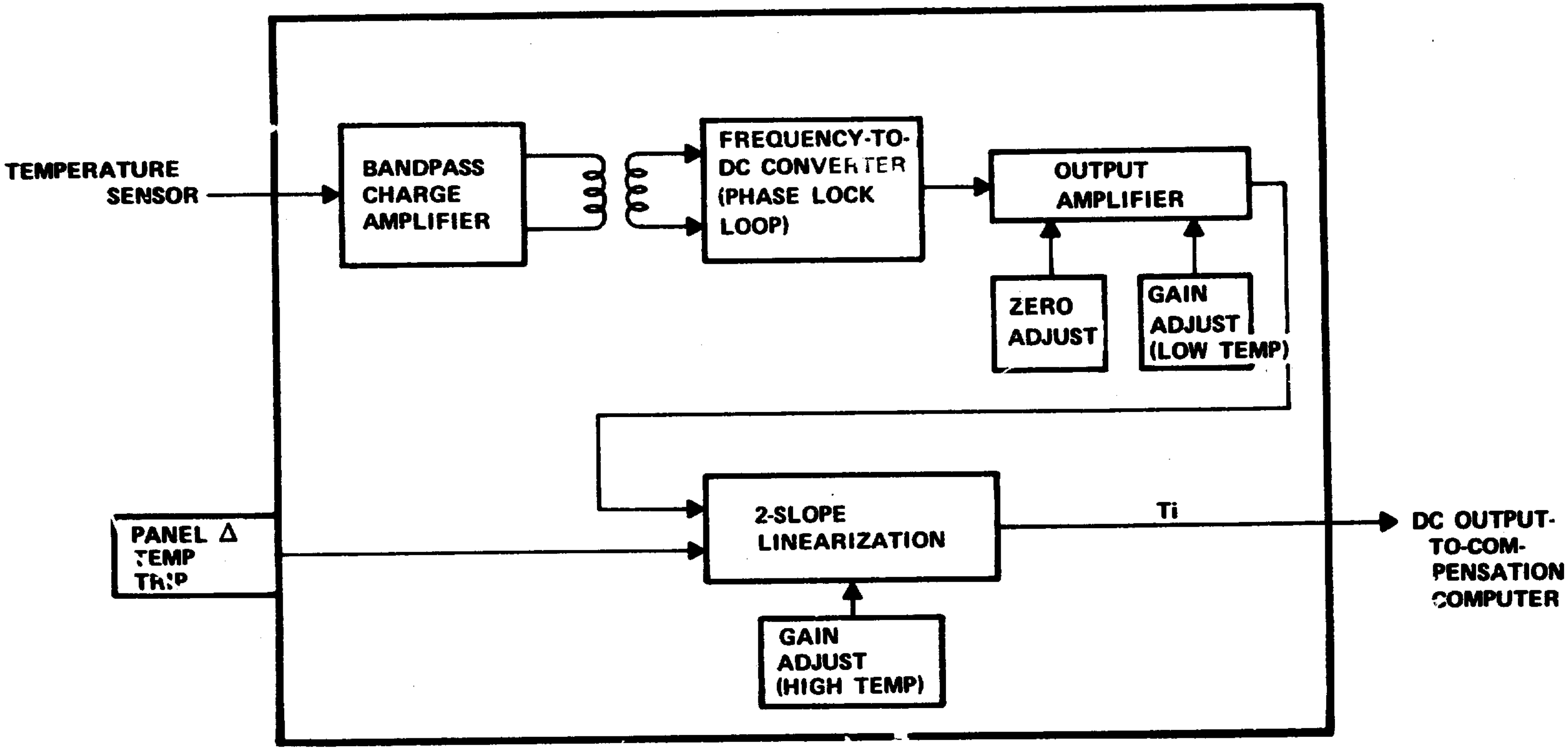

Figure 19. Frequency-to-Analog Converter Block Diagram

FD 81189

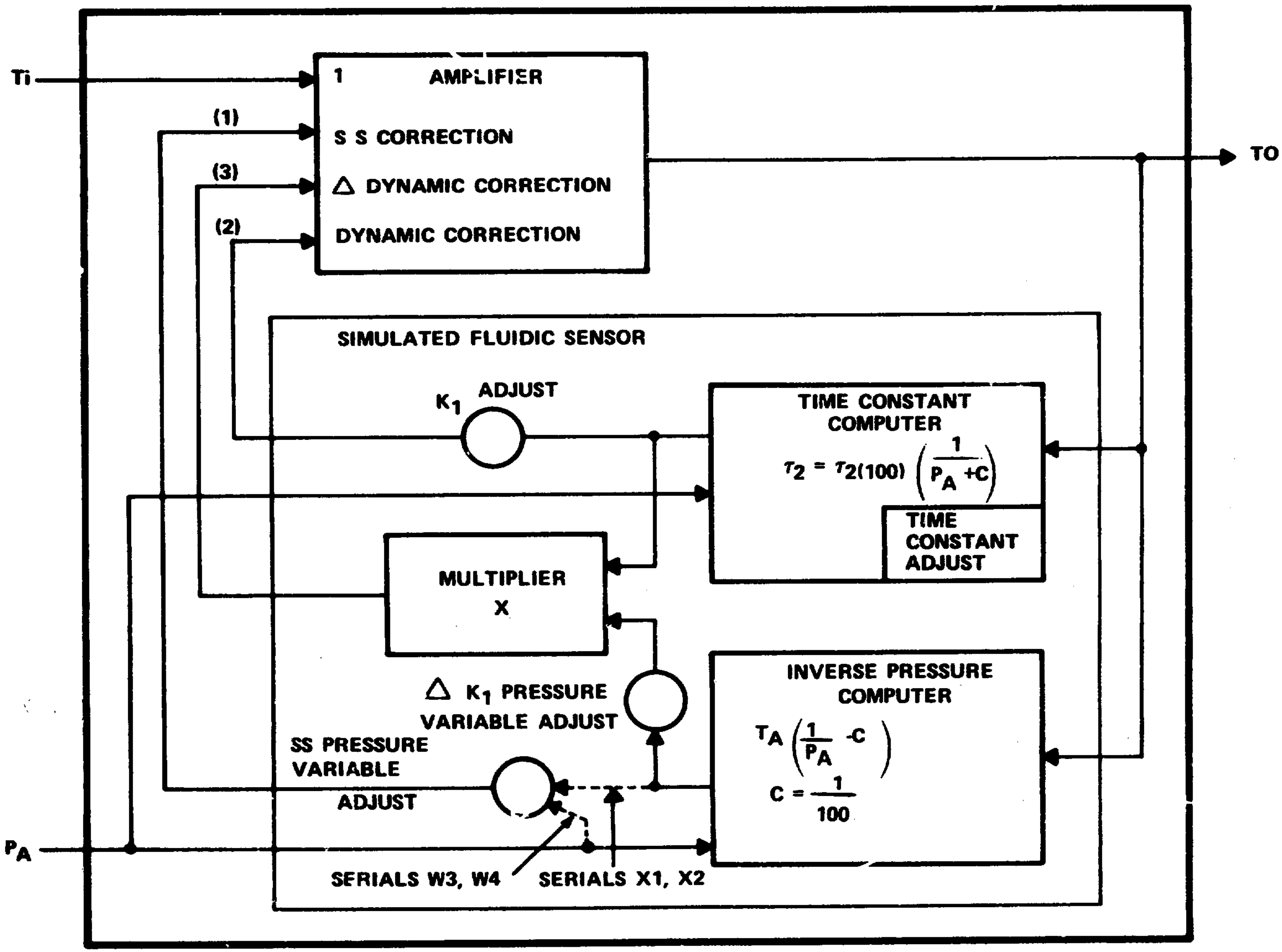

Figure 20. Variable Compensation Computer

FD 81190

Three compensation terms are summed at the amplifier input: (1) is the steady-state correction that varies directly with absolute temperature and inversely with pressure for serials X1 and X2 experimental units and linear (decreasing direction) with pressure for serials W3 and W4 flight test units; (2) this is the basic dynamic compensation that is varied as an inverse function of pressure (τ_2 is varied but the amplitude K_1 is not); and (3) this is the delta change in amplitude of the dynamic compensation and is varied directly with absolute temperature and inversely with pressure.

c. Inverse Pressure Computer

The inverse pressure computer accepts inputs of absolute pressure and measured temperature. The circuitry is mechanized to give an output of zero volt at 100 psia and a maximum output at 20 psia. The temperature input has relatively small authority and varies the output as a function of absolute temperature. Internal trim adjustments are available that can change the authority of both pressure and temperature inputs. The output of the inverse pressure computer is used to control both the steady-state correction and variation in amplitude of the dynamic correction (K_1). (Note: On serials W3 and W4, pressure controls steady-state correction directly.)

d. Time Constant Computer

The time constant computer consists of two amplifier circuits, a multiplier, and an integrator. These components are connected into a closed loop circuit to form a lead circuit. The time constant of the circuit varies inversely with loop gain. The gain of the loop can be varied in two ways, one by a trim pot used to set the basic time constant at 100 psia and the other by the pressure input to the multiplier.

e. Dynamic Compensation

The amplitude of the dynamic compensation at maximum pressure (100 psia) is adjusted by varying the K_1 trimpot. Since a higher amplitude of dynamic compensation may be needed at low pressure, a multiplier circuit was designed in to allow the amplitude to be varied as a function of the inverse pressure computer output.

SECTION III

PHASE II: TIGT MEASUREMENT SYSTEM BENCH TESTING

Bench testing of the TIGT measurement system consisted of component tests of the interface selector and temperature sensor by Honeywell, engine suitability tests of the J58 and TF30 sampling probes by P&WA and engine suitability tests on the TIGT System. These tests are described below.

A. J58 HOT GAS SAMPLING PROBE TEST

1. Vibration

A J58 gas sampling probe was subjected to 50 hr of heated (2300°F) vibration (3 g's) endurance.

The TIGT probe assembly (P/N 2167905 probe and P/N 2167908 sleeve) was installed in the test rig shown in figures 21 and 22. The resonant frequency was determined at 1 g input at the probe mount flange by observing the probe tip response. The resonant frequency was determined to be 1580 Hz at room temperature. A test vibration level of 3 g's was selected as shown in figure 23. The test piece was placed in an oven and heated to 2300°F while vibrating. The input vibration frequency was adjusted to keep the probe at resonance as the frequency changed with heat addition. The test included five thermal cycles with each cycle preceded by a resonance search. The probe appearance at these inspections was as follows:

1. At 10.5 hr, the probe was dark gray with a scale over about 30% of the area.
2. At 20.0 hr, the probe was dark gray at the tip and changed to a green yellow about 1/3 the distance toward the sleeve. Scaling was limited to the probe sleeve joint.
3. At 41 hr, the probe tip was green and dark gray and changed to reddish orange 1/3 the distance toward the sleeve.
4. A photograph of the probe after 50 hour test is shown in figure 24.

2. Performance Tests

The J58 hot gas sampling probe was subjected to tests to determine the steady-state and transient temperature loss due to heat transfer and airflow. A thermocouple was mounted in the probe with the sensing junction located at the same immersion depth as the fluidic sensor inlet. Fluidic sensor airflow through the probe was simulated by placing 0.050 in. spacers between the probe flange and the thermocouple flange. Steady-state tests results as obtained from rig testing are tabulated below and show little steady-state temperature error as measured by two thermocouples of the same material.

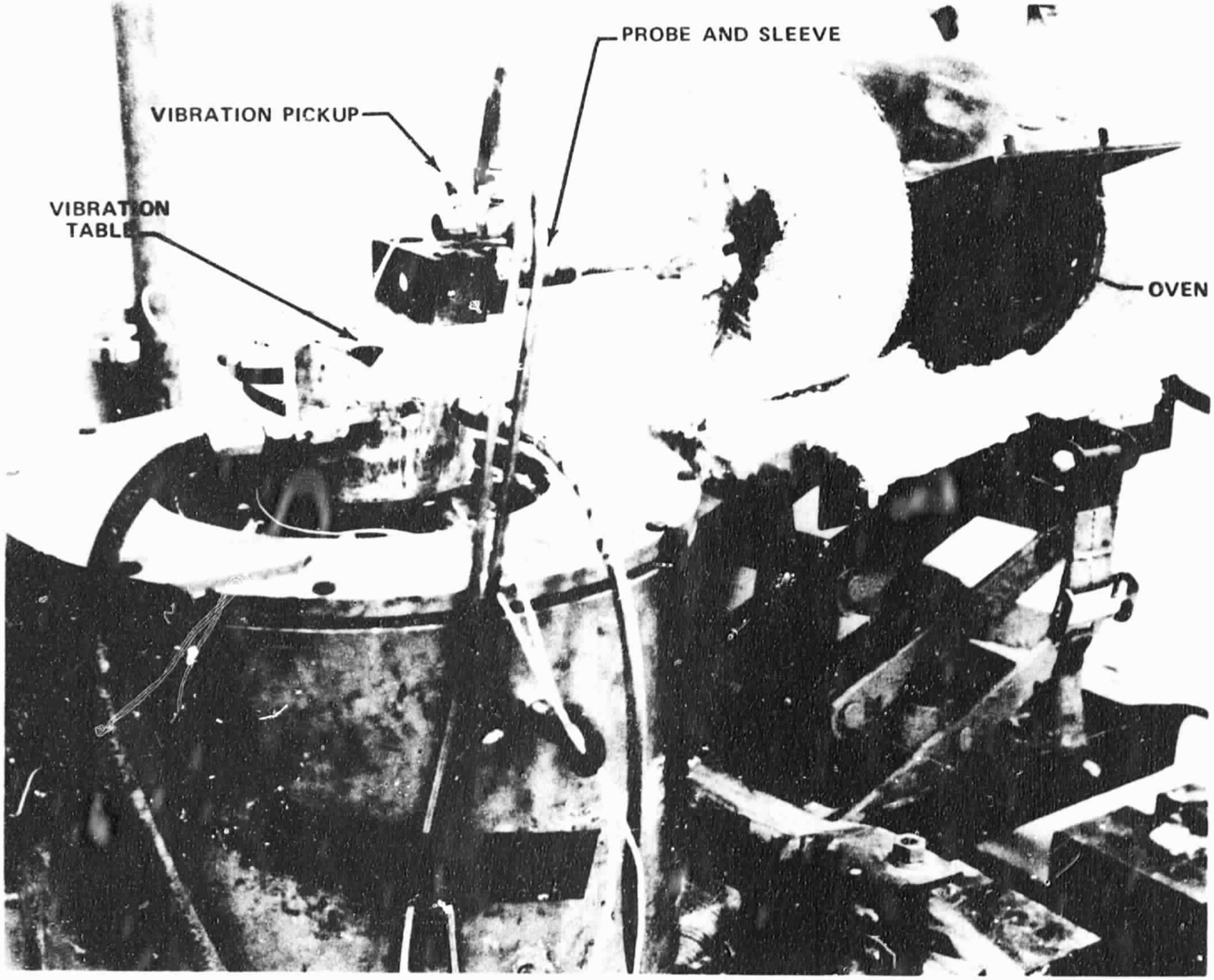

Figure 21. TIGT Probe Heated Endurance Test Setup

FD 81191

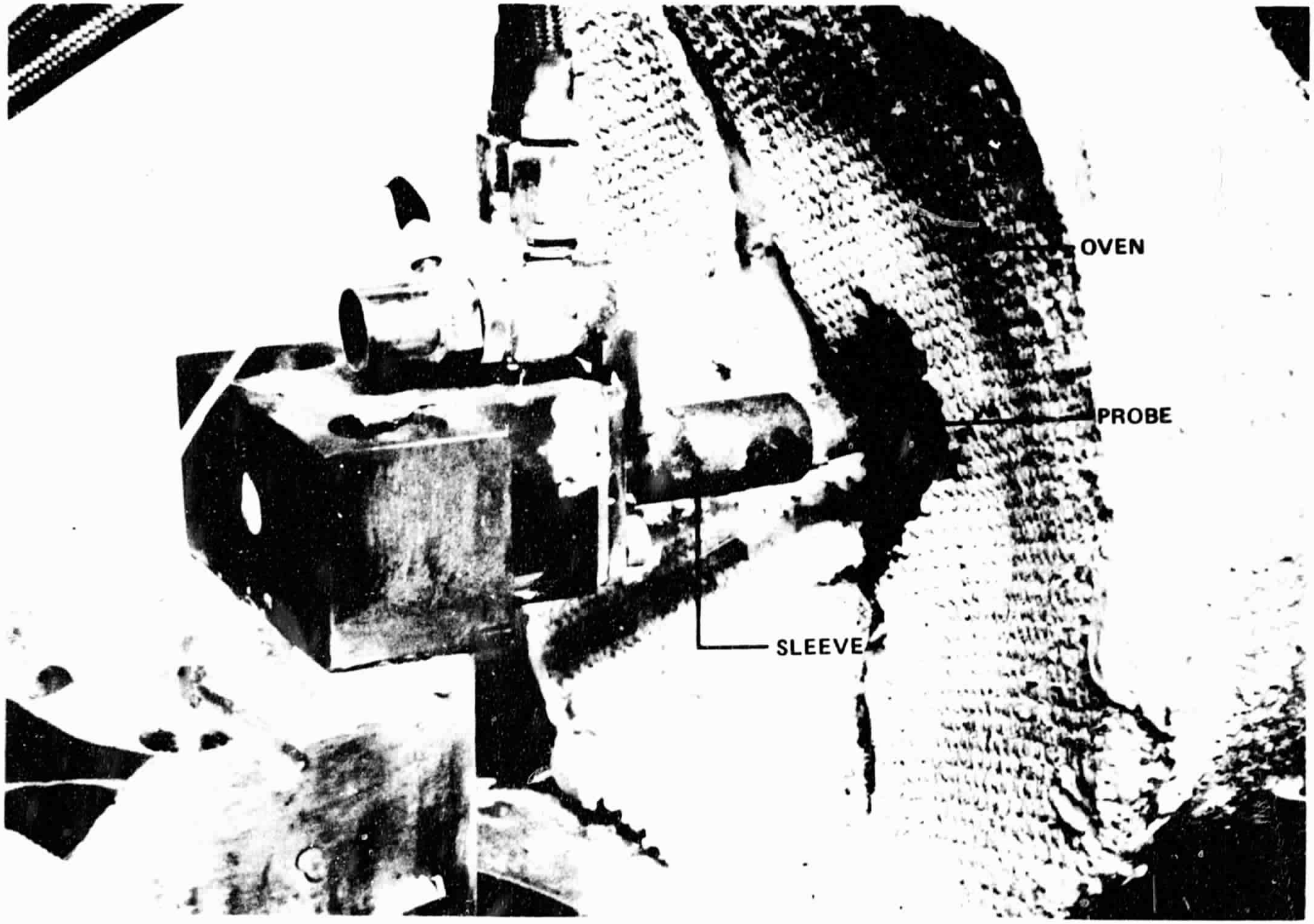

Figure 22. TIGT Probe Heated Endurance Instrumentation Detail

FD 81192

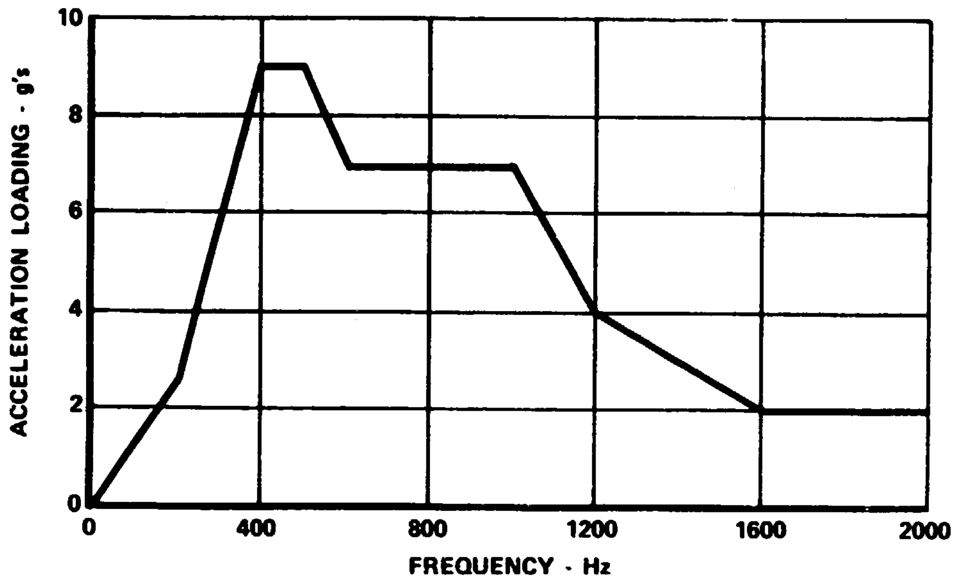

Figure 23. Tangential Plane Vibration - J58 Engine Turbine Case FD 76208

Set Point Temperature, °F	Sampled Gas Temperature, °F
1550	1550
1680	1700
1920	1900
2230	2200

Transient response tests were conducted by changing the fuel flow into a combustor rig. Slow transients (ramp inputs) were made by the rig operator manually regulating the fuel flow while rapid transients (step inputs) were made using a solenoid valve bypassing fuel flow upon command of the rig operator. These parts are illustrated in figure 37.

Tests were conducted with both slow changes and rapid changes in combustor temperature. The probe mounted T/C agreed with the burner mounted T/C within instrumentation accuracy throughout the test with a 6°F/sec input rate and a temperature change of 600°F. Therefore, for a ramp rate of 6°F/sec, the hot gas sampling probe contributes no identifiable error. The results of the probe tests when subjected to rapid temperature changes show a maximum error occurring 2 sec after the initiation of the disturbance. A tabulation of the probe response to a rapid temperature decrease is shown in table I. The thermocouples used for the tests were fabricated to the same design and have a response time of approximately 0.04 second.

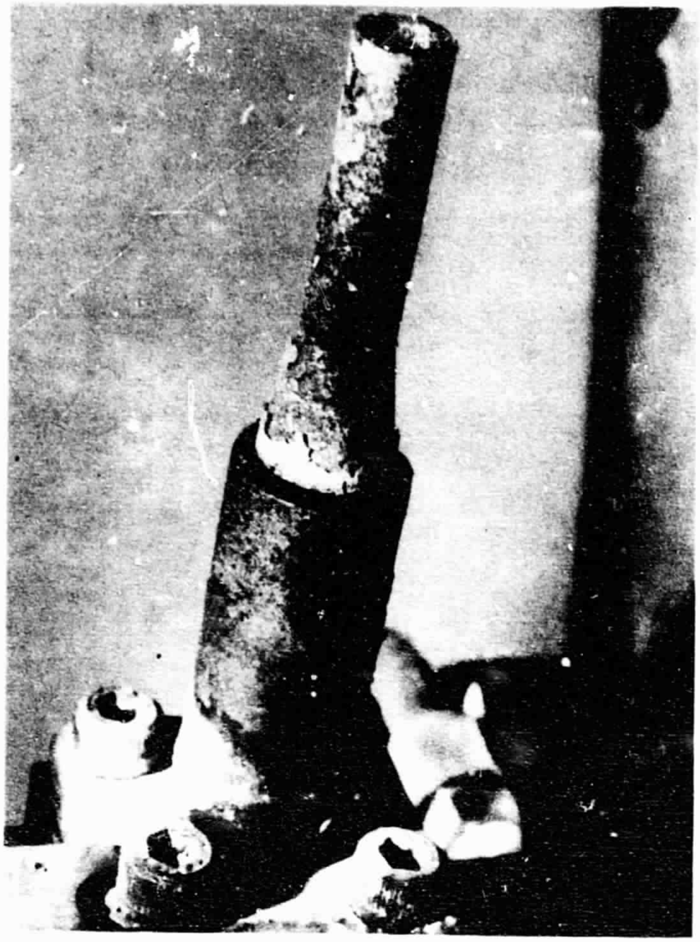

Figure 24. TIGT Probe After 50 Hour/2300°F Test FE 124408

Table I. Probe Response To A Rapid Temperature Decrease

Time, sec	T/C Burner, °F	T/C Probe	ΔT, °F
0	2300	2280	-20
.38	1960	2000	40
1	1940	1980	40
2	1770	1860	90
3	1715	1780	65
4	1650	1720	70
5	1590	1670	80
6	1580	1620	40
7	1580	1630	50
8	1560	1600	40
9	1510	1570	60
10	1510	1550	40
11	1540	1560	20

B. TF30 HOT GAS SAMPLING PROBE DURABILITY TESTS

The sample probe successfully demonstrated its design reliability and structural integrity by passing a 50-hr engine simulated vibration and temperature test. The probe was subjected to ±13 g's and ±15 g's excitation for 20 and 30 hr respectively at resonant frequency and 2300°F.

First bending mode (resonance) was determined at ambient temperature to occur at 2231 Hz. An acceleration gain of 21.0 existed between the mount flange and probe tip at this frequency. This resulted in a tip acceleration of ±210 g's and 800 micro in. double amplitude with ±13 g's excitation. At heated conditions, the frequency of this mode varied from 2129 Hz to 2473 Hz.

Excitation frequency was varied as necessary to maintain resonance of the probe. The majority of the 2300°F testing was done around 2300 Hz. A photo of the probe taken after completion of the 50-hr test is presented in figure 25. Part of the strain gage and its retaining cement is visible in the figure. The gage was used to ascertain resonance at temperature.

Figure 25. TF30 Probe After 50 Hour/2300°F Test FE 125922

The TF30 probe was also subjected to a 15 hr test in a TF30 1/8 segment burner rig. The test conditions were 230 psia and 2170°F temperature. A visual inspection following the test revealed a structurally sound probe. However, there was a loss of material at two places around the probe airflow entrance (tip). A materials analysis indicated that the loss of material was a result of base metal (B66 columbium) oxidation which occurred when the silicide coating dissipated from the sharp edges. The probe design was revised to radius the probe tip and eliminated the sharp corners. Following reoperation of the TF30 probe to provide a smooth tip, it was delivered to NASA, FRC.

C. TEMPERATURE SENSOR

Temperature sensor component tests were conducted at Honeywell, Inc. on a prototype unit. These tests consisted of a 50-hr performance check, 20-hr hot vibration, and calibration and response checks. Acceptance tests were conducted on the four sensors delivered in Phase I and the two units delivered in Phase IV.

1. Performance Test

The objective of the sensor performance test was to determine capability of the device to perform for 50 hr at maximum design conditions of sensor inlet temperature and pressure of 2200°F and 125 psia. The test was conducted on the Honeywell, Inc. Sudden Expansion (SUE) burner facility on the test fixture shown in figure 26 and the drawing (figure 27). The 50-hr duration was accomplished in approximately 8-hr increments.

Test results of output frequency and signal amplitude as a function of test time showed no measurable performance changes. Visual inspections at intervals showed acceptable performance of the sensor material. At the conclusion of the test, visual inspection with the aid of optics revealed a slight erosion of the oscillator splitter material at the geometric center of the splitter leading edge. This erosion was not considered abnormal for the severe operating environment, and it had no measurable effect on sensor operating characteristics.

2. Vibration Test

A 20-hr vibration test on the temperature sensor to determine structural integrity of the device consisted of 5- to 2000-Hertz vibration scans at specified acceleration levels in each of two axes with the oscillator body in a 2200°F environment. The test setup is shown in figure 28. The axes selected were parallel and perpendicular to the plane of the splitter. The 20-hr duration was logged with 10 hr in each of the two directions. No well defined resonance points could be detected, and the sensor completed the test without failure.

3. Calibration

Calibration tests were conducted on the prototype unit for design assurance and on all delivered units as part of the acceptance tests. For the Phase I calibration tests, the sensors were mounted directly in the test fixture as illustrated in figure 26. The test fixture was mounted on the electric hot-gas facility as shown in figure 29. A typical temperature sensor calibration curve is shown in figure 30. A detail presentation of the temperature sensor calibration data is included as Appendix A.

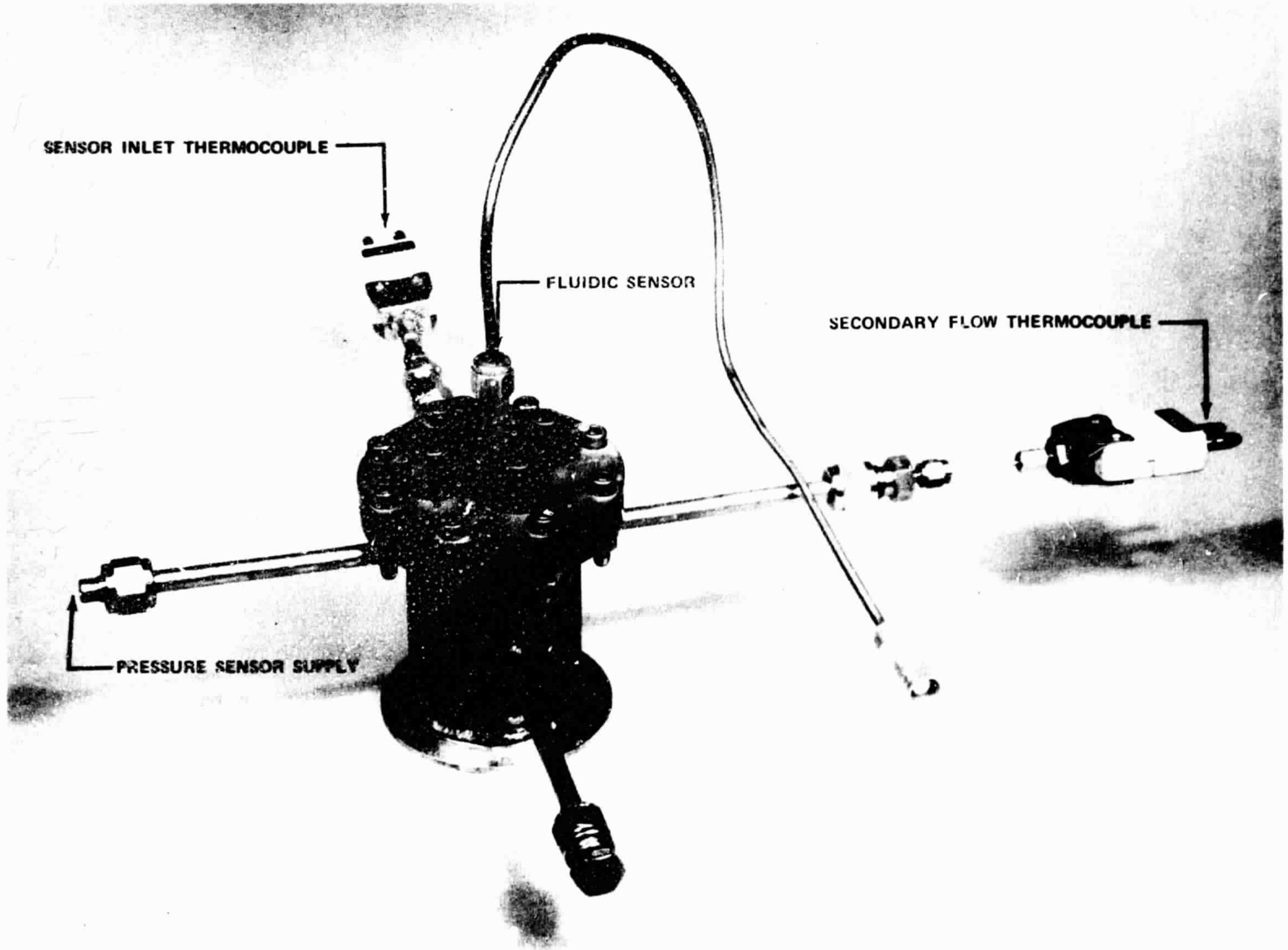

Figure 26. SUE Burner Test Fixture FD 81193

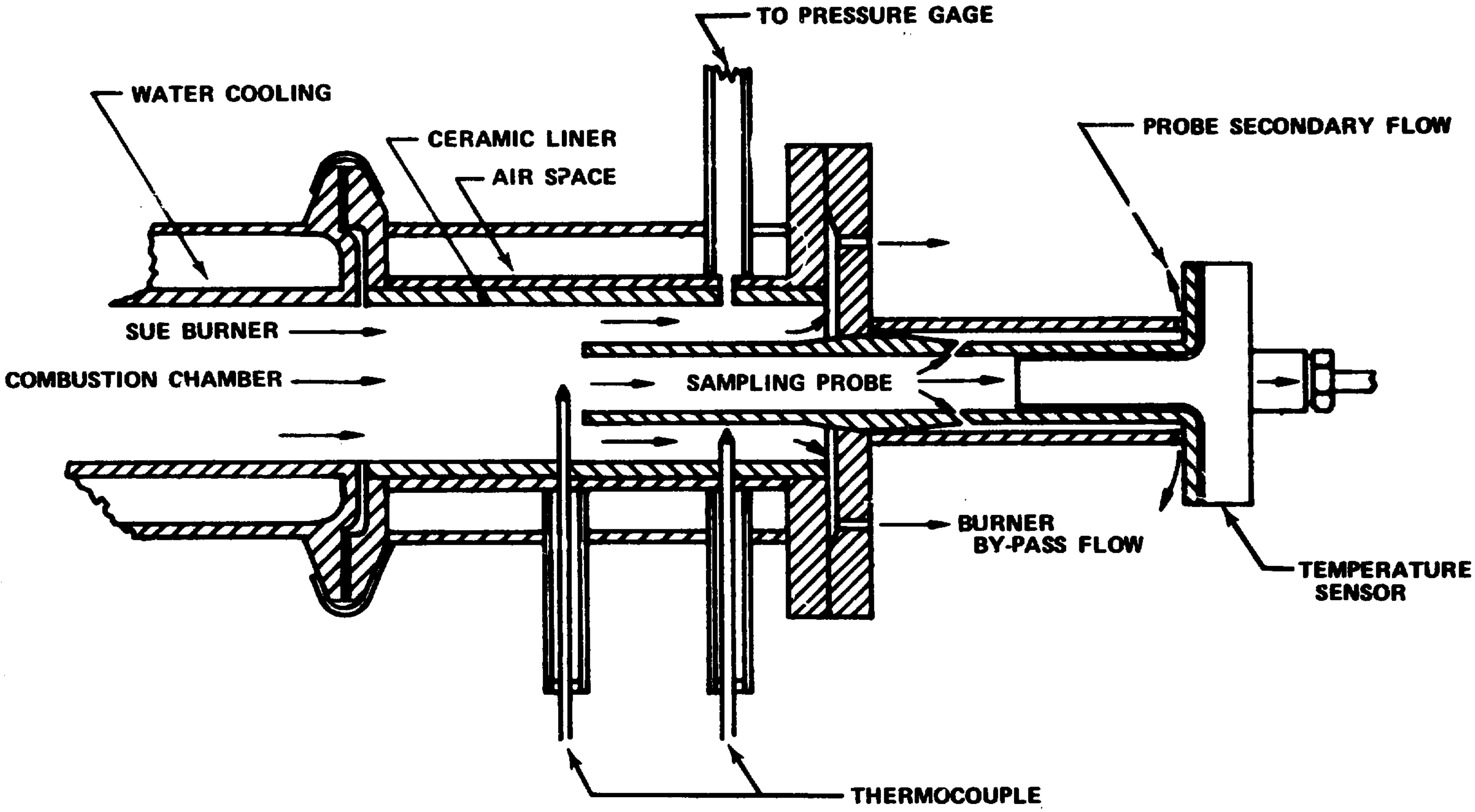

Figure 27. SUE Burner and Test Fixture

FD 81194

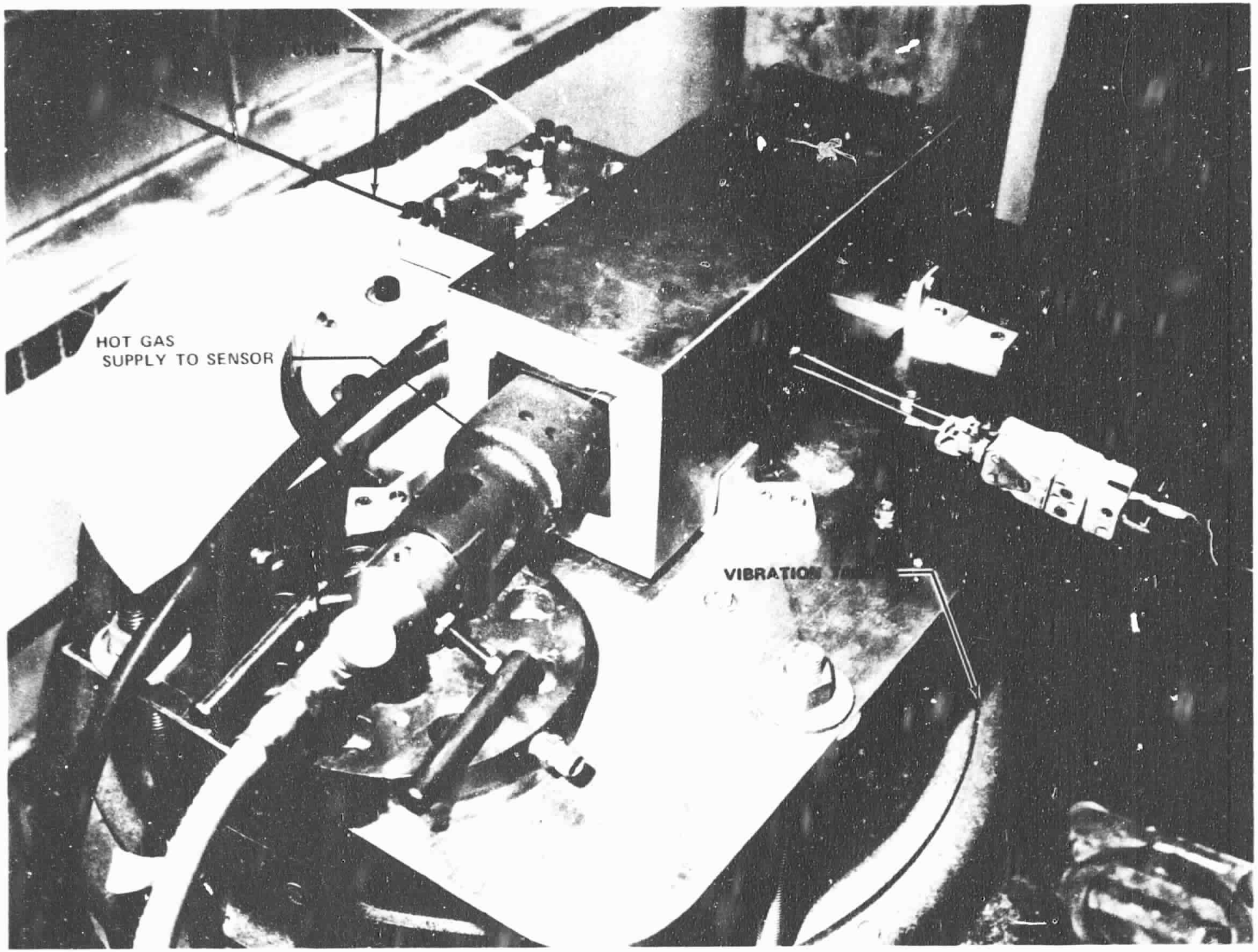

Figure 28. Sensor Vibration Test Setup

FD 81195

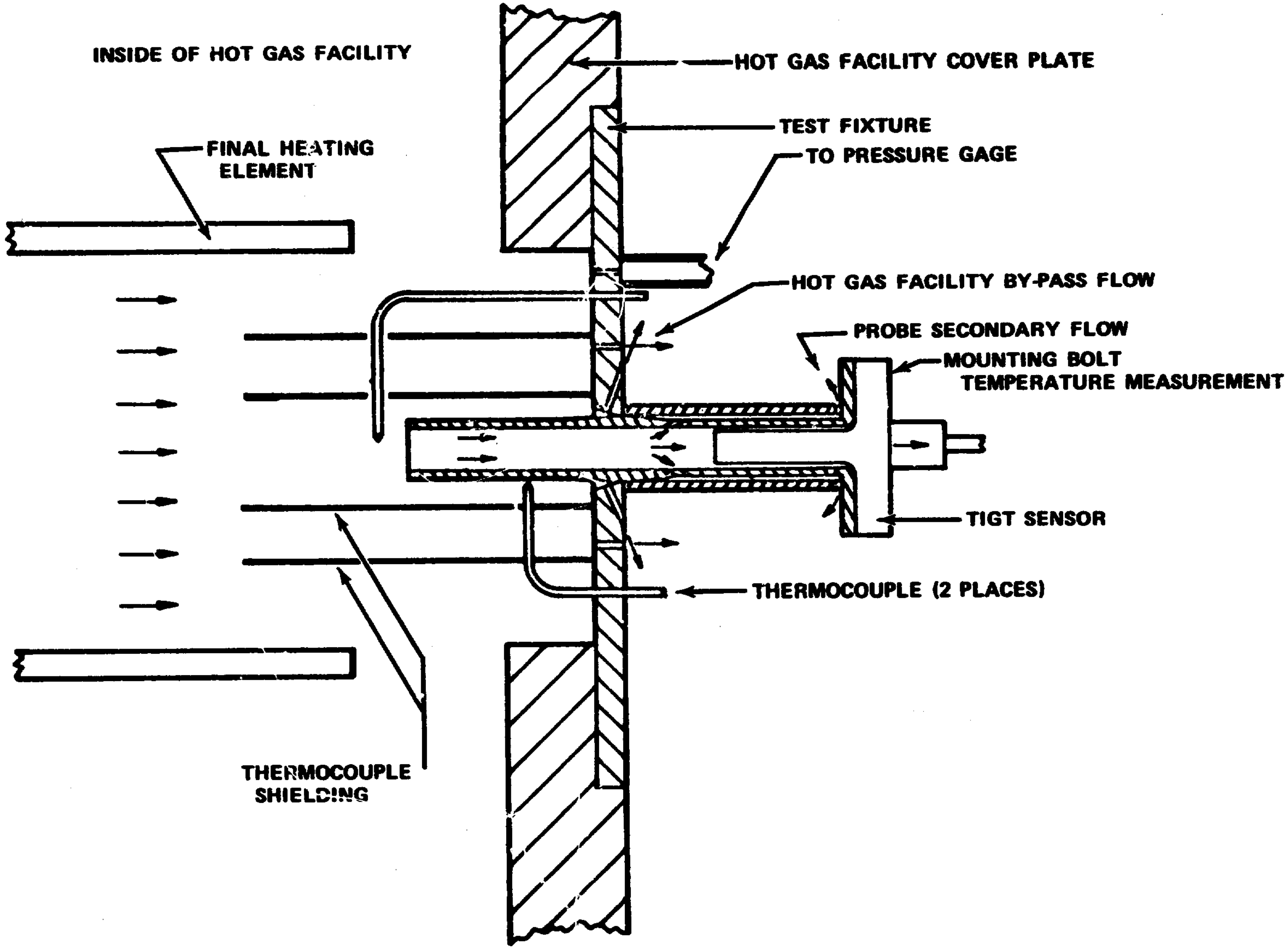

Figure 29. Sensor Calibration Fixture Showing Sensor Probe Installation

FD 81196

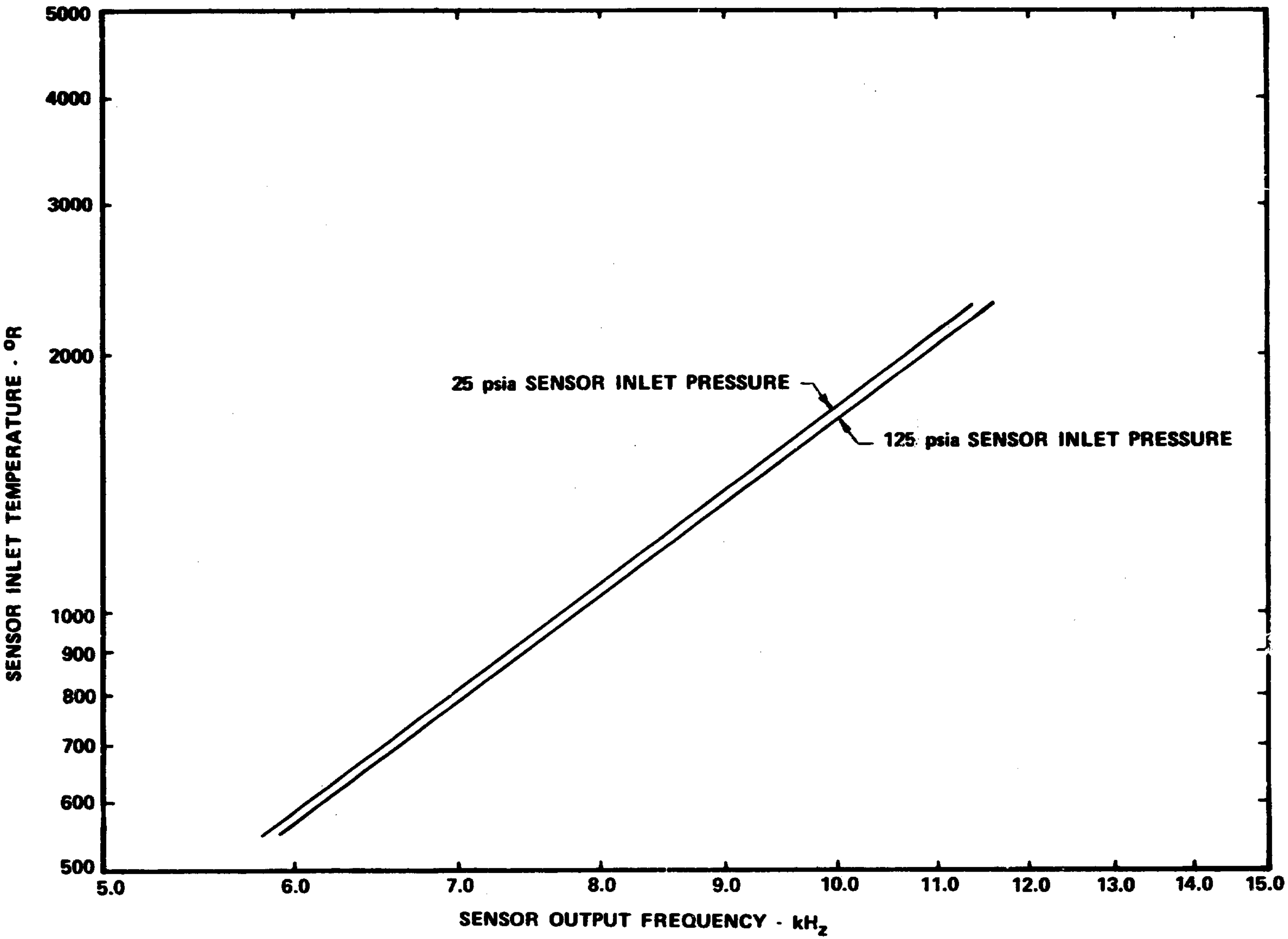

Figure 30. Sensor Calibration Test Data

FD 81197

D. INTERFACE SELECTOR ELECTRONICS

1. Prototype Calibration

The prototype interface selector was calibrated as a unit using the fluidic sensor frequency output data shown in figure 30. The sensor was simulated with a sine wave generator and burner pressure was simulated by shop air. In this manner, the interface selector was checked for performance at each stage through the circuit. Mirror adjustments were made at various points to get the desired gain and range on the output signals. The dynamic compensation amplitude (K_1) was set for 0.67 (50% overshoot to a step change in input frequency). The time constant τ_2 was set as follows (refer to figure 10):

Pressure, psia	Time Constant, sec
100	6.6
50	8.8
20	11

These values were based upon the sensor performance when subjected to rapid temperature changes on the Honeywell, Inc. SUE Burner test facility.

The final calibration of interface selectors X1 and X2 prior to shipment to FRDC are presented in tables II, III, and IV and figures 31 and 32.

The indicator output (0 to 5 volts) data are shown in figure 31 plotted as volts versus temperature. As mentioned above, the temperature was a simulated frequency.

The TIGT output (21.95 to 38.14 millivolts) data recorded at the same time as the indicator output is presented in figure 32.

a. Hardware Calibration for Phase I

The first two interface selector units, serials X1 and X2, were calibrated to give output signals shown in the following tables. Table II is a tabulation of the steady-state calibration at 100 psia; table III is for 50 psia; and table IV is for 20 psia. The indicated temperature for a given frequency is higher at 20 psia than 50 psia than 100 psia. This is to compensate for the lower frequency produced by the fluidic sensor at lower pressures.

Table II. Steady-State Calibration at 100 psia

Input Frequency, Hertz	Output TIGT, millivolts	Output Indicator, volts	Indicated Temperature, °F
10,690	21.95 + 0.46	0.000 + 0.142	1500
10,817	23.13	0.3571	1550
10,944	24.32	0.7142	1600
11,072	25.50	1.0713	1650
11,199	26.68	1.4284	1700
11,326	27.85	1.7855	1750
11,453	29.02	2.1426	1800
11,580	30.18	2.500	1850

Table II. Steady-State Calibration at 100 psia (Continued)

Input Frequency, Hertz	Output TIGT, millivolts	Output Indicator, volts	Indicated Temperature, °F
11,690	31.34	2.8571	1900
11,800	32.50	3.2142	1950
11,910	33.64	3.5713	2000
12,020	34.77	3.9284	2050
12,130	35.90	4.2855	2100
12,240	37.02	4.6426	2150
12,350	38.14	5.0000	2200

Table III. Steady-State Calibration at 50 psia

Input Frequency, Hertz	Output TIGT, millivolts	Output Indicator, volts	Indicated Temperature, °F
10,690	22.40 ± 0.46	0.136 ± 0.142	1519
10,817	23.61	0.500	1570
10,944	24.79	0.857	1620
11,072	26.00	1.221	1671
11,199	27.17	1.578	1721
11,326	28.37	1.943	1772
11,453	29.53	2.299	1822
11,580	30.72	2.664	1873
11,690	31.88	3.021	1923
11,800	33.05	3.385	1974
11,910	34.18	3.742	2024
12,020	35.34	4.106	2075
12,130	36.46	4.463	2125
12,240	37.58	4.820	2175

Table IV. Steady-State Calibration at 20 psia

Input Frequency, Hertz	Output TIGT, millivolts	Output Indicator, volts	Indicated Temperature, °F
10,563	22.54 ± 0.46	0.178 ± 0.142	1525
10,690	23.77	0.550	1577
10,817	24.98	0.914	1628
10,944	26.21	1.285	1680
11,072	27.47	1.657	1732
11,199	28.67	2.029	1784
11,326	29.86	2.400	1836
11,453	31.07	2.771	1888
11,580	32.27	3.142	1940
11,690	33.46	3.514	1992
11,800	34.64	3.886	2044
11,910	35.81	4.257	2096
12,020	36.98	4.628	2148
12,130	38.14	5.000	2200

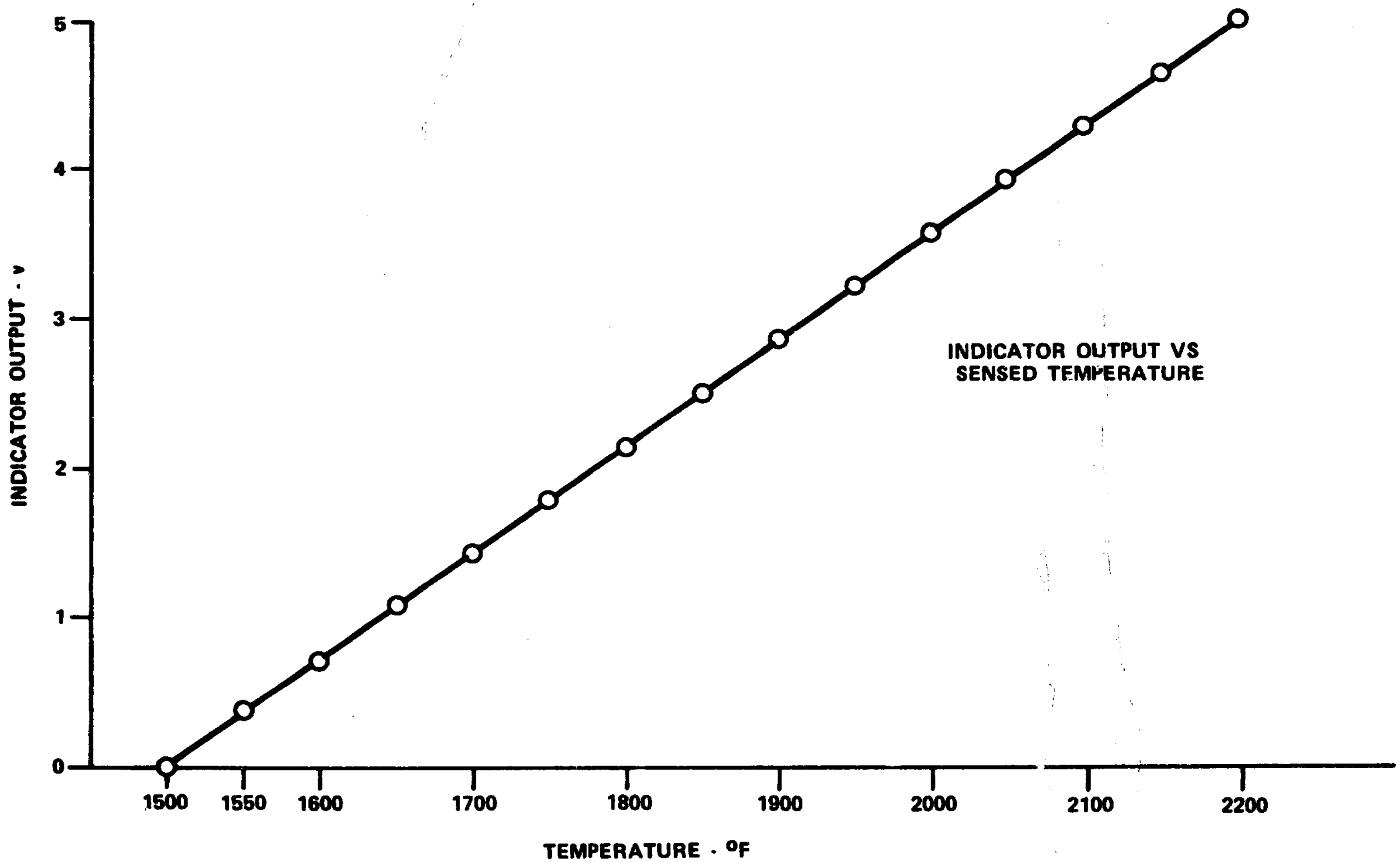

Figure 31. Indicator Output Versus Temperature With 100 psi Simulated Pressure

FD 81198

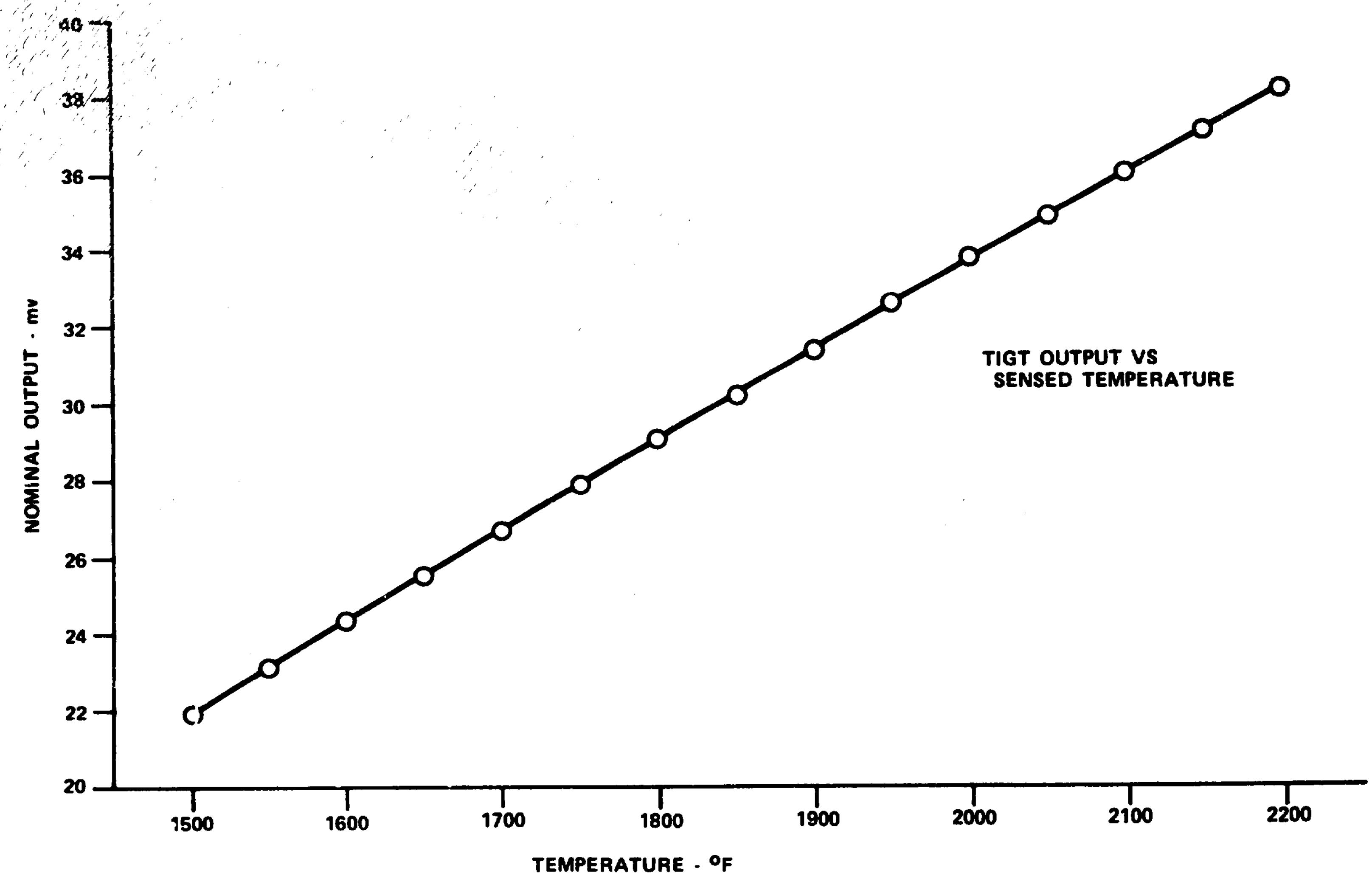

Figure 32. TIGT Output Versus Temperature With 100 psi Simulated Pressure FD 81199

The TIGT millivolt signal output lag was set at 1 sec to achieve stable operation when connected to the CG319 EGT control.

Initial calibrations of serials X1 and X2 were based on component test results conduct at Honeywell, Inc. System and component tests described in Section IV at FRDC indicated that recalibrations for steady-state volts versus temperature, steady-state change in volts versus pressure and transient volts versus pressure were required to meet system performance goals. Changes in the steady-state calibrations were made on Serial No. X1.

2. Ambient Temperature Tests

The prototype unit of the interface selector was used to determine the interface selector sensitivity to ambient temperature. A set of performance data were measured at room temperature, -65°F, +160°F and post room temperature. These data are presented in the form of output error versus input temperature for each condition of ambient temperature. In addition, various inputs to the pressure compensation circuits were simulated to verify temperature effects on these circuits. Figure 33 is a graph of the indicator output errors at the initial room temperature calibration. Figure 34 is a graph of the indicator output errors at -65°F. Figure 35 is a graph of the indicator output errors at +160°F. Figure 36 is a graph of the indicator output errors at room temperature after temperature tests were completed. The unit was subjected to a 4-hr nonoperating soak at the ambient temperature before each set of data were taken.

3. Vibration Tests

Vibration tests were conducted per MIL-STD-810B, paragraph 4.5.1.3 and 10 g level. Vibration was applied at the rate of MIL-STD-810B. Total time of vibration was 13 min in each axis. The indicator output was monitored during the vibration tests with no deviations outside the +20°F allowable error band and no resonant points detected.

4. EMI Tests

Radiated and conducted emission and susceptibility EMI tests were carried out on the prototype interface selector unit per MIL-E-5007 using the methods of MIL-I-6181 with the open circuit voltage increased from 100,000 microvolts to one volt for the susceptibility tests. The unit successfully passed all EMI tests.

5. Prototype System Tests

The prototype system test was the first functional checkout of the components integrated together as a system. Tests were conducted to determine if interface selector adjustments would eliminate both steady-state and transient temperature sensor errors. During these tests, the sensor was mounted with the gas sampling probe on the SUE burner and subjected to temperature input transients. Preliminary adjustments were made on the interface selector to bring system output within specified requirements.

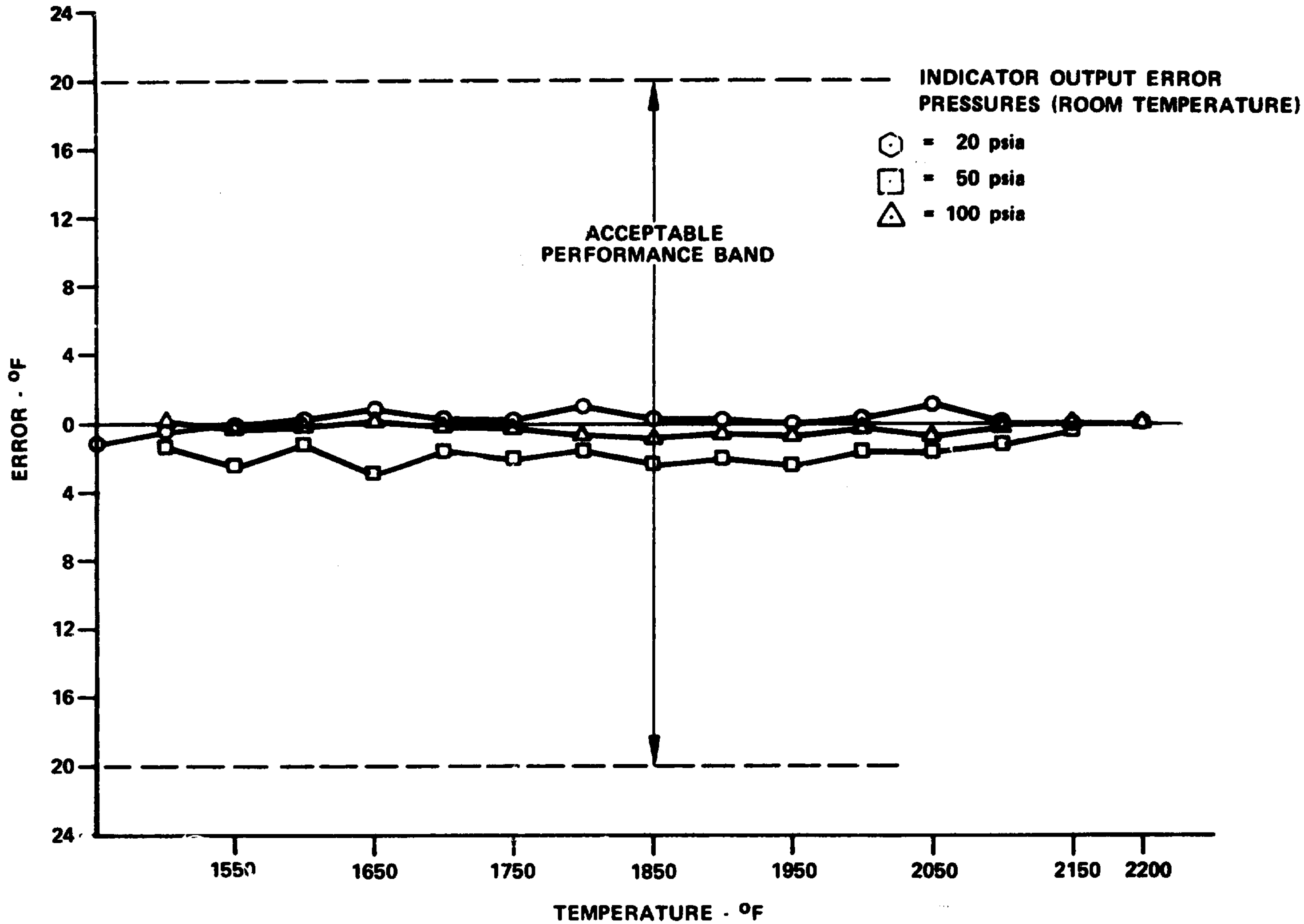

Figure 33. Interface Selector Basic Calibration Error (Room Temperature)

FD 81200

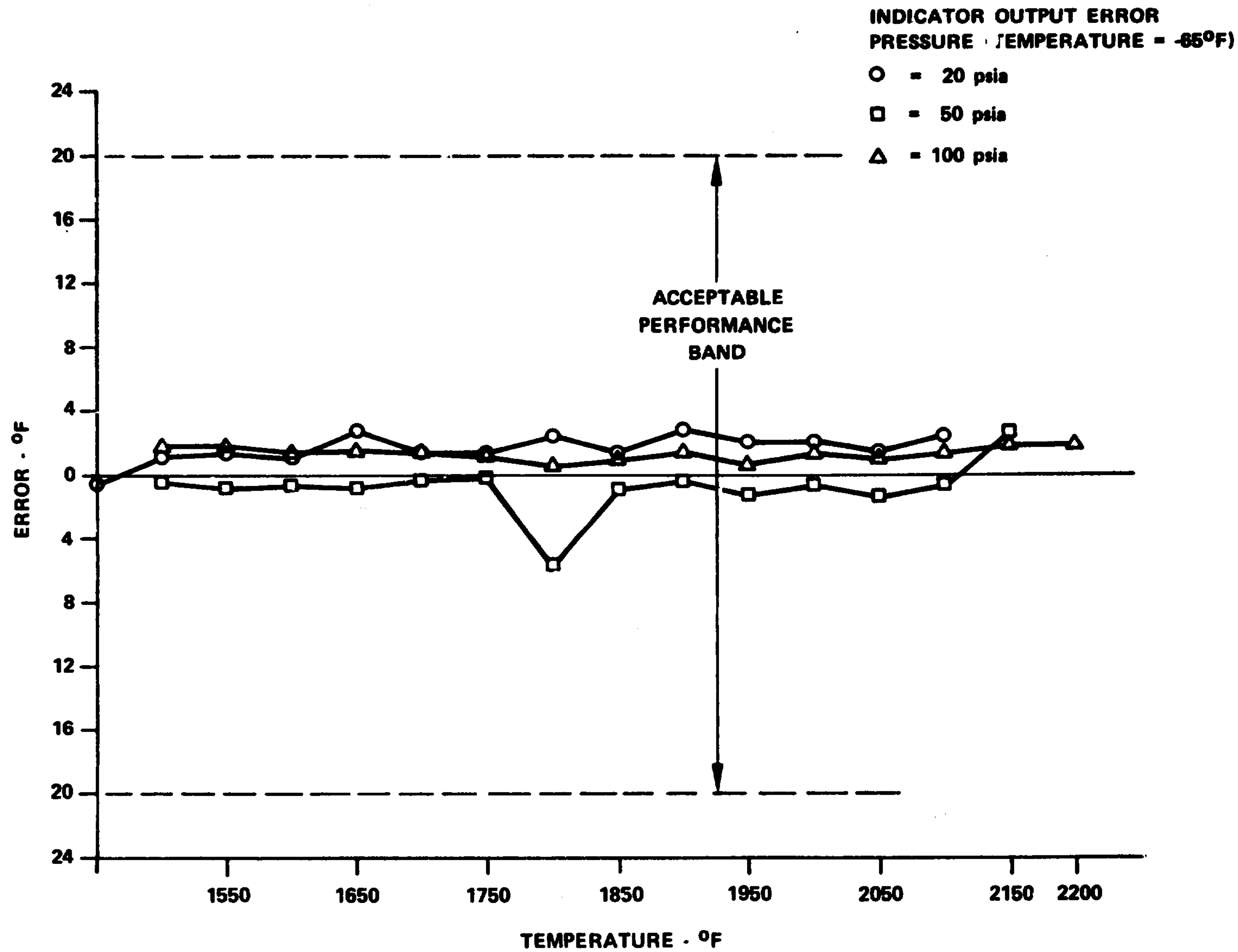

Figure 34. Interface Selector Indicator Output Error Versus Temperature (-65°F)

FD 81201

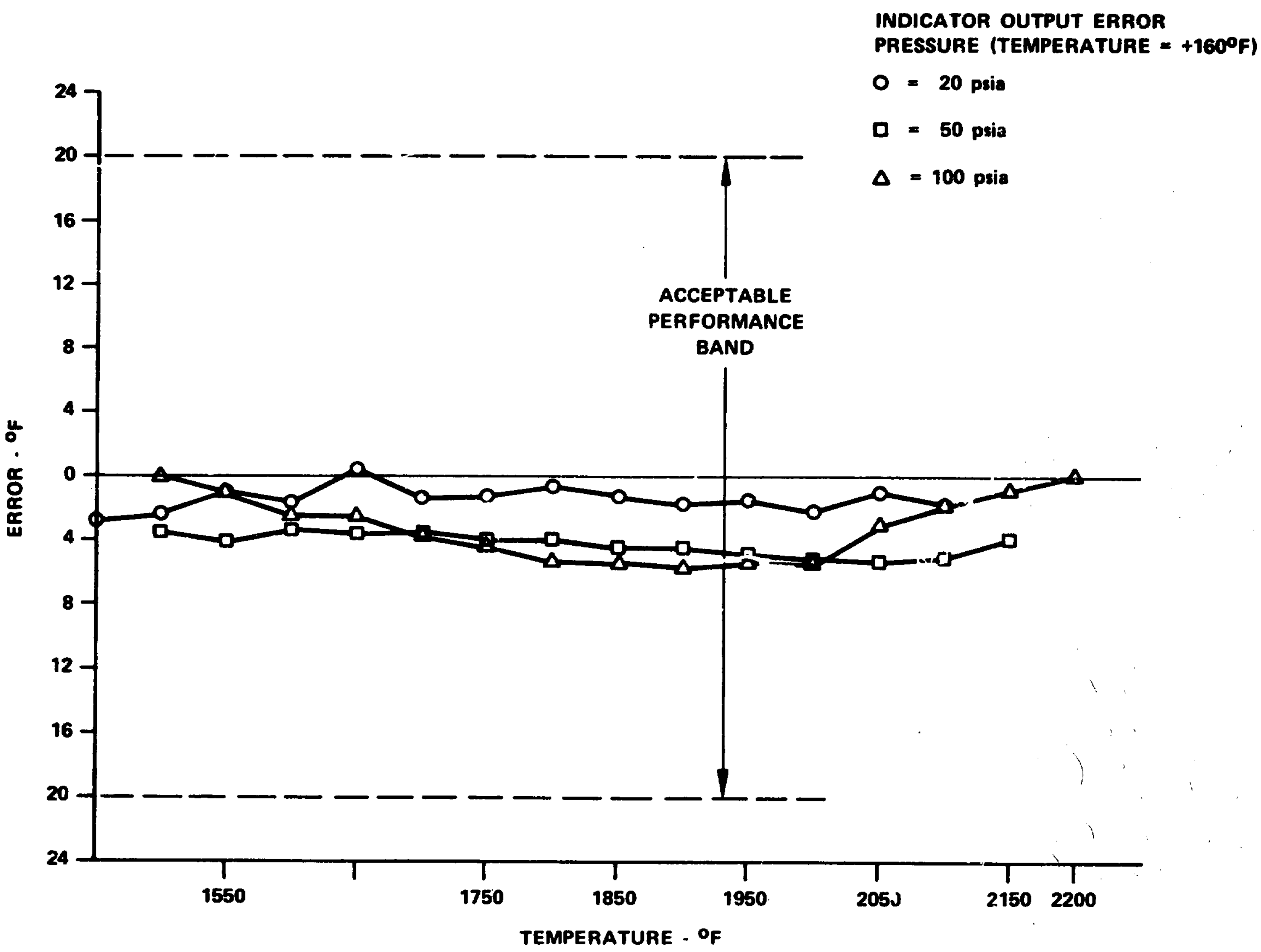

Figure 35. Interface Selector Indicator Output Error Versus Temperature (+160°F) FD 81202

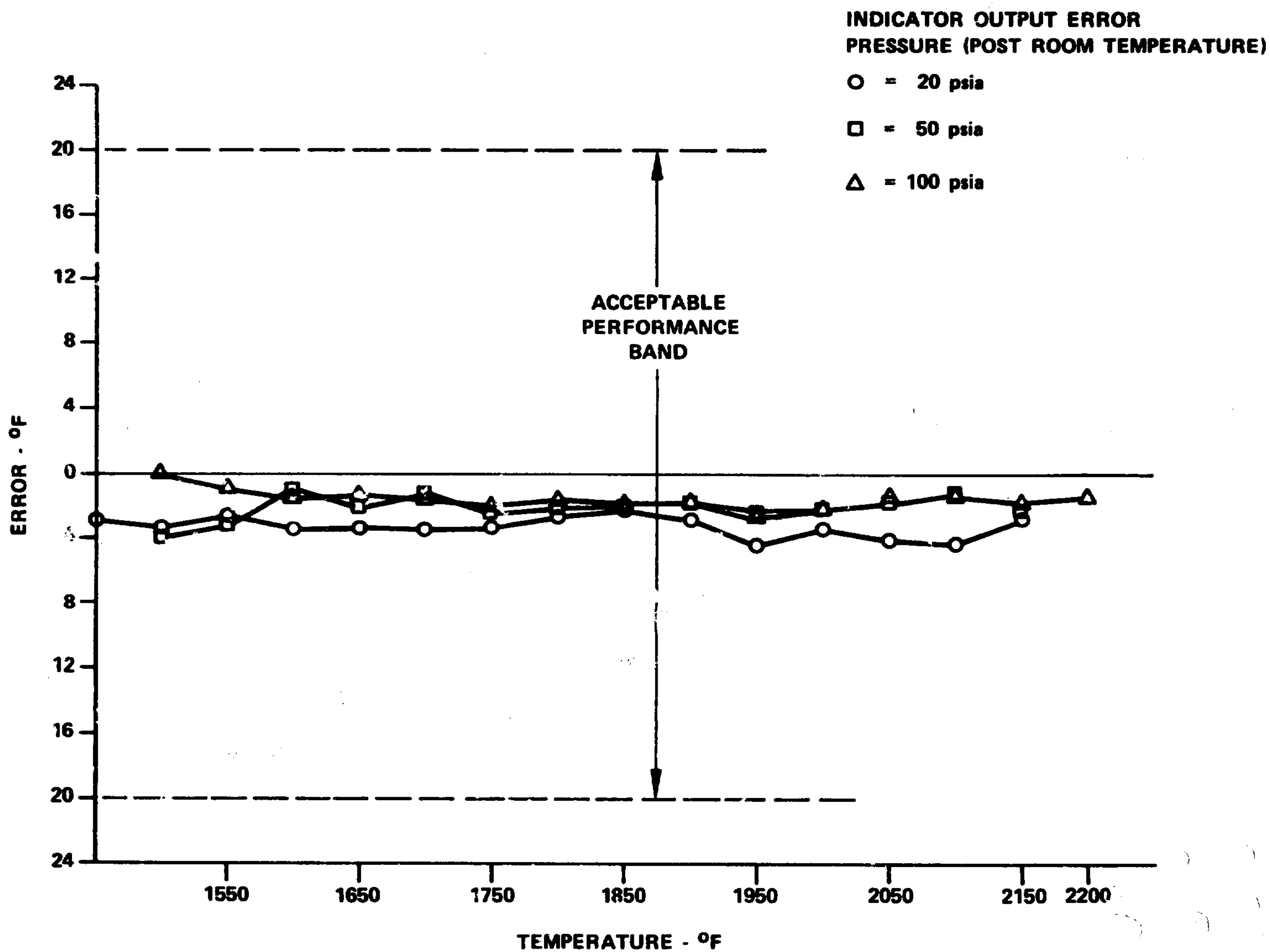

Figure 36. Interface Selector Indicator Output Error Versus Temperature (80°F) FD 81203

The system was then connected to a CG 319 vernier trim control and a trim control test panel having an indicator light system showing trim output signal status, i.e., up or down trim and no trim. Using a simulated compressor inlet temperature input to the CG 319 vernier trim control, a functional check was made of the complete TIGT measurement and control system. The time constant of the TIGT millivolt output was adjusted to eliminate excessive dither in the trim system. This was required since response of the TIGT measurement system exceeds that of the normal EGT input to the CG 319 trim control. The control system performed as required when adjustments were set to simulate a one second time constant.

6. Nonflight Configuration TIGT Measurement Systems

Two TIGT measurement systems suitable for nonflight investigations of the fluidic sensing part of the flight test configuration were fabricated, calibrated and delivered to NASA FRC under this contract.

The nonflight configuration systems included (1) hot gas sampling probe, (2) fluidic temperature sensor, and (3) a frequency to voltage converter. The probe and sensor were fabricated to the same requirements as the experimental units. The frequency to voltage converter was fabricated to an existing Honeywell, Inc. design. It provides two outputs of ±9 volts for input frequency of 7,000 (450°F) to 13,000 Hertz (2200°F). One of the outputs is compensated for a 3 sec time constant (τ_2) and the other is an uncompensated voltage signal of the fluidic sensor output.

A photograph of the converter is presented in figure 37. These converters were calibrated to the values listed in table V at Honeywell and delivered to FRDC for laboratory investigation purposes. The results of bench tests conducted at FRDC are presented in Appendix B.

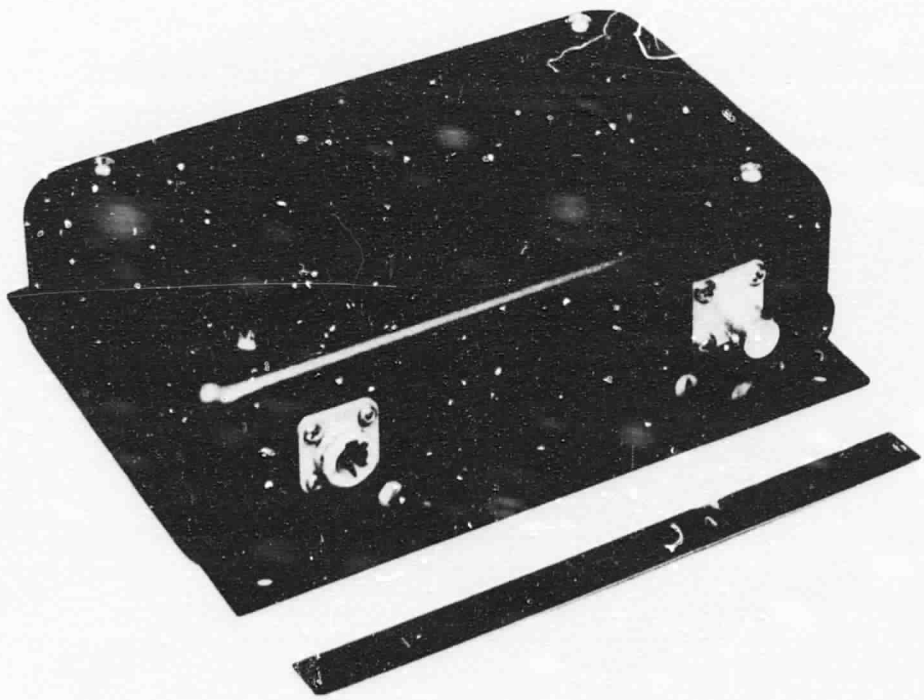

Figure 37. Frequency to Voltage Converter (CSX 19406) FE 125428

Table V. Calibration Data for Frequency-to-Analog Converters Part No. CSX 19406

Input Frequency, KHz	Uncompensated Output, dc volts	Compensated Output, dc volts
	Serial No. X9	
7.0	-9.017	-9.047
7.5	-7.509	-7.529
8.0	-6.013	-6.029
8.5	-4.512	-4.518
9.0	-3.011	-3.018
9.5	-1.510	-1.516
10.0	-0.012	-0.013
10.5	+1.487	+1.490
11.0	+2.991	+2.997
11.5	+4.487	+4.497
12.0	+5.995	+6.009
12.5	+7.498	+7.517
13.0	+8.994	+9.019
	Serial No. X10	
7.0	-9.040	-9.046
7.5	-7.536	-7.539
8.0	-6.034	-6.034
8.5	-4.528	-4.528
9.0	-3.025	-3.025
9.5	-1.517	-1.517
10.0	-0.019	-0.017
10.5	+1.484	+1.486
11.0	+2.98	+2.988
11.5	+4.486	+4.491
12.0	+5.988	+5.992
12.5	+7.495	+7.502
13.0	+9.000	+9.013

E. SYSTEM TESTS

Performance tests were conducted on the TIGT measurement system to determine what improvements or changes were required to meet the operational goals. A schematic of the bench test setup used for the system tests at FRDC is presented in figure 38.

The test rig consisted of air supply duct work connected to a J57 engine that is a source of air, a J58 combustor and fuel nozzle assembly, transition duct and TIGT measurement system test nozzle. All temperature instrumentation was mounted in the test nozzle and burner pressure was taken from the combustion chamber section. A photo of the test nozzle assembly is presented in figure 39.

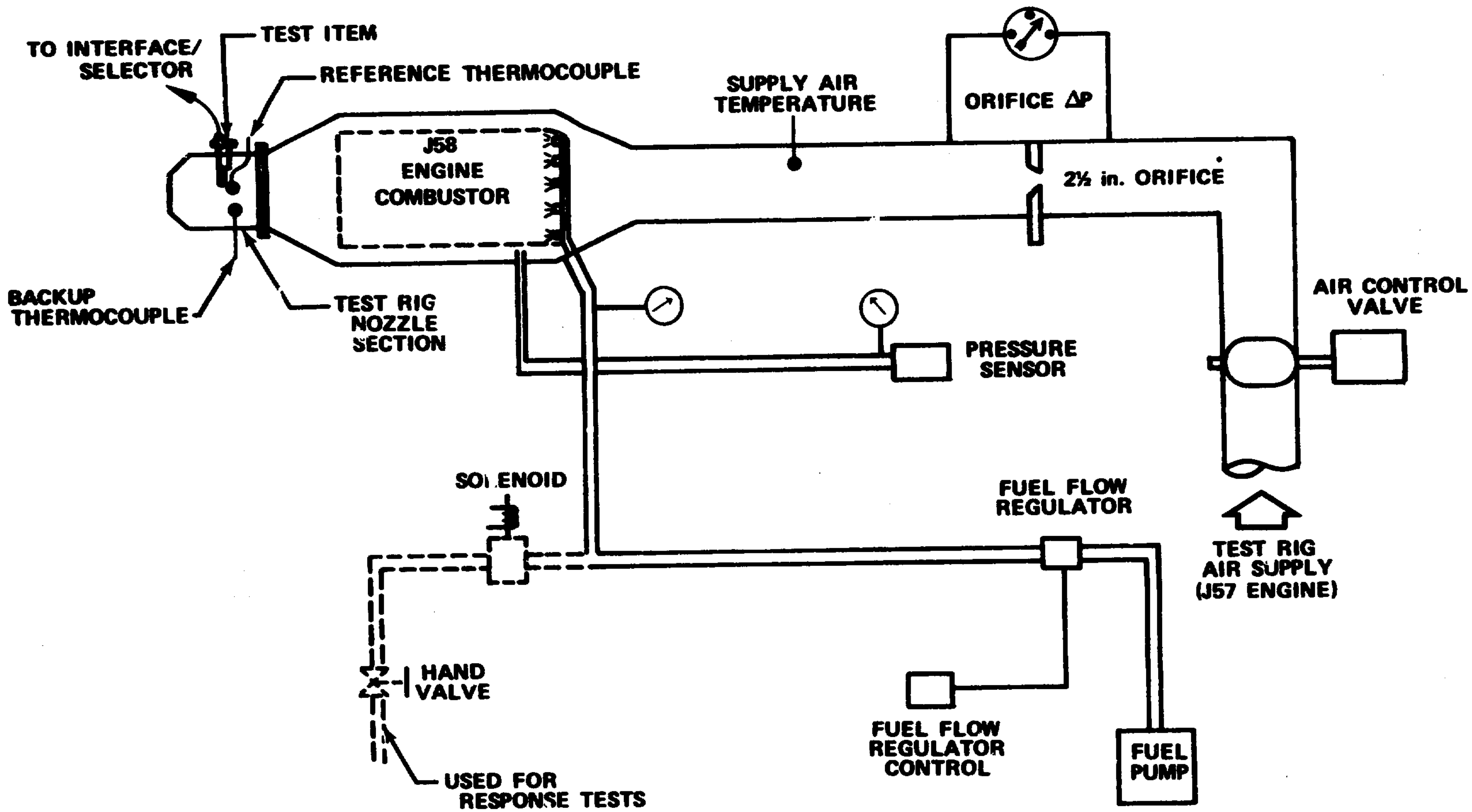

Figure 38. TIGT Measurement System Bench Test Setup

FD 74959A

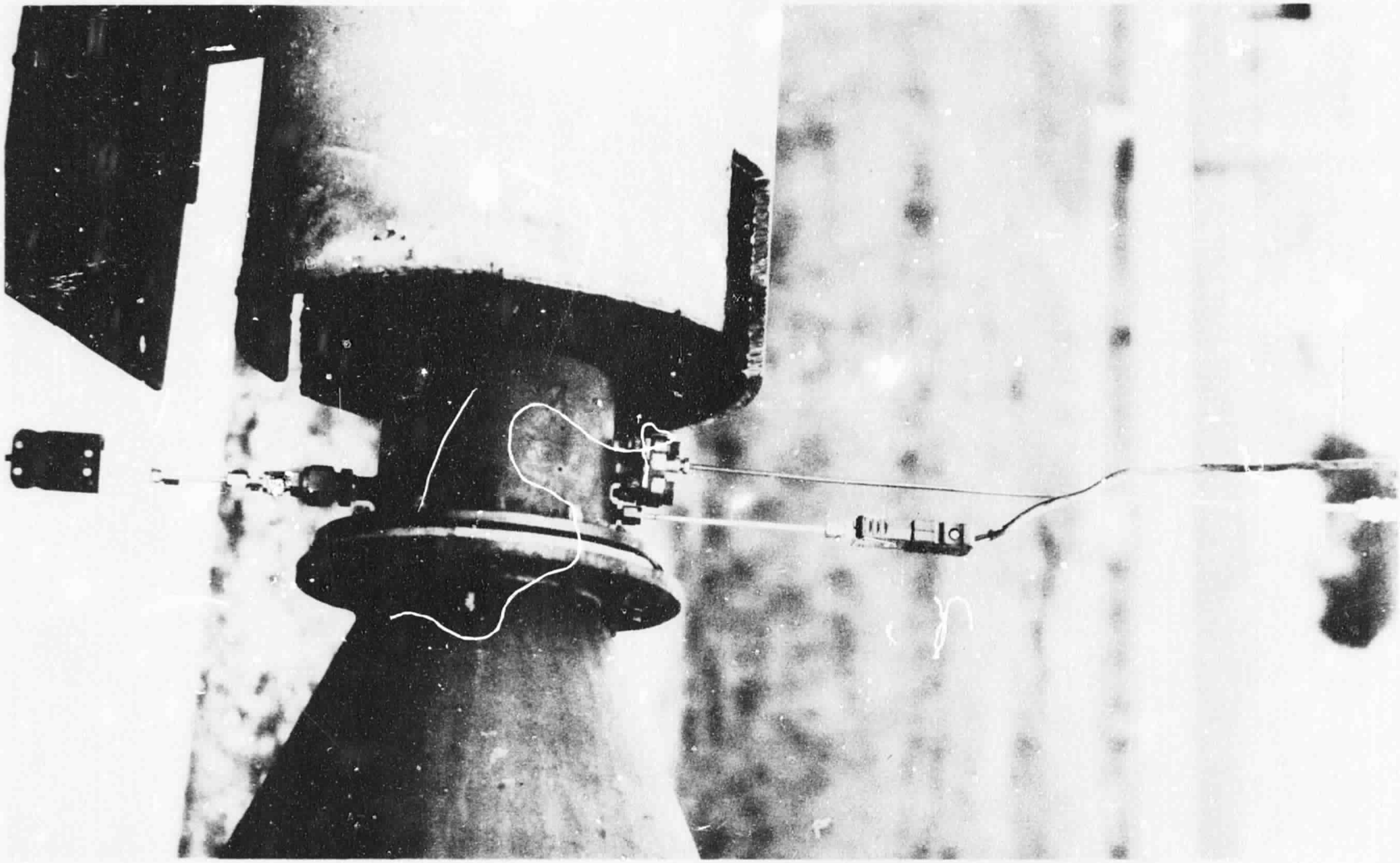

Figure 39. TIGT Test Nozzle Assembly

FE 333470

Two experimental TIGT measurement systems were subjected to performance tests with gas temperature ranging from 1500°F to 2200°F and pressure from 25 psia to 80 psia. A plot of these data referenced to a ±40°F accuracy band is presented in figure 40. The data represents 87 randomly selected points with two outside the steady-state performance goal. The interface selectors used in these calibrations were set for steady-state pressure compensation of 4 Hz/psi (1.5°F/psi) at 25 psia and 2 Hz/psi (1°F/psi) at 75 psia. The fluidic sensor performance of sensors tested at FRDC during the development phase is shown in figure 41.

Creation of a step temperature change in a real combustion system is impossible since control dynamics and combustion delays combine to add finite time delays to what may have started as a step. However, any combustion system does exhibit a certain amount of noise, with a frequency content that can be assumed to appear as a step change to the sensors and can be used to indicate the dynamic response of the sensing system. A plot of TIGT measurement system indicator output response to TIGT "noise" is shown in figure 42. The temperature reference was a shielded aspirated platinum-87% platinum/13% Rhodium thermocouple, fabricated to a design that had been determined to have approximately a 0.04 sec time constant for the test conditions of figure 41. Examination of the two traces shows the TIGT measurement system to indicate temperature peaks at the same time as the high response thermocouple and also indicate the same peak-to-peak temperature changes, thereby demonstrating acceptable response to small temperature changes. The performance of the TIGT sensor assembly (probe, mount, fluidic sensor) changes with the level of absolute pressure. Biases were incorporated into the interface selector to compensate both the steady-state and transient temperature indication as a function of combustor pressure. The degree of steady-state compensation was determined by observing the output of the sensor at constant temperature and the various combustor pressures. These tests led to the conclusion that steady-state compensation of 5.6 Hz/psi was required which will result in a correction of 160°F over design pressure range. Dynamic compensation requirements for the variables shown previously in figure 10 were defined as follows:

Time Constant (τ_2) - 21 seconds at 33 psia
7 seconds at 100 psia
$K_1 = K_2$ - 0.5

A comparison of the TIGT sensor test results at Honeywell and FRDC shows a significant difference in frequency versus temperature. This indicated temperature difference is attributed to the different combustor test rigs. The Honeywell facility was constructed for generation of a well controlled temperature source while the FRDC facility was constructed to simulate conditions existing at the J58 turbine inlet. Consequently, the FRDC sensor calibration was accepted as the standard for the program, furthermore, the FRDC results were verified by probe inlet to sensor inlet tests using thermocouples of the same design as discussed in paragraph A.2 of this section. Subsequent tests in the engine installation correlating TIGT as measured by the fluidic sensor and a thermocouple to EGT at the same engine conditions confirmed this selection. Further discussion of this is included in Appendix B.

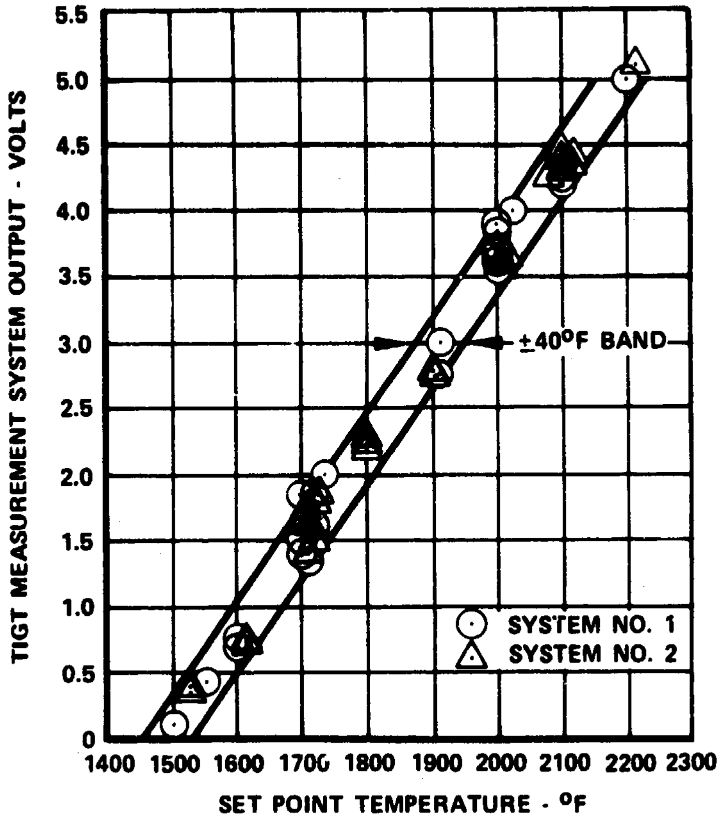

Figure 40. TIGT Measurement System Performance With Pressure 25 to 80 psia FD 74960

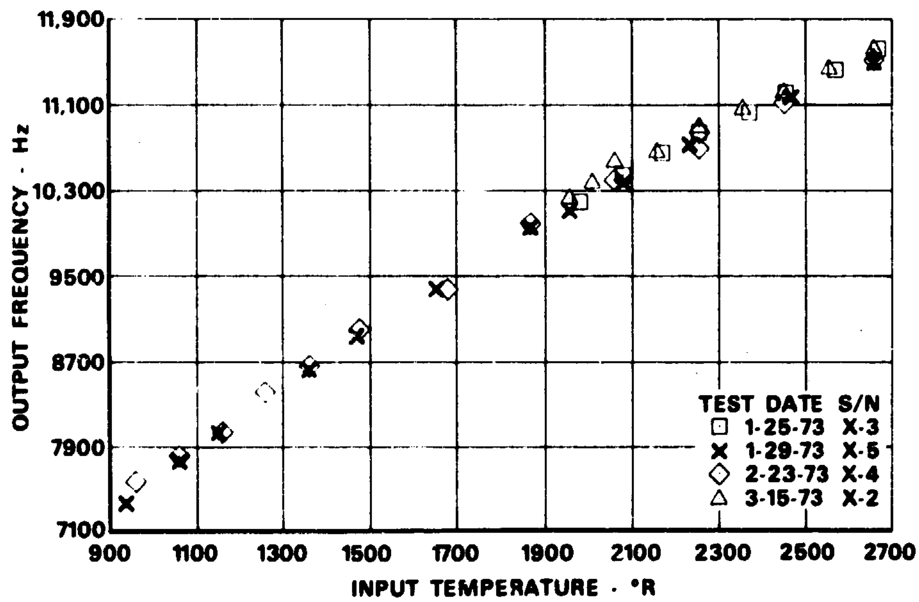

Figure 41. TIGT Sensor Performance With Pressure 25 to 80 psia FD 76209

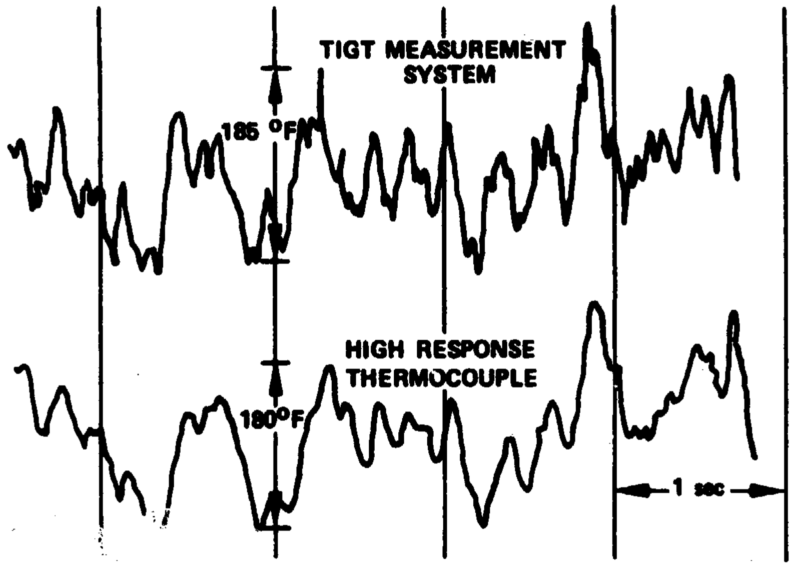

Figure 42. TIGT Measurement System Response to Combustion Noise FD 74961

Throughout the FRDC bench test phase of the program the validity of the temperature reference for data taken on the TIGT measurement system performance was checked and rechecked. The reference temperature of TIGT for steady-state tests in the program were based upon Pt-Pt/13% Rh enclosed junction thermocouples and Pt-Pt/13% Rh with radiation shielded exposed junction were used for transient tests. Combustion noise was at all times greater than the steady-state performance goals of the system. The enclosed junction T/C and the interface selector control (22 to 38 millivolt) output being slow response devices, did not pass the noise. However, the interface selector indicator (0 to 5 volt) output circuit did pass the noise as well as the exposed junction thermocouples. For this reason, different configuration references were used depending on the type of test being conducted. The TIGT noise increased as a function of increased pressure and temperature and ranged from approximately 100°F peak-to-peak at low settings to approximately 250°F peak-to-peak at high settings.

Development of a quieter calibration rig and temperature references less susceptible to the standard errors was beyond the scope of this program. However, the results presented herein are within the acceptability of turbine engine development tolerances.

SECTION IV

PHASE III: ENGINE TESTS TIGT MEASUREMENT AND CONTROL SYSTEM

The TIGT system shown in figure 43 was installed on a J58 engine for flight suitability tests. The TIGT Measurement and Control system was configured as a single sample system to minimize complexity and cost while providing the capability of evaluating the fluidic method of temperature sensing in an operational environment. All engine testing was accomplished piggyback on the current J58 sustaining engineering program. These constraints prohibited the simultaneous measurement of the TIGT by a thermocouple and the fluidic sensor. Therefore, correlation was established by determining the relationship between TIGT and EGT using the Bill-of-Material engine EGT thermocouples and by alternatively installing a thermocouple and a fluidic TIGT sensor installed in the gas sampling probe. A comparison of the engine to bench steady-state data showed agreement within 50°F as illustrated in figure 69, Appendix B.

An analysis of the data taken during base line calibrations also indicated that when engine operating conditions were constant as measured by indicated average EGT, TIGT at the single sample location was not constant. This condition was monitored on two builds of one engine and one build of another engine. The magnitude of the TIGT "drift" at constant indicated average EGT was 120°F. Therefore, it was anticipated that when on TIGT control there would be some EGT wander. Figure 44 is a plot of the system performance while on TIGT control. The range of EGT as shown in figure was 55°F (30°C) which is about 1/2 the earlier observed drift. This can be explained to some degree in that the EGT thermocouples have about a 2 sec time constant and the millivolt output of the interface selector also has a lag equal to about 1 sec. These two combine with the slow trim rate of the EGT vernier control to "clip" peaks that occur in the observed TIGT.

Response of the TIGT measurement system to a snap throttle decrease is presented in figure 45. The response is measured against indicated power lever angle and burner fuel flow. The TIGT indication lags fuel flow by 0.11 sec and leads the EGT indication by about 3.5 sec. The TIGT indication saturates at 1500°F TIGT therefore the noise does not come through.

During this engine test, erratic operation of the TIGT measurement system was observed. Investigations revealed the cause to be originating in the connector of the high temperature cable (Cable IB of figure 48). The female end of the connection had relaxed under thermal loading. A temporary "fix" was made and the measurement system performance observed during a subsequent engine test. The system performed correctly during this test which included simulated mission cycles with heated environment. The system was removed from the engine and the high temperature cable returned to the vendor for investigation and repair.

A test for the integrity of the high temperature cable connectors of the flight test units was agreed to between P&WA and Honeywell. One of the two cables on hand at Honeywell proved defective and all cables were returned to the cable vendor (Kaman Sciences Corp) for incorporation of design changes.

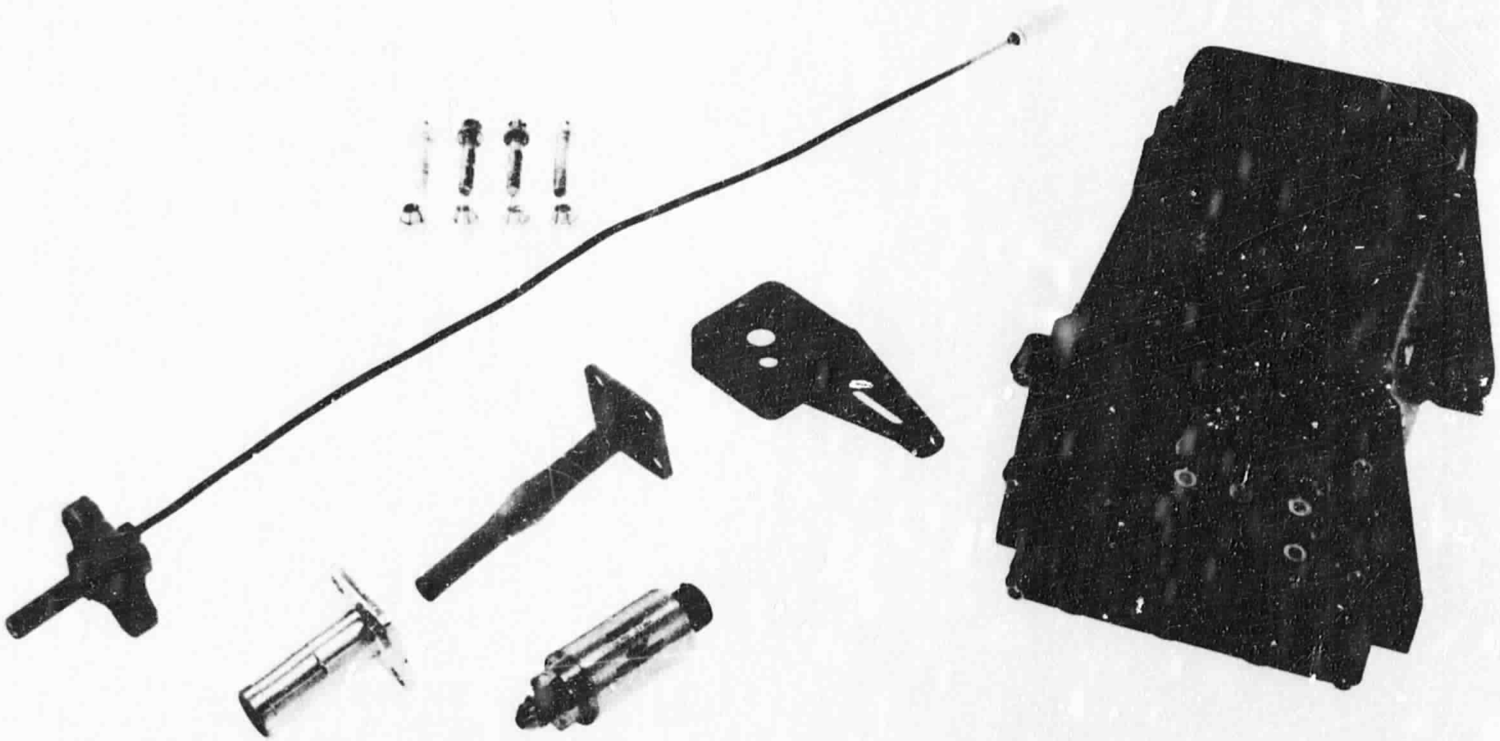

Figure 43. TIGT Measurement System FE 128269

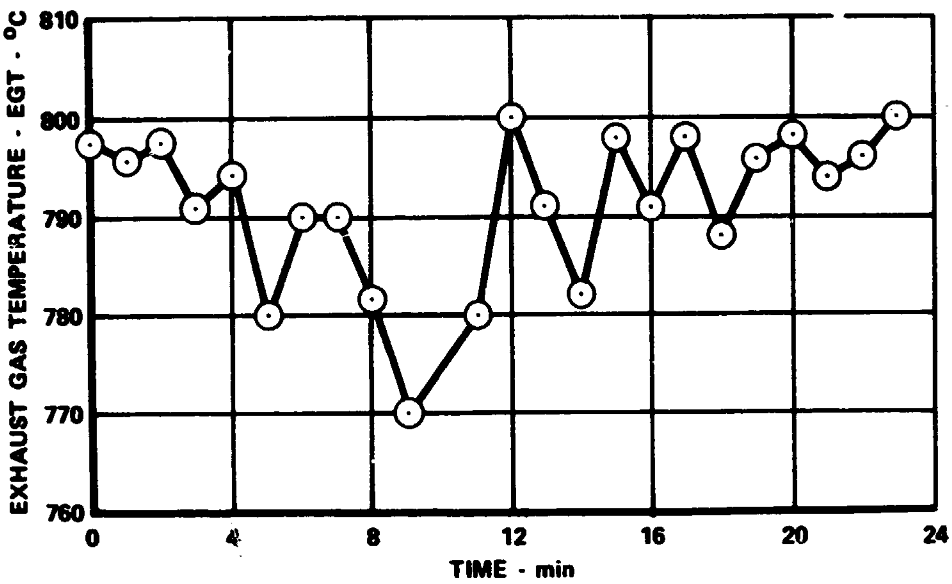

Figure 44. Observed EGT While on TIGT Control FD 74962

Durability of the TIGT Measurement System was demonstrated by completion of at least 60 hr of engine endurance time. Component time on endurance engines are as follows:

TIGT Sensor	S/N X 3	75.5 hr
	S/N X 2	13.5 hr
TIGT Probe and Sleeve		106.5 hr
Interface/Selector	S/N X-1	58.8 hr
	S/N X-2	30.3 hr

The engine vanes were inspected following this test and showed no distress.

The number of fluidic sensor of a specific configuration with more than 50-hr high temperature operation is limited, but has revealed certain characteristics that were again observed in this program. The most significant of these characteristics was that when a new diaphragm and piezoelectric transducer (figure 8) are installed in the sensor, a "burn in" time is required to stabilize the frequency output at constant input conditions. Honeywell, Inc. analysis of this phenomenon is that the diaphragm goes through an initial oxidation period that decreases the receiver volume thereby increasing the output frequency of the assembly. This analysis leads to the supposition that continued oxidation will result in continued shifts in the output frequency. The results of a post engine test calibration on S/NX3 fluidic sensor after 75.5 hr of engine time compared to the pre-engine test calibration (figure 46) shows a slight shift in the increased temperature direction which corresponds to the predicted trends. This sensor continued on engine tests accumulating a total of 158 hr. The sensor performance was then checked by Honeywell and compared to the original calibration. This comparison revealed an increase in indicated temperature of approximately 15 F at 900°F (110 psig) input temperature and 10°F at 1500°F (110 psig) implying that no additional shift in the indicated temperature occurred during the last 80 plus hr of engine operation. It should be noted, however, that all the above shifts are within the performance goals of the TIGT measurement system.

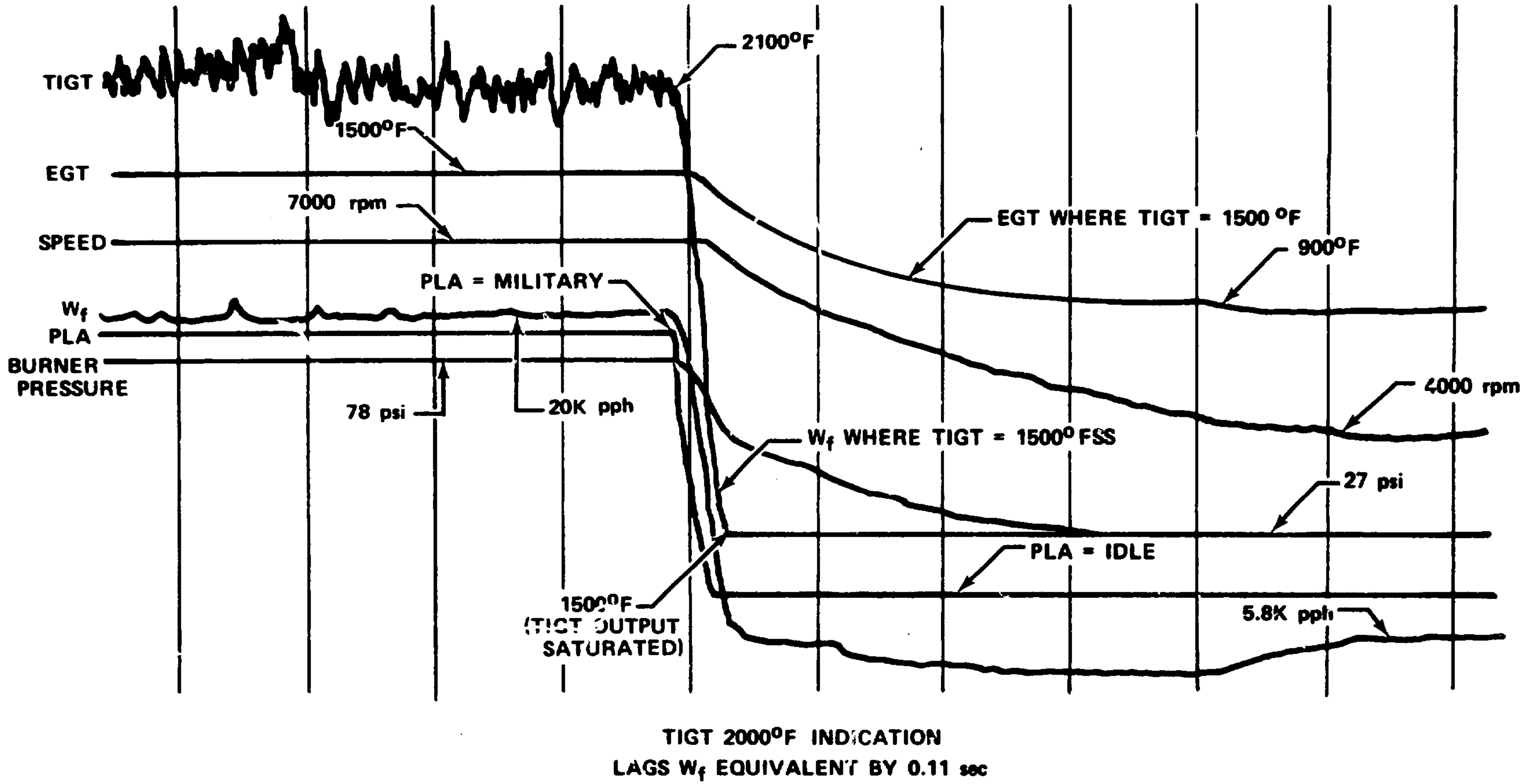

Figure 45. TIGT Measurement System Response To A Snap Decrease of Engine Power

FD 74963A

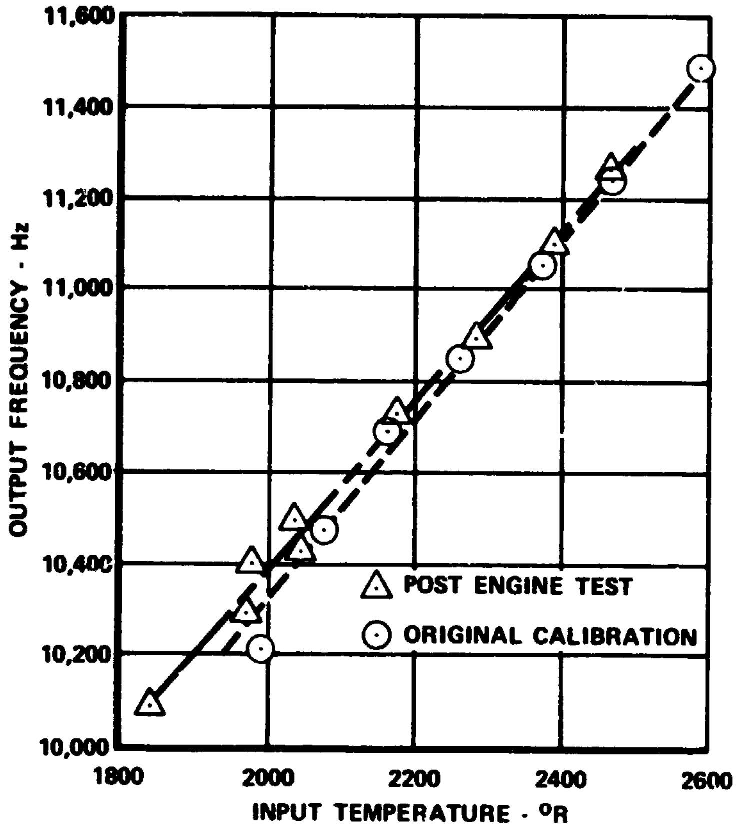

Figure 46. TIGT Sensor S/NX3 Calibration, 75.5 Hours Engine Time (35 psia) FD 74964

The hot gas sampling probe had accumulated 106 hr at the end of the engine test. A visual inspection revealed the details shown in figure 47. The silicide coating was oxidized and flaky in places but there was no indication of base metal deterioration.

The high temperature cable was repaired by adding a support to the female part of the connector and a second engine test conducted to substantiate the redesigned cable. The same TIGT system was used throughout both engine tests.

A total of 75.5 hr endurance time was accumulated on the TIGT measurement system during the second engine test. The TIGT probe accumulated 128 total hr during the second engine test.

The TIGT sensor used in the engine tests has accumulated a total of 156.5 total engine hours and the hot gas sampling probe had a total of 234 hours engine time at the completion of Phase III.

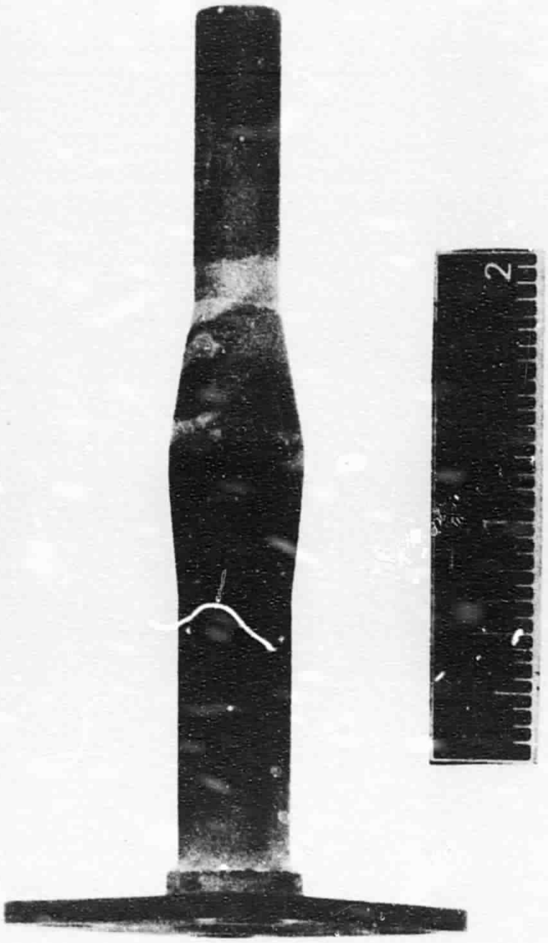

Figure 47. TIGT Probe, 106.5 Hours Engine Time FE 129172

A visual inspection of the hot gas sampling probe assembly and high temperature cable showed all parts to be in good mechanical condition. The fluidic sensor had ceased operating during the last hour of the engine test. A teardown inspection showed the ceramic electrical insulator to be cracked. The sensor assembly was returned to Honeywell, Inc. The broken part was replaced and a post engine test calibration check made. The post engine test of 156.5 hr results were compared to the initial calibration made in January of the same year and showed agreement within instrumentation accuracy, therefore indicating that no deterioration occurred during the additional 81 hr of engine testing over that shown in figure 46.

SECTION V

PHASE IV: FABRICATION AND DELIVERY OF FLIGHT TEST HARDWARE

Two TIGT measurements systems were fabricated and delivered to NASA FRC during this Phase. The delivered hardware included probes, sensors, (TIGT and pressure) interconnecting cables and connectors, interface selector, and adapter hardware required for engine installation of the TIGT sensor. A schematic of the electrical installation with cable lengths and thermal environmental requirements identified is presented in figure 48. The system was tested with the pressure sensor remotely mounted approximately 10 ft from the point of sampling. This distance could be as much as 20 ft without affecting the system performance since the system as installed in the airplane will utilize only steady-state pressure.

Interface/Selector Calibration is based on results obtained at FRDC during the bench and engine tests. Calibration of interface selector serials W3 and W4 was changed from that used for serials X1 and X2 as described in Section III.

The steady-state pressure compensation was changed to a linear function of pressure with a correction of 3°F/psi. This corresponds to 5.63 Hz/psi above 11,080 Hz (1850°F at 50 psia) and 6.43 Hz/psi below 11,080 Hz.

The time constant on the TIGT millivolt output signal was increased from 1 to 2 sec to compensate for the higher than anticipated noise level found during the engine tests.

Amplitude of the dynamic compensation was increased from 50% overshoot to 100% overshoot for a step change in input frequency. This increase allows compensation for a sensor/probe K1 performance value (equation 2 of Section II) of 0.5 as compared to 0.67.

The time constant of the dynamic compensation was changed to allow for sensor/probe τ_2 as shown below.

Pressure, psia	Time Constant (τ_2), sec
100	7
50	14
33	21
20	35

The steady-state calibration curves for serials W3 and W4 with the 3°F/psi correction are shown in figure 49. Tabulated data is included in Appendix A.

Figure 50 is a recording of the output of interface selector serial W3 with a step change in input frequency. The indicated temperature (Ti) curves are the output of the frequency-to-analog converter and reflect the step change in input frequency. The temperature output (To) curves represent the system indicator (0 to 5 volts) output. It is on these curves that the variation-in-time constant as a function of pressure can be seen. The time constant varies from 7 sec at 100 psia to 14 sec at 50 psia and to 35 sec at 20 psia. The TIGT curves have the same compensation as the To curves but with a 2-sec lag added to this output.

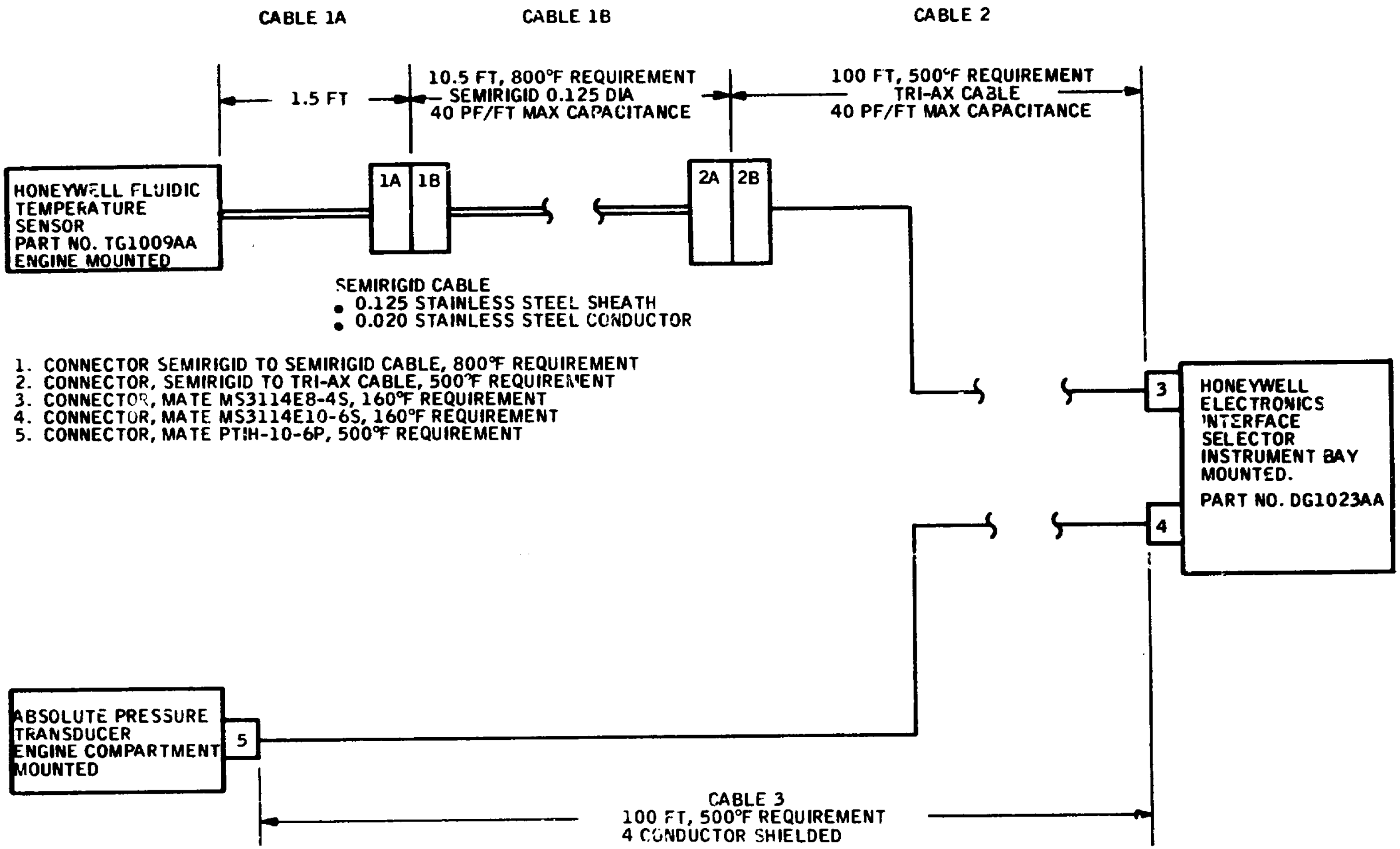

Figure 48. Cable and Connector Requirements

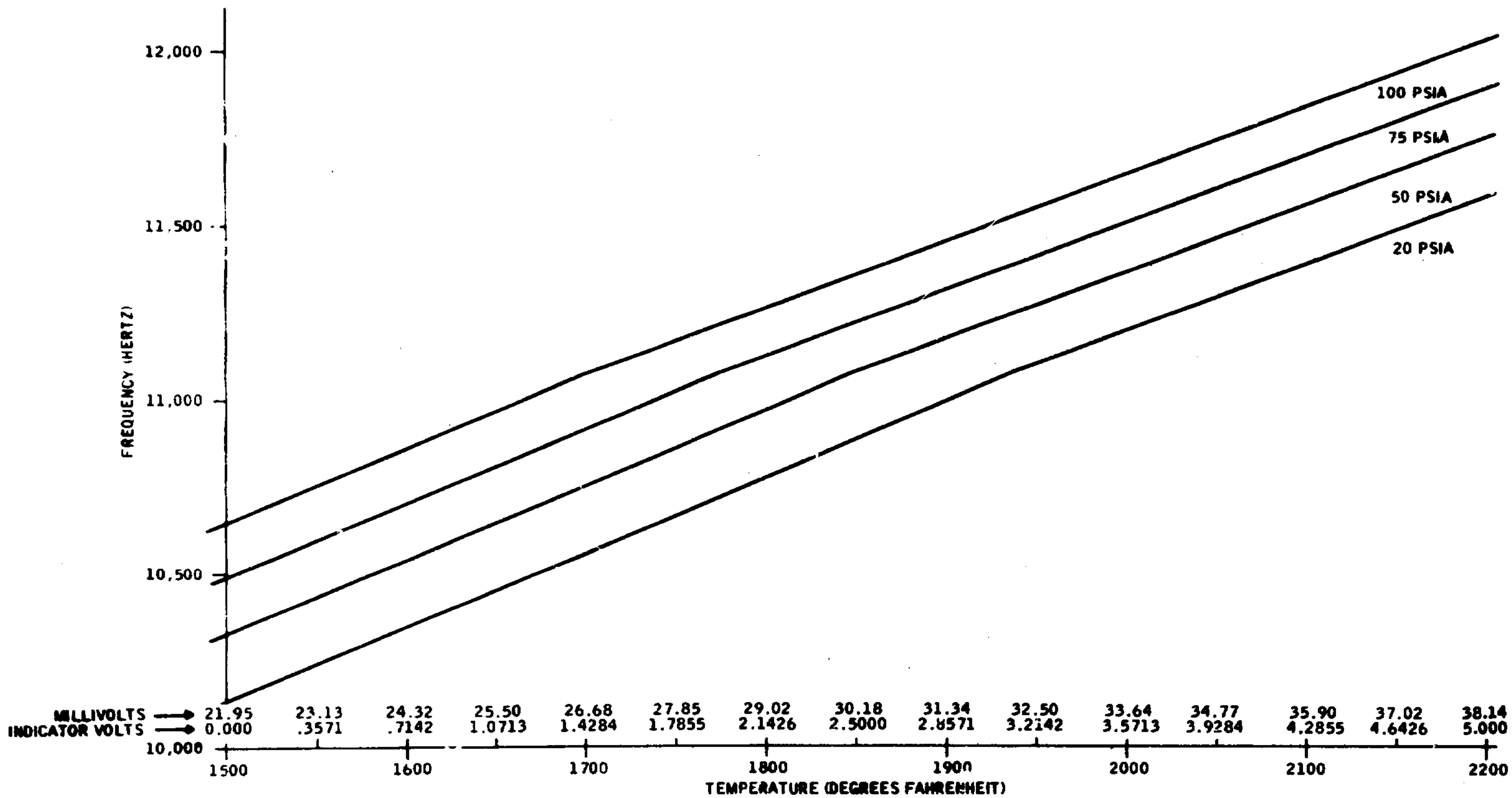

Figure 49. Steady-State Calibration Curves TIGT Interface Selectors Serial W3 and W4

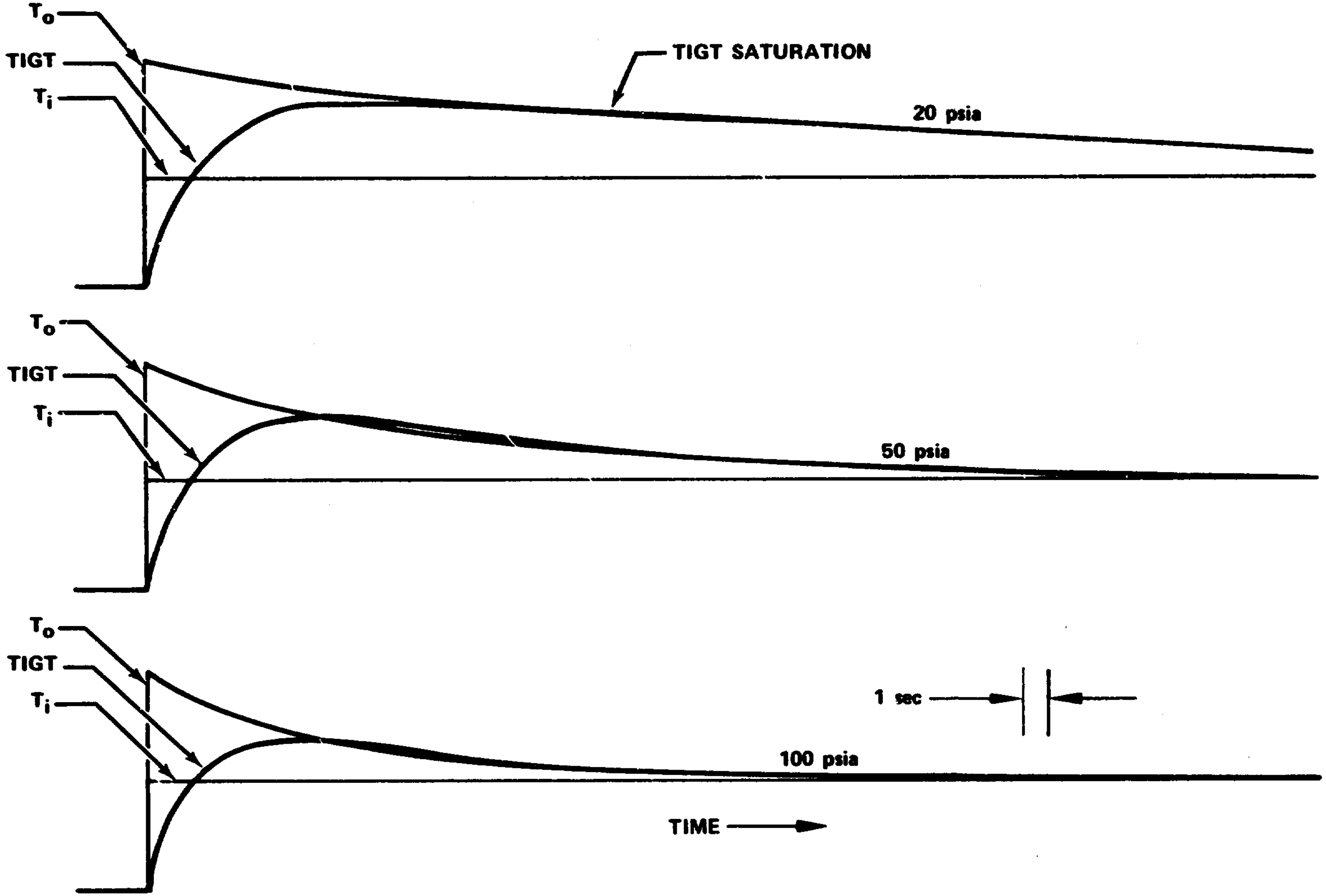

Figure 50. Visicorder Traces

FD 81228

The dynamic response goals of the TIGT measurement system are described in Section II. A. 2. Dynamic testing of the TIGT measurement system was initiated early in the bench test (Phase III) effort. The first attempt at creating a step change was made using the fuel valve as shown in figure 38 and moving it rapidly to create a step change in combustor exit temperature. This method proved unsatisfactory because the response of the fuel control valve was slower than required to generate the desired rate of temperature change.

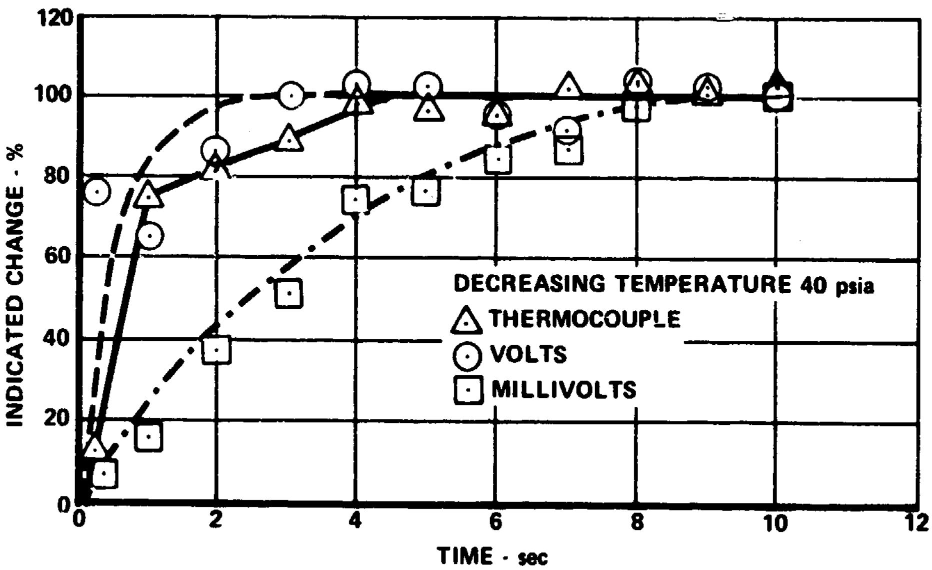

Figure 51. Response Test Data of TIGT Flight Test System FD 76206

The test rig was then modified to include the solenoid valve and downstream hand valve shown in figure 38 to provide an instantaneous bypass of fuel away from the combustor fuel nozzle. This configuration allowed temperature rates of about 1500°F sec on the initial ramp and about 700°F sec over the first sec of the transient. A plot of the development systems dynamic performance using this configuration is shown in figure 52. It shows that about 80% of the initial ramp was indicated. The experimental interface selector contained a dynamic compensation level of 50% which was adequate for small changes in gas temperature as illustrated in figure 42. However, the 50% level was not adequate for changes over 200°F in gas temperature. Figure 52 shows the unacceptable level of dynamic response provided by the experimental units.

The flight test units, calibrated with increased dynamic compensation, were subjected to transient response tests using the same test rig configuration described above. The flight configuration TIGT system indicated a higher change in temperature than the thermocouple at the 0.1-sec time for all tests. At the 3-sec time the indicated temperature was 0 to 10% of the change indicated by the thermocouple and agreed within 4% of the temperature change after 10 sec. The combustor temperature was varied from about 1600°F to about 2200°F during these tests making approximately a 600°F change. Therefore the 4% difference, which was a worse case, represented 24°F. The steady-state tolerance band is 40°F. Therefore, it is concluded that the TIGT measurement system met the design goals for steady-state and dynamic performance. Figure 51 shows the level of dynamic response provided by the flight test units. The millivolt indication shown in figure 51 lags the two rapid indicators due to the 2-sec lag included for compatibility with the J58 EGT control system. Additional dynamic response data is included in Appendix B.

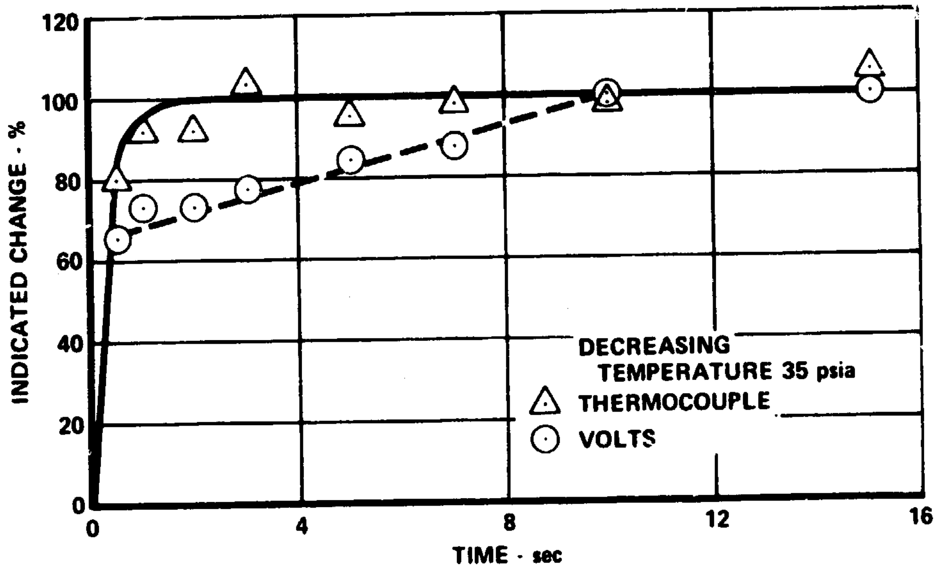

Figure 52. Response Test Data of TIGT Experimental System FD 76205

SECTION VI

RECOMMENDATIONS

This program has accomplished the established objectives that should lead to a successful flight test demonstration of the temperature measurement system. A major effort was devoted to system performance improvement through design of system response compensation in the signal conditioner electronics. During this design effort, much was learned about sensor installation effects, and later testing with the high response system provided new data on turbine inlet temperature noise characteristics and possible changes in temperature profiles. These efforts have defined the following areas for continued development.

1. Conduct the planned flight test with emphasis on TIGT Measurement System susceptibility to (1) operational thermal environment, (2) operational electromagnetic environment, and (3) operational physical environment (vibration, acoustic, etc.).

2. The TIGT system was applied to a steady-state trim control with limited authority. Future effort will be required to address the application of TIGT measurement technology to a high response, authoritative control system.

3. Sensor performance analyses indicate the need for a sensor/probe design effort with the objective of a fully integrated design.

4. Multiple point temperature measurement is required to assess the potential to optimize engine performance and protection. Application of multiple sensors in a propulsion system control, filtering of signals from sensors indicating true combustion noise, and signal averaging efforts are required.

5. Programs are in progress that address the materials and sensor concept problems associated with the advent of engines having TIGT in the range of 2500°F to 3500°F. Continuation of these programs is also required to meet the temperature measurement needs on advanced turbine engines.

SECTION VII

CONCLUSIONS

This program concluded with the development of a TIGT measurement system using a fluidic temperature sensor. The purpose of this program was to expose the fluidic temperature sensing technology to an operational environment and to explore the unknowns of turbine inlet temperature control. A single point sample of temperature was chosen to accomplish the assigned task to minimize cost and risk. Although some knowledge of the TIGT dynamics existed prior to this program the full scope of dynamic TIGT frequency and amplitude was not exposed until well into the engine test. (See Phase III.) An additional phenomenon discovered was that the characteristics of local TIGT varied with time at constant average EGT. This characteristic revealed that a single point sample was inadequate for use in an operational engine control system. However, exploratory stand and flight testing could be conducted.

The system configured in this program utilized advanced state-of-the-art materials that could be procured. The hot gas sampling probe was constructed of a columbium alloy B66 which had previously demonstrated over 50-hr life at 2300°F. The fluidic sensor was constructed of a thorium dispersed nickel chromium with aluminum (TD Ni Cr Al). This material had been previously developed by an independent contractor sponsored by NASA. A 50-hr life test at 2200°F was successfully conducted on a prototype sensor constructed of TD Ni Cr Al. Based upon the materials survey conducted as part of this program and the negative results of other programs that were funded for the purpose of identifying materials capable of withstanding more severe conditions, a conclusion is made that the above temperatures represent the upper limits of uncooled fluidic temperature sensing at this time.

Causes of performance degradation in fluidic temperature sensors have been identified as the absolute temperature and the absolute pressure (density) of the gas passing through the sensor. These parameters cause erosion of the inlet nozzle and leading edge of the splitter which cause the sensor output frequency to change at fixed inlet condition. This also introduces noise into the pressure wave that is sensed to indicate temperature and thereby become a source of noise. An additional degradation characteristic that has been identified is the oxidation of the diaphragm that seals the hot gas from the frequency sensor and also excites the frequency sensor. This oxidation decreases the receiver volume causing an increase in output frequency. This latter degradation was found to be minimized by a "burn in" process induced as part of the assembly and calibration procedure.

The applicability of turbine inlet temperature sensing to control modes for future engines has revealed that, in complex cycle engines, TIGT is not the unique performance parameter that it is in turbojet engines with few cycle variables. This is caused by TIGT becoming a dependent variable when the engine cycle includes variable compressor geometry, variable turbine geometry and variable turbine cooling airflow. Table VI compares the performance variation of such an engine using TIGT and pressure ratio.

Table VI. Engine Performance Comparison Using TIGT and Pressure Ratio

WF Control Mode	Variation Due To Sensing Errors % FN	Variation Due To Extractions 0 → 50 HP % FN	0 → 2 PPS Bleed % FN
Pressure Ratio	0.26	0.09	-0.86
TIGT (55°F Error)	1.40	-0.11	-3.88
TIGT (No TIGT Error)	0.41		

It can be concluded from table VI that complex cycle engine control mode studies do not favor TIGT for thrust control. However, the application of TIGT for use as thrust control mode in simple cycle engines remains a potential.

FUTURE DEVELOPMENT

The fluidic temperature sensor designed to measure the turbine inlet gas temperature of the J58 engine has been developed and qualified for flight tests in a YF-12 aircraft.

The transient response and steady-state accuracy of the TIGT measurement system meet the YF-12 flight test requirements.

Due to TIGT fluctuations at a single location, overall engine control system performance cannot be adequately evaluated without a multiple TIGT sampling system.

A program to define; (1) the number of sampling locations required for an adequate TIGT average, (2) the most effective method of averaging multiple individual electrical frequency signals and, (3) the demonstration of such a system is the next logical step in the development of a fluidic turbine inlet gas temperature control system.

REFERENCES

1. Small, Capt. L., "Turbine Engine Sensors for High Temperature Applications," Technical Paper Presented at 17th Annual International Gas Turbine Conference, March 1972.

2. Johnson, J. L., "Turbine Inlet Temperature Measuring System," Technical Report, AFFDL-TR-69-92, November 1969.

3. Kunkle, C. B., "Advanced Hybrid Propulsion System Control Program," Final Report, Technical Report, AFAPL-TR-71-8, February 1971.

APPENDIX A

TIGT MEASUREMENT SYSTEM TEST RESULTS

The results of TIGT sensor and interface selector calibrations at Honeywell are presented in this section.

TIGT sensors used in the development program were identified as SN X-1 through SN X-5. TIGT sensors delivered for flight tests were identified SN W6 and SN W7. The data taken as final calibrations on these units prior to shipment from Honeywell are included in tables VII through X.

Table VII. Result of TIGT Sensor and Interface Selector

SN X-1			SN X-2		
Sensor Inlet Temperature, °F	Sensor Inlet Pressure, psig	Output Frequency, Hz	Sensor Inlet Temperature, °F	Sensor Inlet Pressure, psig	Output Frequency, Hz
70	15	5702	90	15	5828
70	30	5725	90	30	5855
70	50	5745	90	50	5874
71	70	5756	91	70	5887
71	110	5770	91	110	5900
305	15	6744	305	15	6749
291	30	6737	299	30	6775
291	50	6770	300	50	6811
284	70	6765	301	70	6834
283	110	6774	300	110	6848
602	15	7868	606	15	7886
598	30	7910	600	30	7928
593	50	7936	598	50	7956
598	70	7985	606	70	7997
600	110	8038	606	110	8037
908	15	8931	902	15	8847
909	30	8966	902	30	8917
900	50	8980	902	50	8962
905	70	9017	902	70	8990
913	110	9079	902	110	9018
1200	15	9800	1200	15	9777
1195	30	9811	1200	30	9798
1196	50	9850	1200	50	9851
1200	70	9897	1200	70	9893
1200	110	9945	1200	110	9930
1512	15	10654	1501	15	10648
1488	30	10645	1501	30	10650
1502	50	10679	1501	50	10684
1508	70	10718	1508	70	10732
1512	110	10761	1501	110	10726
1781	15	11332	1792	15	11348
1781	30	11347	1794	30	11375
1808	50	11430	1802	50	11422
1810	70	11457	1802	70	11450
1817	110	11504	1802	110	11470

Table VIII. Result of TIGT Sensor and Interface Selector

SN X-3			SN X-4		
Sensor Inlet Temperature, °F	Sensor Inlet Pressure, psig	Output Frequency, Hz	Sensor Inlet Temperature, °F	Sensor Inlet Pressure, psig	Output Frequency, Hz
76	15	5755	74	15	5719
76	30	5785	74	30	5750
77	50	5808	74	50	5767
77	70	5819	74	70	5783
77	110	5832	75	110	5805
302	15	6750	306	15	6730
303	30	6802	298	30	6744
302	50	6830	300	50	6793
298	70	6834	300	70	6811
299	110	6873	297	110	6828
600	15	7872	596	15	7816
599	30	7925	599	30	7880
601	50	7985	600	50	7928
603	70	8022	603	70	7975
600	110	8053	599	110	8005
900	15	8899	900	15	8846
900	30	8941	900	30	8913
897	50	8989	900	50	8960
900	70	9028	896	70	8980
900	110	9070	900	110	9027
1192	15	9828	1192	15	9741
1200	30	9846	1200	30	9776
1204	50	9896	1200	50	9847
1197	70	9929	1200	70	9870
1200	110	9978	1201	110	9909
1500	15	10658	1504	15	10620
1500	30	10672	1501	30	10590
1502	50	10713	1500	50	10652
1502	70	10738	1503	70	10686
1504	110	10784	1500	110	10710
1774	15	11377	1764	15	11283
1788	30	11418	1773	30	11290
1778	50	11407	1800	50	11374
1800	70	11473	1792	70	11390
1800	110	11510	1800	110	11411

Table IX. Result of TIGT Sensor and Interface Selector

SN X-5		
Sensor Inlet Temperature, °F	Sensor Inlet Pressure, psig	Output Frequency, Hz
86	15	5839
86	30	5864
86	50	5882
86	70	5893
86	110	5906
306	15	6793
301	30	6825
300	50	6850
299	70	6872
297	110	6887
600	15	7892
594	30	7933
600	50	7997
602	70	8034
602	110	8083
900	15	8904
901	30	8980
904	50	9026
900	70	9047
900	110	9087
1202	15	9818
1200	30	9886
1200	50	9916
1210	70	9980
1200	110	9985
1500	15	10705
1500	30	10716
1500	50	10746
1500	70	10775
1500	110	10800
1760	15	11336
1764	30	11339
1783	50	11436
1787	70	11489
1800	110	11535

Table X. Result of Flight Test TIGT Sensors Calibration

SN W6			SN W7		
Sensor Inlet Temperature, °F	Sensor Inlet Pressure, psig	Output Frequency, Hz	Sensor Inlet Temperature °F	Sensor Inlet Pressure, psig	Output Frequency, Hz
72	15	5687	72	15	5723
72	30	5715	72	30	5750
72	50	5734	72	50	5770
72	70	5743	73	70	5783
73	110	5755	73	110	5793
300	15	6661	295	15	6750
300	30	6739	295	30	6768
300	50	6764	295	50	6817
300	70	6778	298	70	6835
298	110	6785	298	110	6860
600	15	7835	600	15	7853
600	30	7845	600	30	7895
600	50	7889	596	50	7931
600	70	7940	596	70	7963
600	110	7978	600	110	8003
900	15	8880	900	15	8927
907	30	8926	916	30	9001
900	50	8943	914	50	9057
913	70	8999	916	70	9041
900	110	9003	916	110	9084
1200	15	9796	1193	15	9817
1200	30	9819	1210	30	9890
1205	50	9851	1210	50	9914
1205	70	9865	1210	70	9935
1205	110	9898	1227	110	9997
1496	15	10537	1503	15	10654
1501	30	10567	1508	30	10669
1500	50	10618	1508	50	10730
1500	70	10651	1508	70	10748
1526	110	10744	1530	110	10796
1755	15	11000			
1783	30	11283	1778	30	11329
1800	50	11346	1802	50	11410
1801	70	11362	1815	70	11460
1802	110	11388	1820	110	11496

Interface selectors delivered for flight tests were identified as SN W3 and SN W4. Both units were calibrated to the same test specification which is presented in tables XI through XIII. This is the tabular data from which figure 49 was plotted.

Table XI. Calibrated Test Specifications
(Max Pressure - 0.025 (100 psi))

Simulated Temperature	Frequency	TIGT (mv)	Indicator (volts)
1500	10651	21.95 ± 0.46	0.000 ± 0.142
1550	10759	23.13	0.3571
1600	10866	24.32	0.7142
1650	10973	25.50	1.0713
1700	11080	26.68	1.4284
1750	11172	27.85	1.7855
1800	11265	29.02	2.1426
1850	11358	30.18	2.5000
1900	11451	31.34	2.8571
1950	11543	32.50	3.2142
2000	11636	33.64	3.5713
2050	11729	34.77	3.928[illegible]
2100	11822	35.90	4.2855
2150	11915	37.02	4.6426
2200	12008	38.14	5.0000

Table XII. Calibrated Test Specifications
(Pressure 20 psi (0.005 volts))

Simulated Temperature	Frequency	TIGT (mv)	Indicator (volts)
1540	10223	22.9[illegible]	0.2851
1590	10330	24.08	0.6428
1640	10437	25.27	0.9999
1690	10544	26.45	1.357
1740	10651	27.62	1.7141
1790	10759	28.79	2.0712
1840	10866	29.95	2.4286
1890	10973	31.11	2.7857
1940	11080	32.27	3.1428
1990	11172	33.41	3.4999
2040	11265	34.55	3.8570
2090	1135[illegible]	35.68	4.2141
2140	11451	36.80	4.5712
2190	11543	37.92	4.9281

Table XIII. Calibrated Test Specifications
(Pressure 50 psi (0.0125))

Simulated Temperature	Frequency	TIGT (mv)	Indicator (volts)
1500	10330	21.95	0.000
1550	10437	23.13	0.3571
1600	10541	24.32	0.7142
1650	10651	25.50	1.0713
1700	10759	26.68	1.4284
1750	10866	27.85	1.7855
1800	10973	29.02	2.1426
1850	11080	30.18	2.500
1900	11172	31.34	2.8571
1950	11265	32.50	3.2142
2000	11358	33.64	3.5713
2050	11451	34.77	3.9284
2100	11543	35.90	4.2855
2150	11636	37.02	4.6426
2200	11729	38.14	5.000

APPENDIX B

Test data taken during the FRDC Bench and Engine testing of the TIGT measurement system are contained in this appendix. The data included are for both system and component test results and are presented in the chronological order that it was generated.

Two nonflight configuration TIGT measurement systems were delivered for laboratory testing purposes. These systems as described in paragraph III. D. 6 consisted of a fluidic sensor, hot gas sampling probe, and frequency to voltage converter. The fluidic sensors were identified as SN X-4 and SN X-5 and the converters were identified as SN X-9 and SN X-10.

Both converters were calibrated with sensor SN X-5 and these data are presented in figure 53. Figure 54 shows a comparison of the two converters with simulated TIGT sensor input. The performance of SN X-4 sensor and SN X-9 converter is shown in figure 55.

TIGT sensors calibrated at FRDC operated at a lower frequency for a given temperature than when tested at Honeywell as illustrated in figure 56. Analysis and tests were conducted to identify the source of this difference. The Honeywell calibration was made using air heated in an electric oven and the FRDC calibrations were made using a JP fuel fired combustor. The Honeywell data were corrected for Gas Constant (R) and specific heat difference (τ) between air and combustion gases and resulted in approximately 25°F.

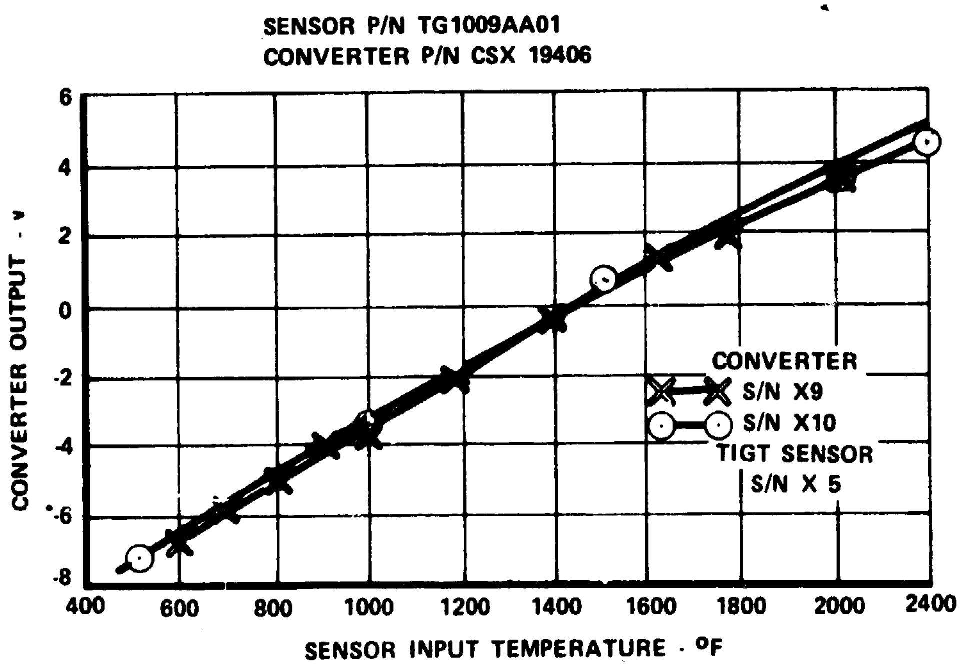

Figure 53. Nonflight TIGT Measurement System Calibration FD 81205

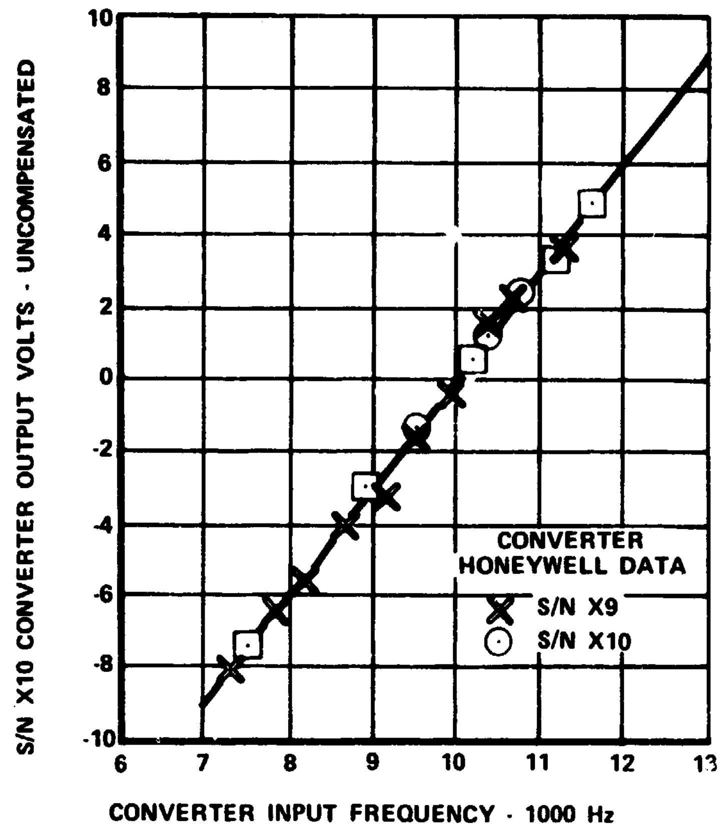

Figure 54. Calibration for Frequency to Voltage Converters FD 81204

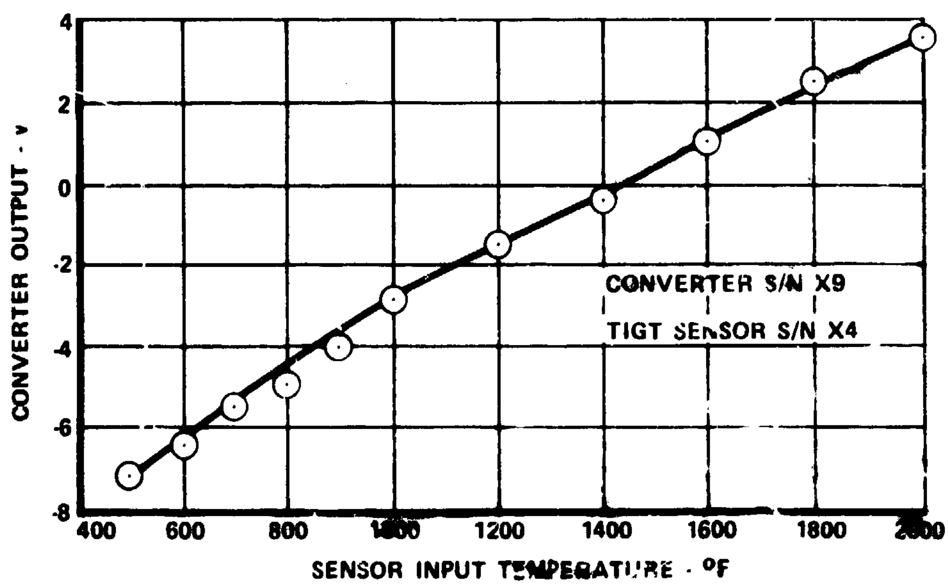

Figure 55. Nonflight Turbine Inlet Gas Temperature Measurement System Calibration FD 81206

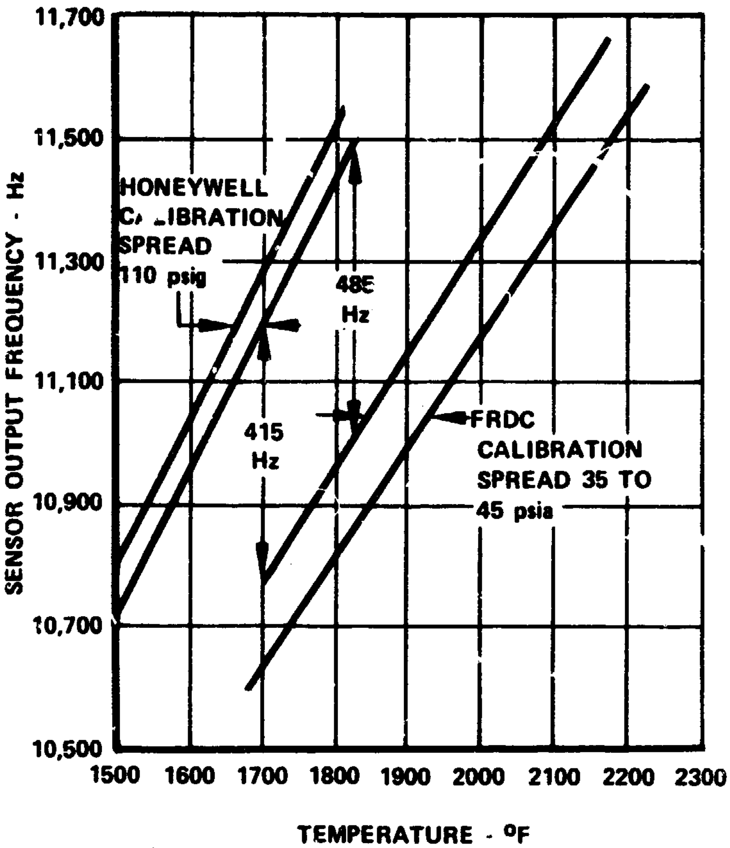

Figure 56. Comparison of Honeywell and FRDC TIGT Sensor Calibrations FD 81207

Subsequent testing led to the conclusion that the major part of the calibration difference was steady-state pressure sensitivity of the sensor/probe assembly. Continued efforts included rig testing the hot gas sampling probe as a component using a bare wire Pt-Pt/Rh (13%) thermocouple to replace the fluidic sensor as shown in figure 57. Initial test results shown in figure 58 indicated a significant difference in temperature (200°F at 2200°F input) between hot gas source and the sampled gas. Further investigation led to the addition of a 0.03 inch gap between the thermocouple flange and thermocouple flange to simulate probe flow as when the fluidic sensor was installed. Tests with this configuration showed the sampled gas to be within 25°F of the hot source (diamonds of figure 58). However, subsequent test of the TIGT measurement system with the fluidic sensor installed and a 0.05 inch spacer between the flanges did not show the same level change, as illustrated by figure 59 indicating that normal fluidic sensor flow was sufficient to flush the probe. These data [figure 60 (3-15-73)] also plotted for fluidic sensor output showed approximately 25°R difference compared to an earlier test [also figure 60 (2-2-73)]. Further analysis revealed that this difference was attributable to a 5 to 10 psi difference in combustor pressure between the two tests.

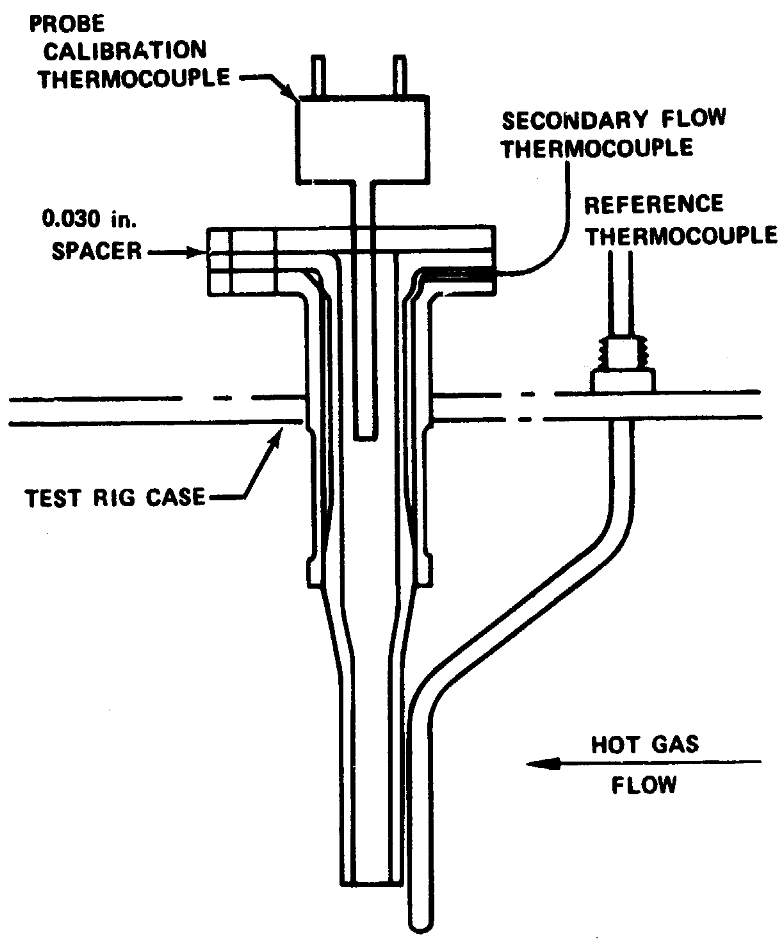

Figure 57. Hot Gas Sampling Probe Calibration Configuration FD 81208

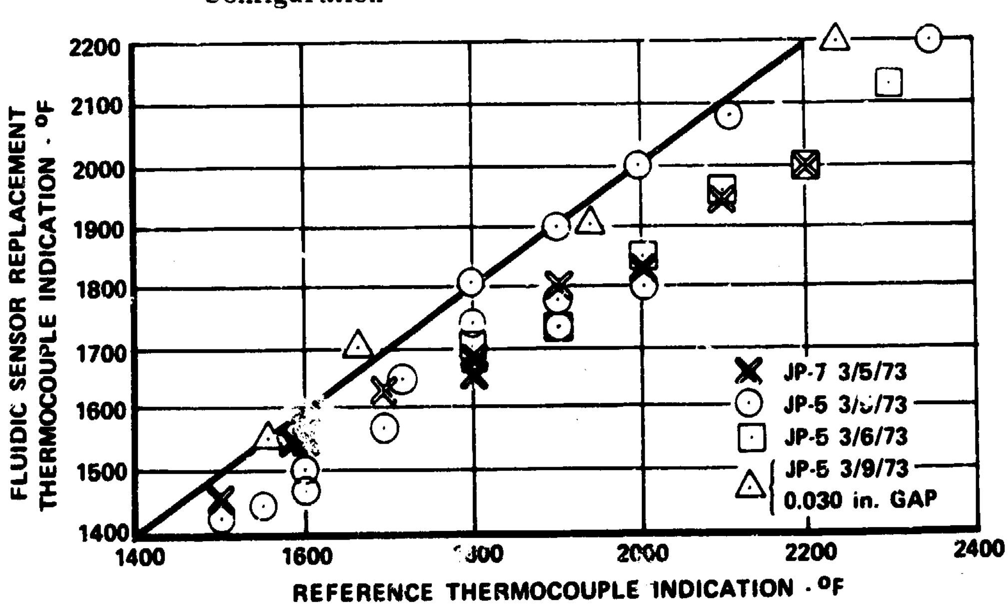

Figure 58. Reference Thermocouple Calibration FD 81209

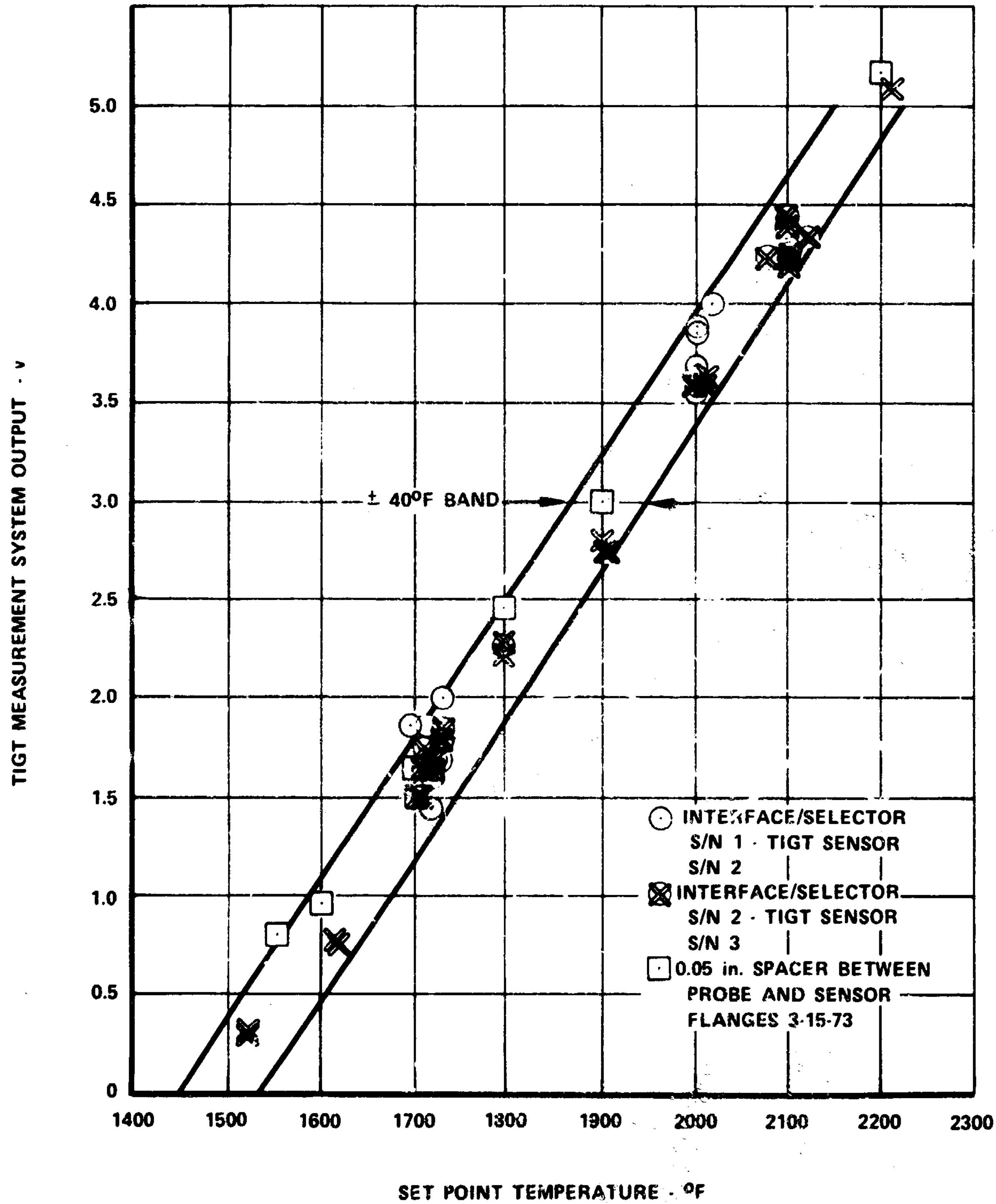

Figure 59. TIGT Measurement System Performance - FD 81210 Pressure Range 25 to 75 psia

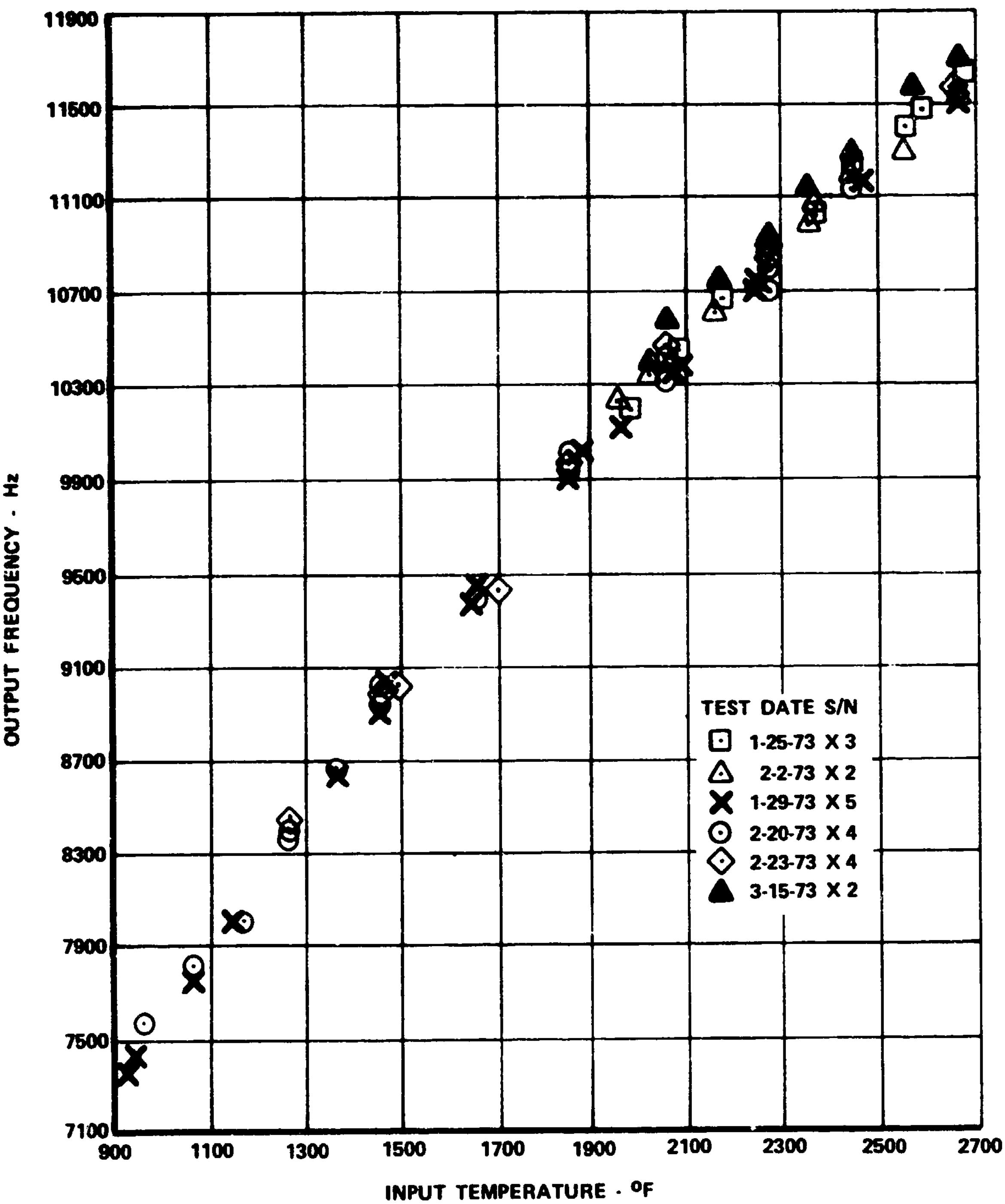

Figure 60. TIGT Sensor Performance FD 81211

One of the functions of the interface selector was to counter bias the effects of gas stream pressure on the fluidic sensor/probe assembly to provide an accurate indication of temperature. Tests were conducted to identify the degree of steady-state bias required. A composite plot of these data shown in figure 61, shows a bias of approximately 5.5 Hz/psi. Interface selector seral number 1 was readjusted to provide additional steady-state compensation as illustrated in figure 62. The X-1 and X-2 units were limited in adjustment capability so the full 5.5 Hz/psi was not available, however, the flight test units were reconfigured and did include full steady-state compensation as described in Section V of the report.

Dynamic tests were conducted on the TIGT measurement system to assess the degree of compliance with the dynamic goals established in the contract and described in Section II of the report. The test rig was modified to include a high (0.04 sec time constant) response Pt-Pt/Rh (13%) thermocouple as shown in figure 63.

Initial dynamic checks were made using the inherent noise of the combustor system. Representative data are shown in figures 64 and 65. The noise level is approximately 160° F as indicated by the thermocouple and the fluidic sensor is indicating 90 to 110% of the noise and leading the thermocouple by approximately 0.05 sec. Rapid changes in combustor temperature were then introduced by alternately opening and closing a valve that dumped fuel flow overboard upstream of the combustor.

Representative plots of the data are shown in figures 66 and 67. It can be seen that the fluidic system led the thermocouple in the early part of the transient but did not provide an accurate indication of the final temperature value. Additional transient data are tabulated on table XIV. The table shows compliance with the 15 sec long time but inadequate 3 sec intermediate time response.

Based upon the results of these tests the dynamic compensation of the flight test units was increased as compared to the experimental units described previously. This is described in Sections II and V of the report.

TIGT measurement system engine tests were initiated with a check of turbine inlet gas temperature versus exhaust gas temperature. The results of these tests are presented in figure 68 and show a phenomenon of variable TIGT at constant EGT. This led to nonconstant engine setting when on TIGT control. This phenomenon is attributed to the fact that EGT is indicated by an average of 36 thermocouple junctions placed around the engine and TIGT is indicated by a single thermocouple junction. A comparison of the TIGT measurement system bench calibration to operation on the engine is shown in figure 69. It shows the engine data to be approximately 30°F higher at low TIGT and 50°F higher at high TIGT. This difference can be explained by the inadequate pressure compensation of the experimental interface selector units described earlier.

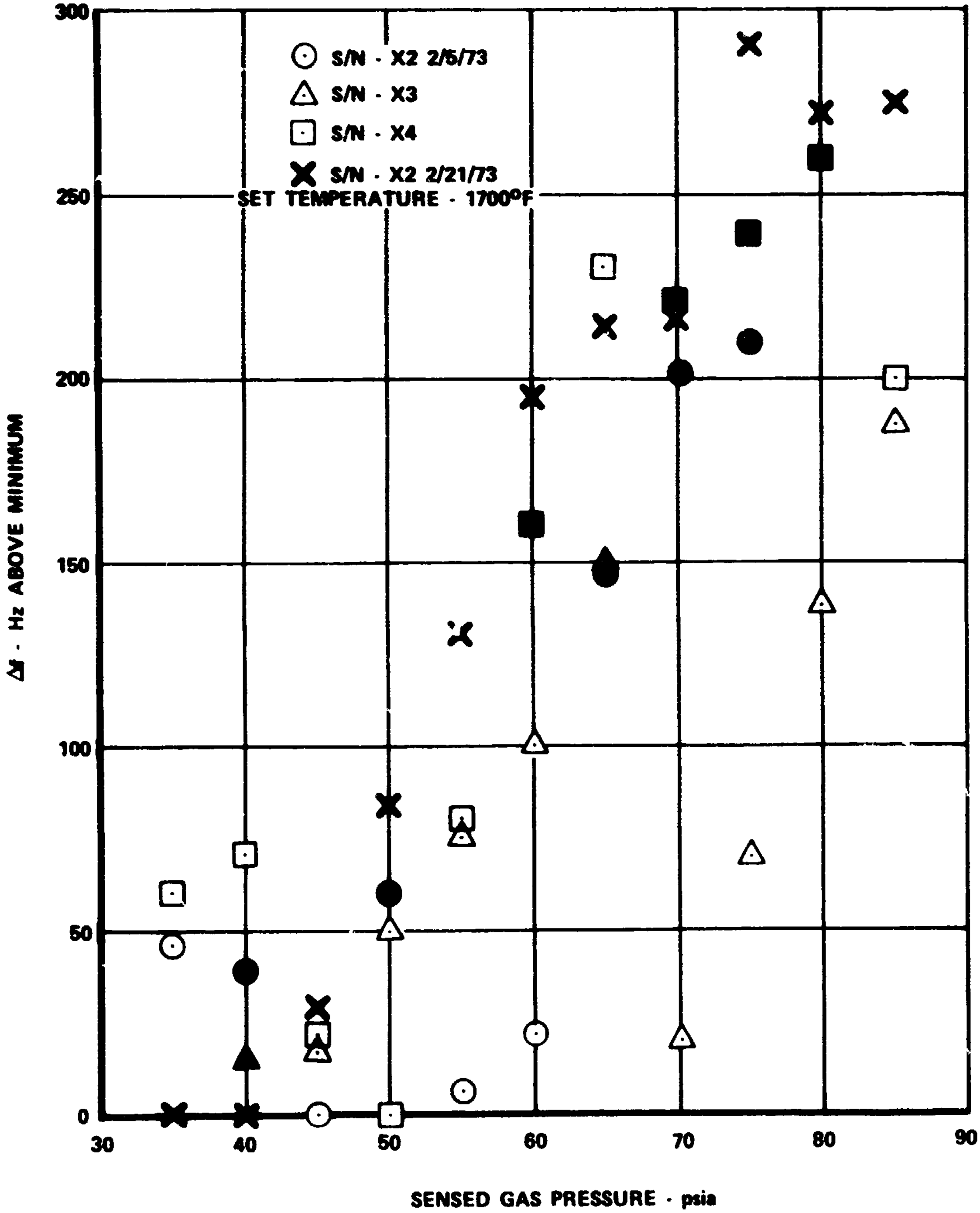

Figure 61. Turbine Inlet Gas Temperature Fluidic Sensors Pressure Sensitivity FD 81212

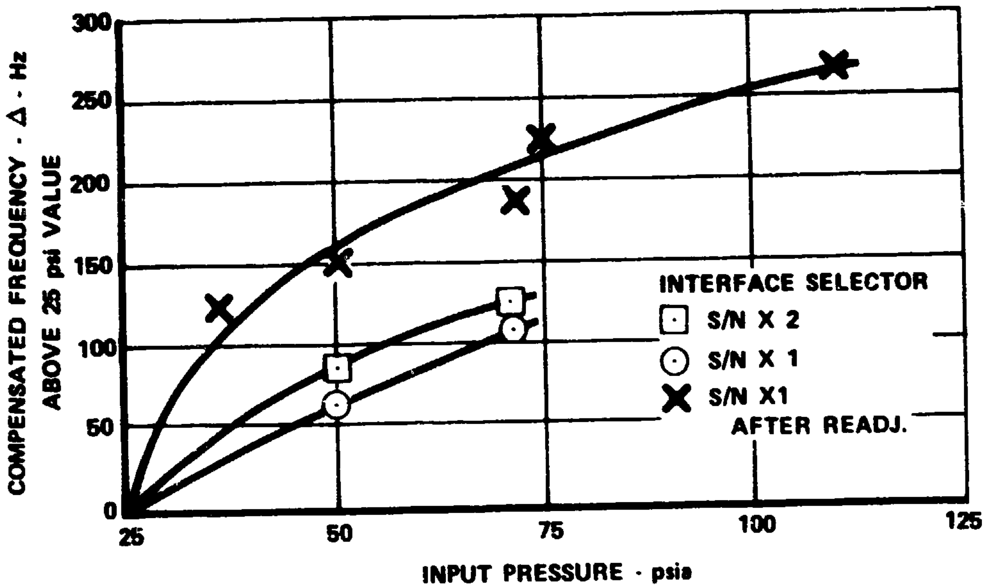

Figure 62. Turbine Inlet Gas Temperature Interface/ Selector Pressure Sensitivity Compensation FD 81213

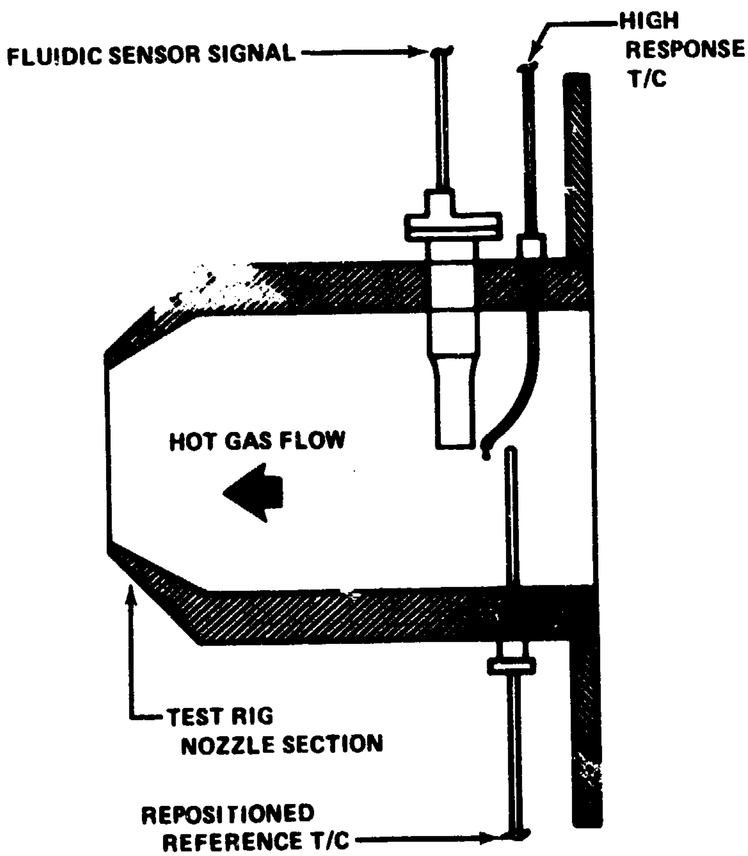

Figure 63. TIGT Measurement System Response Test Setup FD 81214

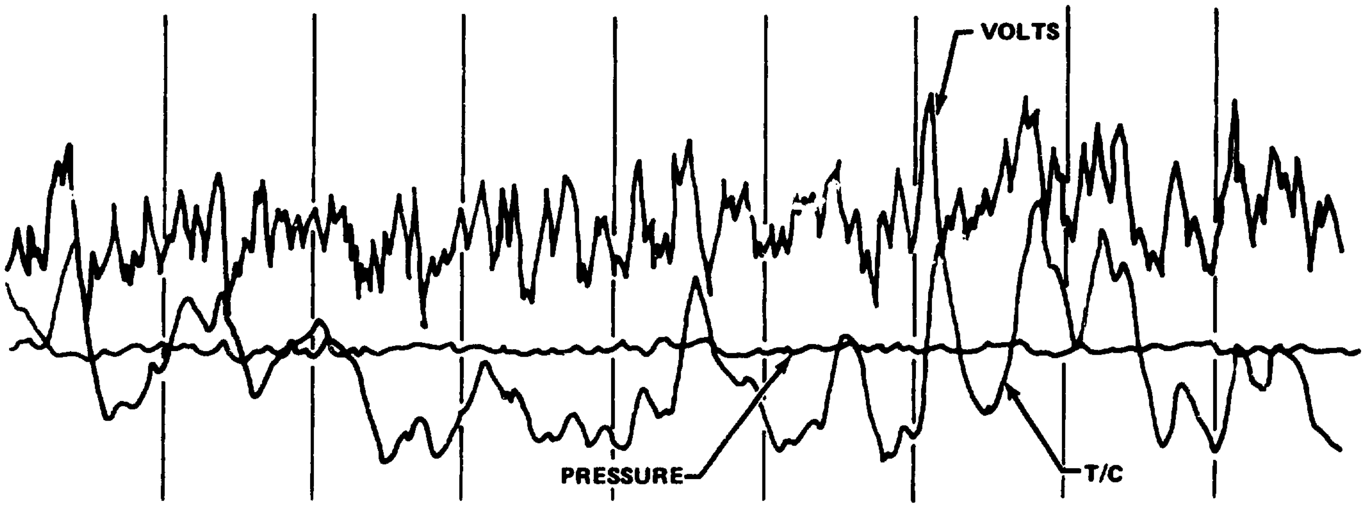

TEST DATE: 3/14/73

TEST CONDITIONS: 2100°F; 30 psia

Figure 64. TIGT Measurement System Resonse: 0.050 in. Flange Spacer

FD 81215

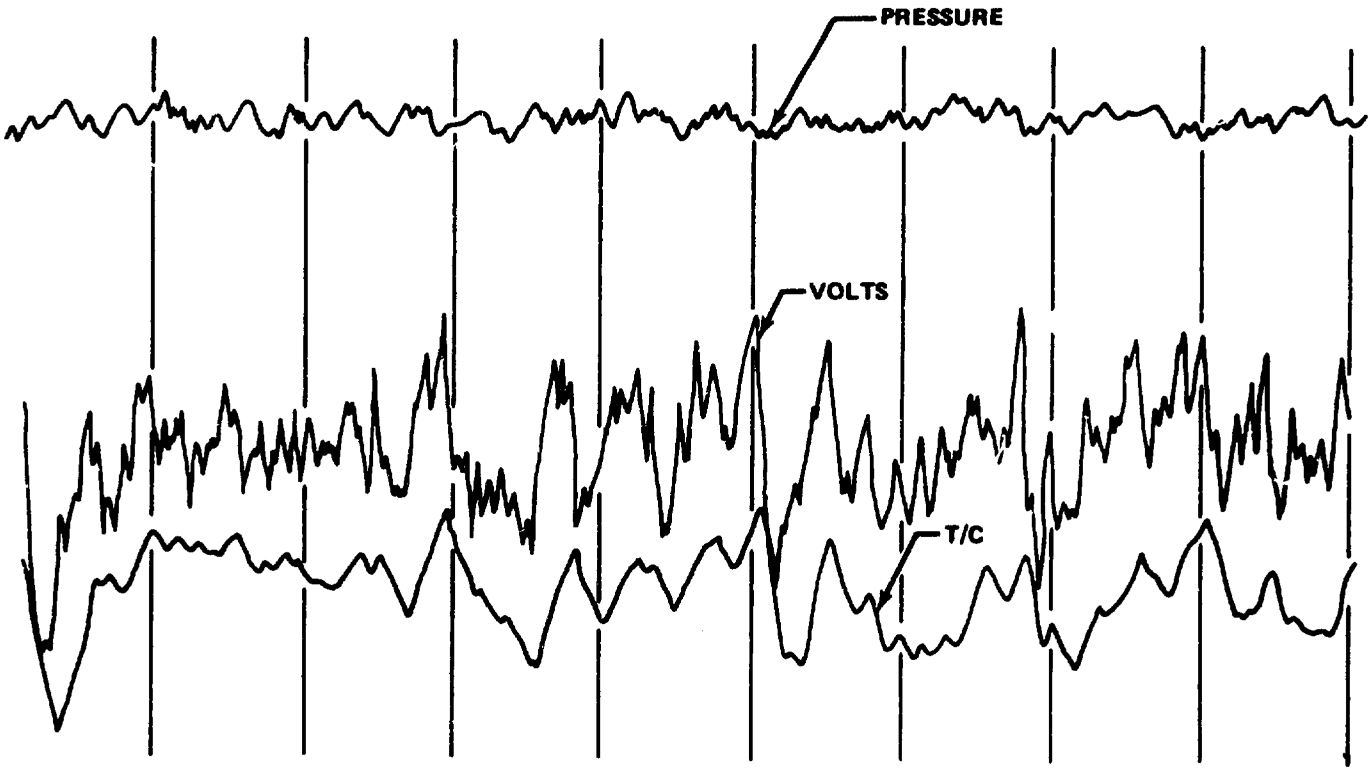

TEST DATE: 3/14/73
TEST CONDITIONS: 2100°F , 50 psia

Figure 65. TIGT Measurement System Response: 0.050 in. Flange Spacer

FD 81216

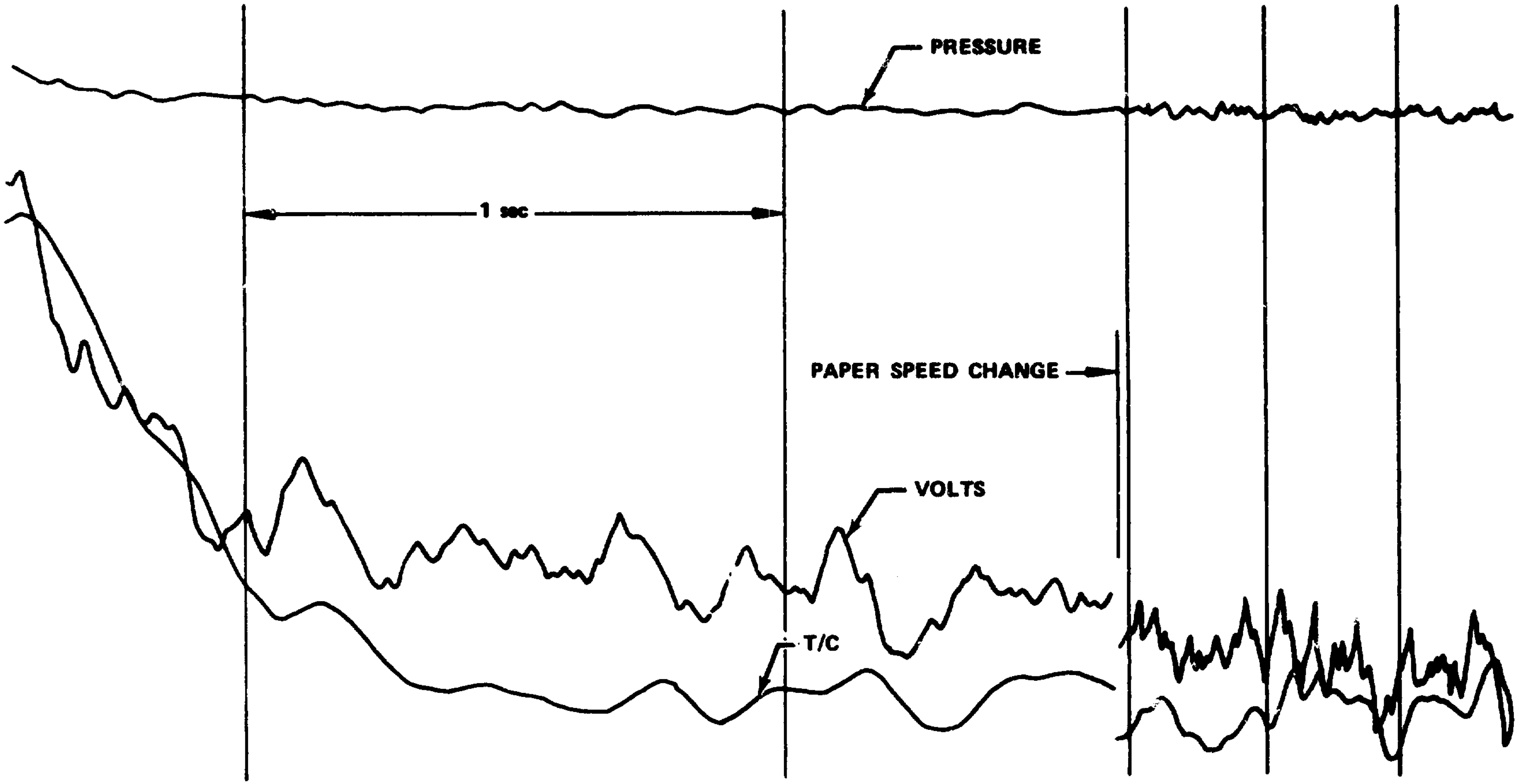

TEST DATE: 3/14/73
TEST CONDITIONS: 2200°F; 50 psia

Figure 66. TIGT Measurement System Response to Step Changes FD 81217

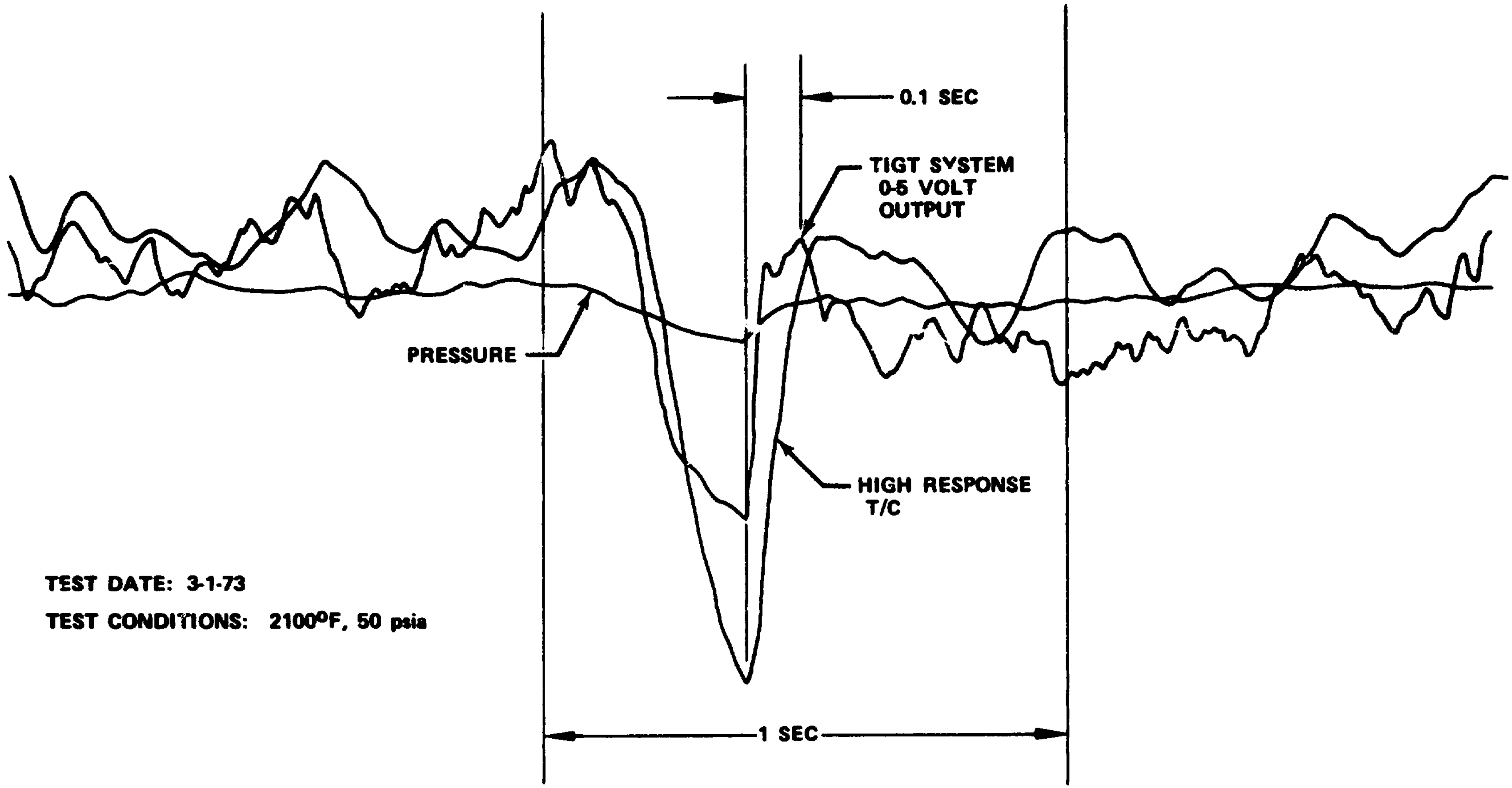

Figure 67. TIGT Measurement System Response to Large Temperature Change

FD 81218

Table XIV. TIGT Measurement System Response to a Step Change

Transient 1

Time	High Response Thermocouple Indication	TIGT Measurement System 0 to 0.5 Volt Indication
0	2370	2260
0.45	1700	1780
1.0	1600	1720
2.0	1600	1730
3.0	1500	1690
5.0	1575	1640
7.0	1550	1620
10.0	1550	1530
15.0	1485	1520

Test Conditions: 50 psia

Transient 2

Time	High Response Thermocouple Indication	TIGT Measurement System 0 to 0.5 Volt Indication
0	2280	2275
0.03	2300	2160
0.38	1850	1790
0.86	1640	1780
1.0	1650	1815
2.0	1660	1675
3.0	1590	1720
4.0	1550	1640
5.0	1470	1650
10.0	1550	1570
15.0	1500	1525

Table XIV. TIGT Measurement System Response to a Step Change (Continued)

Transient 3

Time	High Response Thermocouple Indication	TIGT Measurement System 0 to 0.5 Volt Indication
0	2130	2070
0.02	2150	2025
0.15	1875	1720
0.36	1640	1750
1.0	1500	1680
2.0	1460	1600
3.0	1380	1600
4.0	1400	1535
5.0	1410	1530
10.0	1400	1500
15.0	1450	1500

Transient 4

Time	High Response Thermocouple Indication	TIGT Measurement System 0 to 0.5 Volt Indication
0	1525	1560
0.49	1800	1920
0.60	1875	1710
1.0	2080	1860
2.0	2280	1950
3.0	2125	1920
4.0	2300	2000
5.0	2300	2220
10.0	2300	2140
15.0	2350	2235

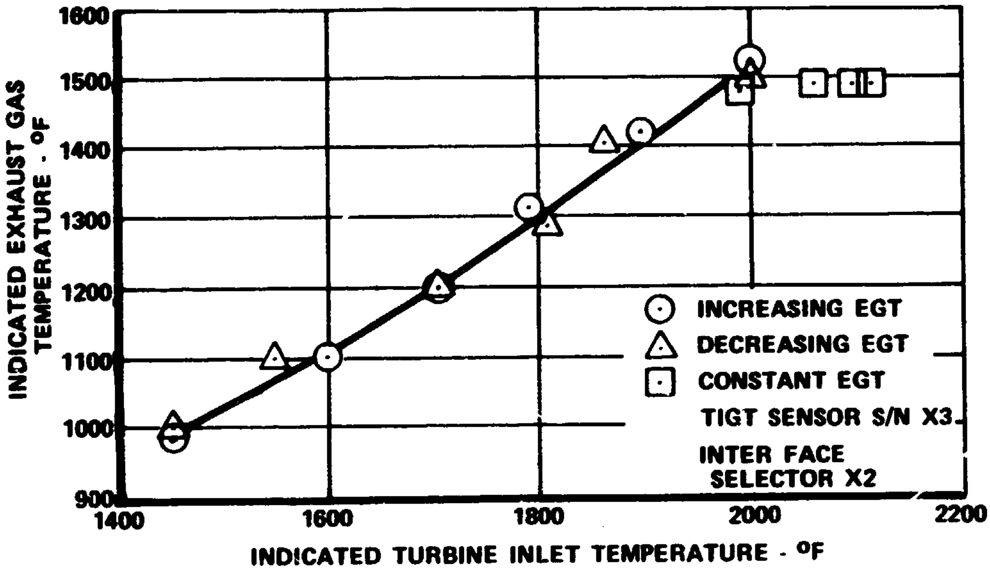

Figure 68. Turbine Inlet Temperature vs Exhaust Gas Temperature FD 81219

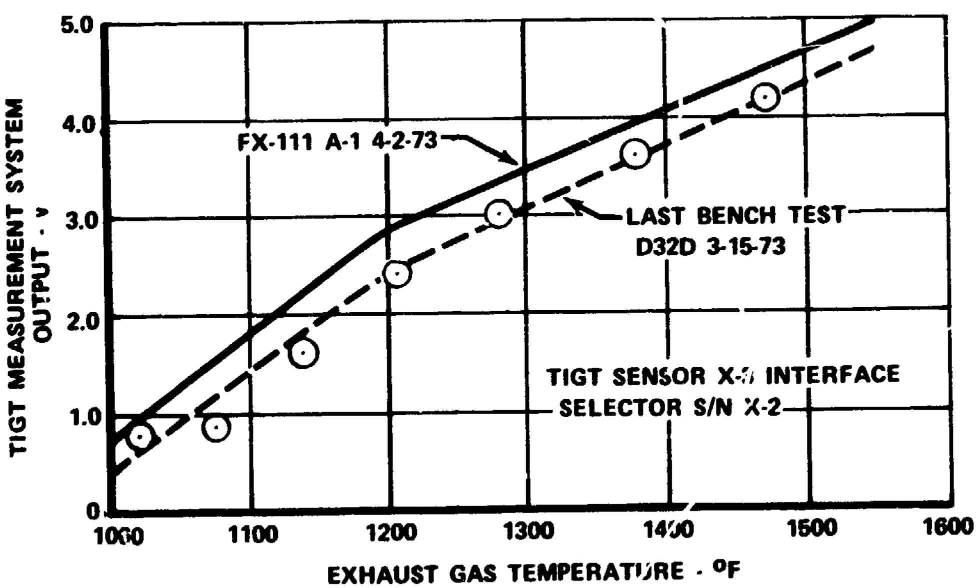

Figure 69. TIGT Measurement System Output Volts Versus Exhaust Gas Temperature FD 81220

Transient data in addition to that shown in Section V taken during the engine tests are shown in figures 70 and 71 and confirm the bench test results that initial response and long time indication conform to the contract goals but intermediate indication is below the goal. A composite plot of 3 days engine operation is shown in figure 72 and illustrates again the variable TIGT at constant EGT. Additional engine operating time history of the fluidic sensor is shown in figures 73 and 74.

Two fluidic sensors were used in the engine test program. Calibration data before and after the engine test are presented in figures 75 and 76 and show minor calibration shifts. Additionally it appears that the calibration shift that did occur took place in the early part of the engine test. As described in Section V, after over 150 engine test hours on SN X-3, no other discrepancy was noted.

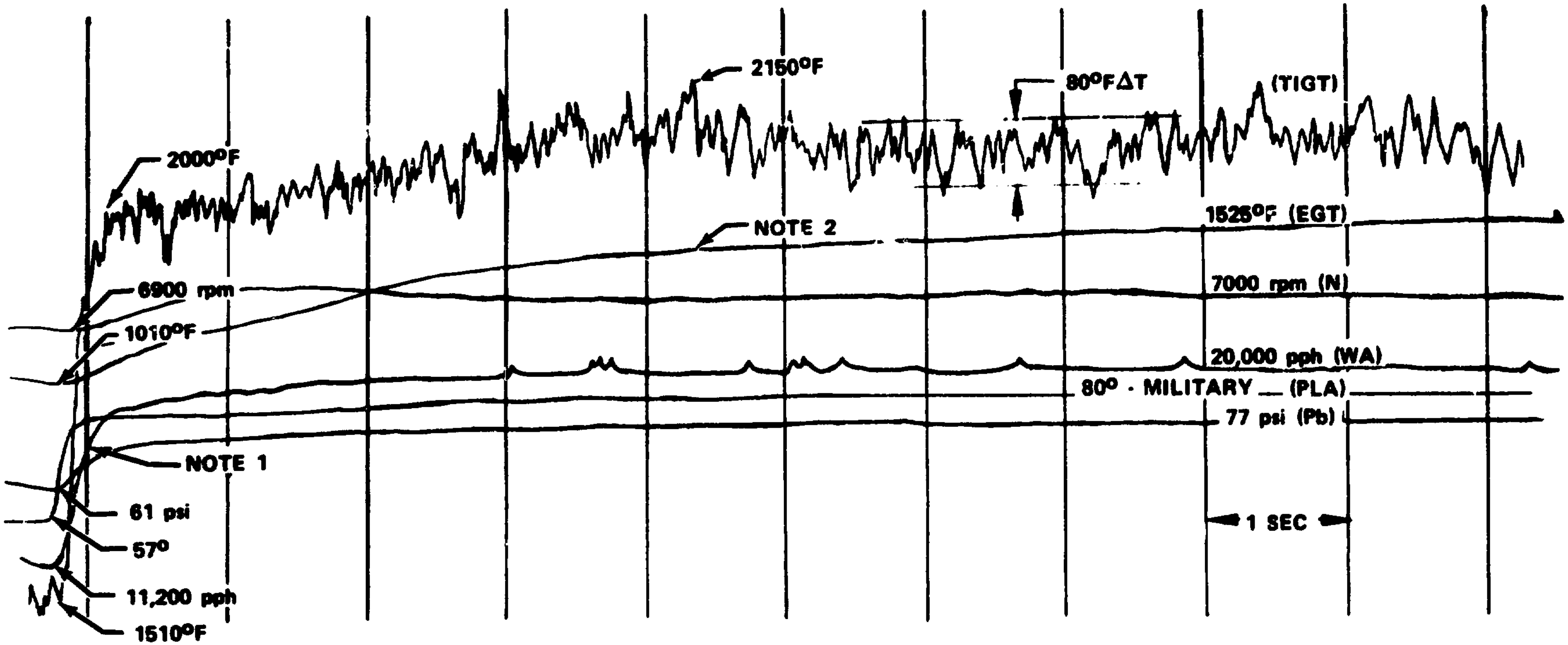

NOTE: 1. FUEL FLOW (W_f) WHERE TIGT WOULD BE 2000°F AT STEADY-STATE
2. EGT WHERE TIGT WOULD BE 2000°F at STEADY-STATE
3. TIGT LAGS W_f BY 0.13 SECONDS AT 2000°F LEVEL

Figure 70. TIGT Measurement System Response: Rapid Increase of Engine Power FD 81221

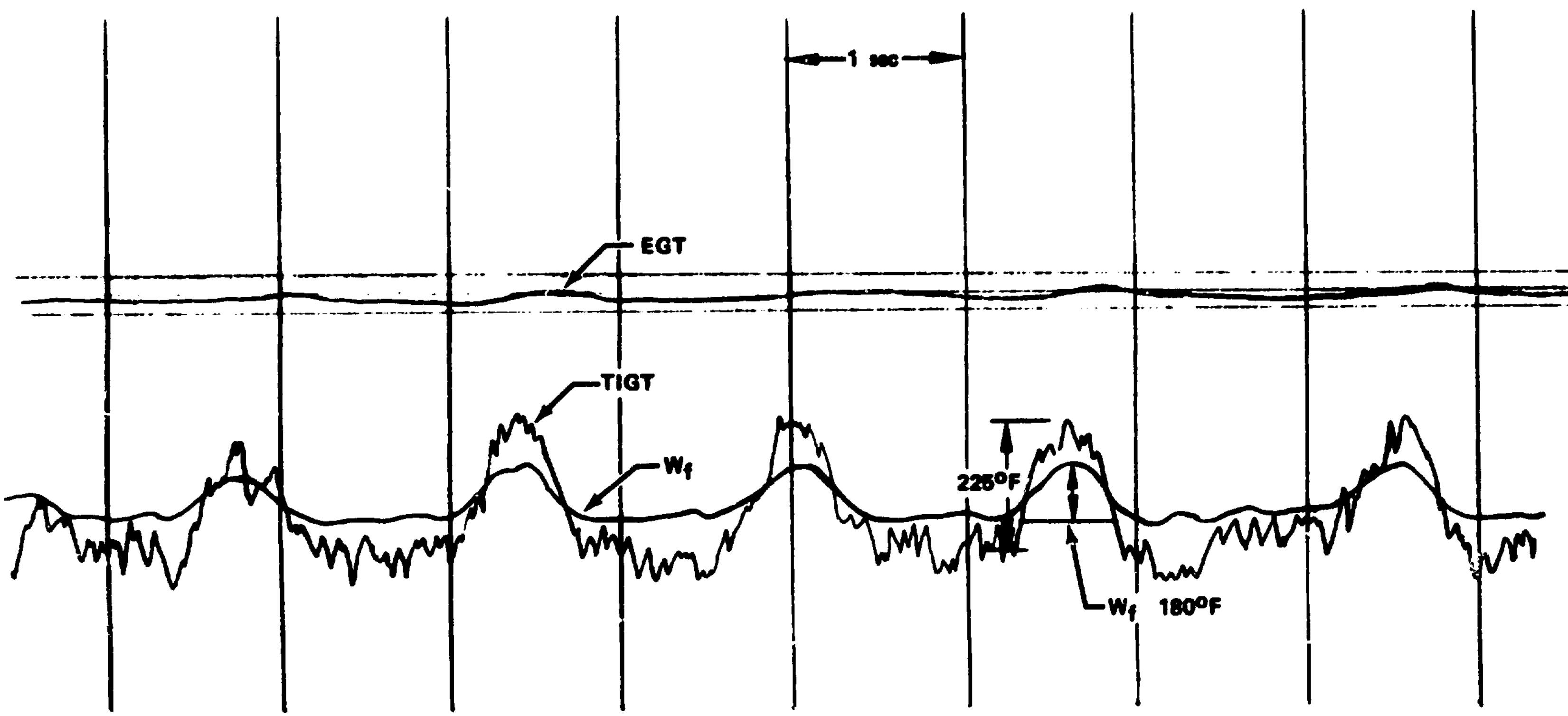

NOTE 1: MAXIMUM W_f RATE IS EQUIVALENT TO 860°F/sec
2: MAXIMUM TIGT RATE IS 700°F/sec

Figure 71. TIGT Measurement System Response to Periodic Engine Fuel Flow Disturbances

FD 81222

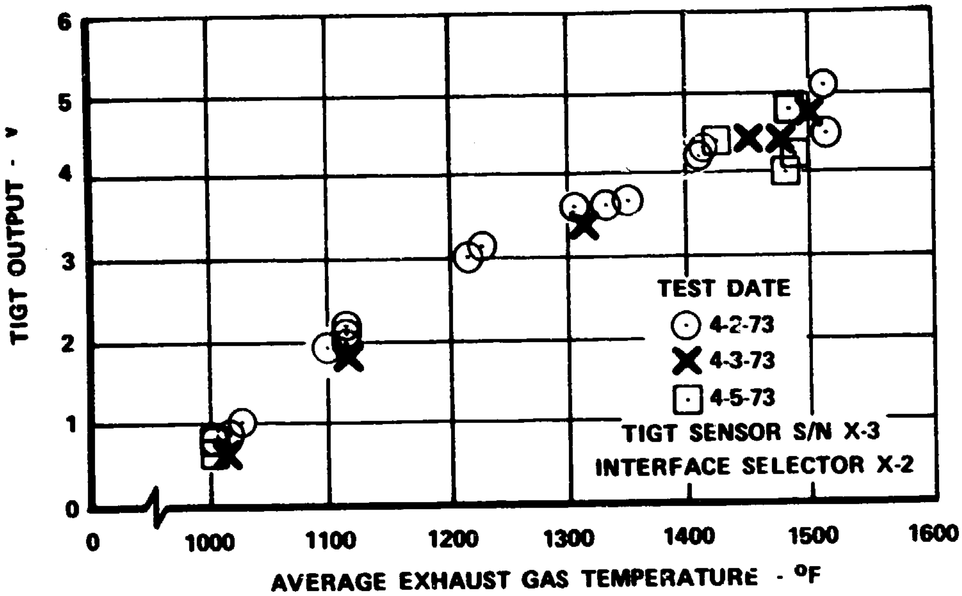

Figure 72. TIGT Measurement System Performance FXlll SL Endurance FD 81223

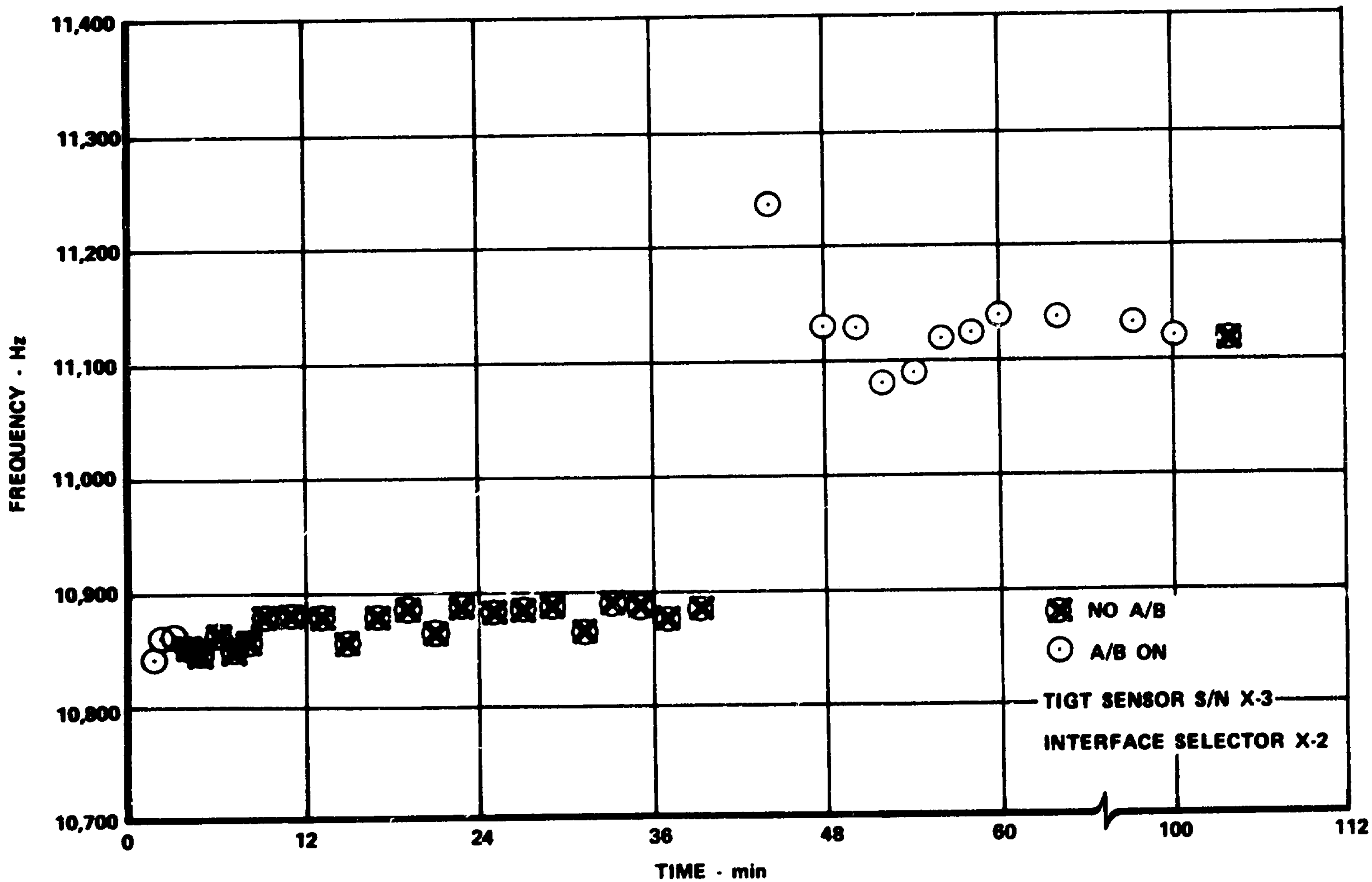

Figure 73. TIGT Sensor Performance Check Beginning of Engine Endurance FD 81224

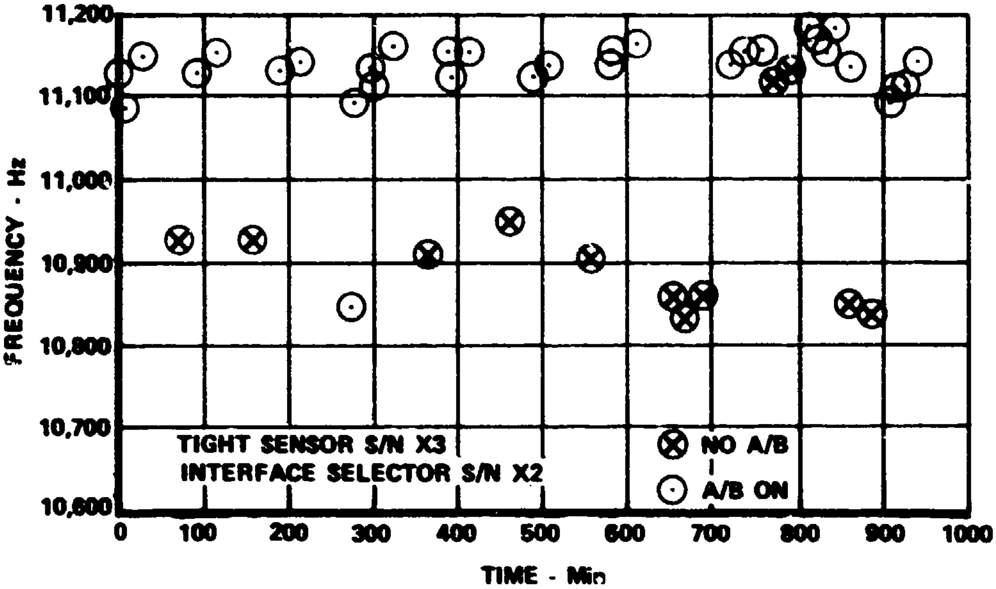

Figure 74. TIGT Sensor Performance Check for FX-111 FD 81225
Engine 75 Through 90 Endurance Hours

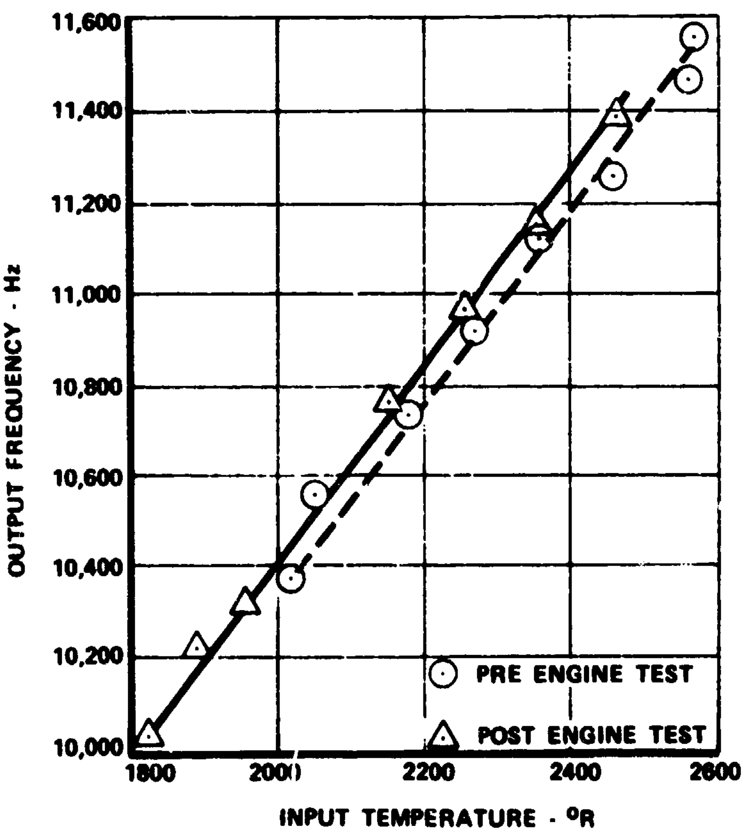

Figure 75. TIGT Sensor SN X2 Calibration FD 81226
13.5 Hours Engine Time

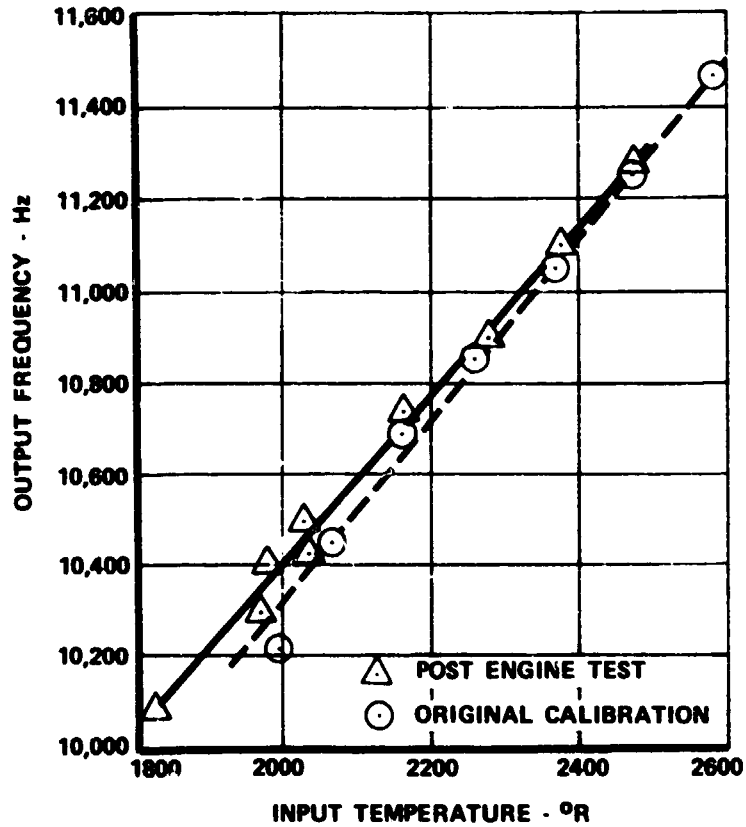

Figure 76. TIGT Sensor SN X3 Calibration 75.5 Hours Engine Time FD 81227